

8-2018

Stretching Vascular Smooth Muscle Cells on Micropatterned Surfaces

Suzanne Nicole Bradley

Clemson University, snbradl@g.clemson.edu

Follow this and additional works at: https://tigerprints.clemson.edu/all_theses

Recommended Citation

Bradley, Suzanne Nicole, "Stretching Vascular Smooth Muscle Cells on Micropatterned Surfaces" (2018). *All Theses*. 2957.
https://tigerprints.clemson.edu/all_theses/2957

This Thesis is brought to you for free and open access by the Theses at TigerPrints. It has been accepted for inclusion in All Theses by an authorized administrator of TigerPrints. For more information, please contact kokeefe@clemson.edu.

STRETCHING VASCULAR SMOOTH MUSCLE CELLS
ON MICROPATTERNED SURFACES

A Thesis
Presented to
the Graduate School of
Clemson University

In Partial Fulfillment
of the Requirements for the Degree
Master of Science
Bioengineering

by
Suzanne Nicole Bradley
August 2018

Accepted by:
Dr. Delphine Dean, Committee Chair
Dr. Bruce Gao
Dr. William Richardson

ABSTRACT

Vascular smooth muscle cells regulate blood flow by contracting and relaxing blood vessels. Vascular smooth muscle cells display one of two distinct phenotypes: contractile or synthetic. The contractile phenotype enables cells to contract, and the majority of cells in healthy blood vessels exhibit this phenotype. Transition to the synthetic phenotype is associated with abnormal mechanical forces and the development of vascular diseases, including hypertension and atherosclerosis. Cell-extracellular matrix interactions and mechanical stimulation are factors that affect phenotypic modulation.

Micropatterning techniques create a microenvironment used to control cell morphology, adhesion, migration, proliferation, and differentiation. Vascular smooth muscle cells are circumferentially arranged in blood vessels, so parallel cell alignment mimics the native environment. Micropatterning vascular smooth muscle cells, either onto topographical features or extracellular matrix protein patterns, has been shown to promote a more contractile, *in vivo*-like phenotype. Vascular smooth muscle cells are exposed to continuous mechanical signaling from pulsatile blood flow, which enforces the contractile phenotype. Applying a physiologically relevant, cyclic stretching regimen to vascular smooth muscle cells also promotes contractile functioning. The purpose of this study was to determine the effects of micropatterning and mechanical stimulation on vascular smooth muscle cell phenotype.

Three micropatterning techniques were implemented to determine the best method for aligning vascular smooth muscle cells. Microstamping was effective at patterning collagen but did not promote sufficient cell alignment. Stencil patterning

vascular smooth muscle cells on a collagen layer was found to promote cell alignment with minimal cell spreading. Stenciled cells were exposed to physiological cyclic stretch using the MechanoCulture FX mechanical stimulation system (CellScale). The combination of stencil patterning and stretching reduced cell proliferation and promoted a more contractile phenotype.

DEDICATION

This thesis is dedicated to all those who have supported me throughout my college career. First, I would like to thank my parents and sister, Meredith, for always encouraging and believing in me. I would like to thank my grandparents Clark and Carol Britt, and the rest of my extended family, for their constant support and encouragement. I would also like to thank my friends, roommates, and other lab members for keeping me sane during grad school and listening patiently about grading lab reports or cell contamination. I would like to thank All In Coffee Shop, Dunkin' Donuts, and Starbucks for keeping me awake during college. Finally, this thesis is dedicated in loving memory of my grandparents John and Barbara Bradley.

“We can rejoice, too, when we run into problems and trials, for we know that they help us develop endurance. And endurance develops strength of character, and character strengthens our confident hope of salvation.” – Romans 5:3-4

ACKNOWLEDGMENTS

I would like to acknowledge all those who have advised and supported me throughout this research project. First, I would like to thank Dr. Delphine Dean for being my research advisor for the last four years, first for an undergraduate Creative Inquiry project, and now for my Master's thesis. I am grateful for your support and guidance, even when micropatterning cells seemed impossible. I would like to thank my committee members, Dr. Bruce Gao and Dr. William Richardson, for their support and the resources provided for this project. I would also like to thank the members of my lab: Hannah Cash, Anika Chowdhury, Nardine Ghobrial, Tyler Harvey, and Scott Slaney. A special thanks to Nardine and Anika for always helping me find things in lab. I would also like to thank Cassie Gregory for her assistance with immunocytochemistry staining, as well as Maria Torres and Jennifer Hogan for their help with all things bioengineering. Finally, I would like to thank Jesse Rogers for answering my many questions about cell stretching, and Kelsey Watts for helping me with microstamping.

TABLE OF CONTENTS

	Page
TITLE PAGE	i
ABSTRACT.....	ii
DEDICATION	iv
ACKNOWLEDGMENTS	v
LIST OF TABLES	xi
LIST OF FIGURES	xii
CHAPTER ONE: INTRODUCTION.....	1
1.1 MOTIVATION	1
1.2 RESEARCH AIMS.....	2
1.3 REFERENCES	3
CHAPTER TWO: BLOOD VESSELS AND VASCULAR SMOOTH MUSCLE CELLS	4
2.1 BLOOD VESSELS	4
2.1.1 Overview of Vascular Anatomy	4
2.1.2 Blood Vessel Structure	5
2.1.3 Mechanical Forces Affecting Blood Vessels	6
2.2 VASCULAR SMOOTH MUSCLE CELLS.....	8
2.2.1 Characteristics of Smooth Muscle	8
2.2.2 Structural Characteristics of Vascular Smooth Muscle Cells.....	10
2.2.3 Functions of Vascular Smooth Muscle Cells.....	14

Table of Contents (Continued)

	Page
2.2.4 Vascular Smooth Muscle Cell Phenotypes	16
2.3 CLINICAL SIGNIFICANCE	19
2.4 MATERIALS AND METHODS.....	22
2.4.1 Vascular Smooth Muscle Cell Culture	22
2.4.2 Immunocytochemistry Staining	23
2.5 REFERENCES	26
CHAPTER THREE: MICROPATTERNING TECHNIQUES AND CELLULAR RESPONSES	29
3.1 MICROPATTERNING TECHNIQUES	29
3.1.1 Microfabrication	29
3.1.2 Micropatterning	29
3.1.3 Photolithography.....	30
3.1.4 Soft Lithography	32
3.1.5 Microstamping	33
3.1.6 Microfluidic Patterning.....	34
3.1.7 Stencil Patterning.....	35
3.1.8 Considerations for Soft Lithography	36
3.2 THE EXTRACELLULAR MATRIX AND CELLULAR RESPONSES	37
3.2.1 Cellular Microenvironments and the Role of the Extracellular Matrix	37
3.2.2 Cellular Responses to Micropatterning.....	38

Table of Contents (Continued)

	Page
3.3 RESPONSE OF VASCULAR SMOOTH MUSCLE CELLS TO MICROPATTERNING	40
3.3.1 Native Microenvironments of Vascular Smooth Muscle Cells.....	40
3.3.2 Motivation for Micropatterning Vascular Smooth Muscle Cells.....	41
3.3.3 Responses of Vascular Smooth Muscle Cells to Micropatterning.....	41
3.4 METHODS, RESULTS, DISCUSSION, AND FUTURE IMPROVEMENTS	43
3.4.1 Photomask Design	43
3.4.2 Photolithography.....	44
3.4.3 Soft Lithography	45
3.4.4 Microstamping	48
3.4.5 Pluronic Solutions to Eliminate Non-Specific VSMC Adhesion.....	50
3.4.6 Microfluidic Patterning.....	51
3.4.7 Stencil Patterning	52
3.5 REFERENCES	54
CHAPTER FOUR: STRETCHED TO THE LIMIT: CELL STRETCHING	57
4.1 CELL STRETCHING DEVICES.....	57
4.1.1 Device Specifications and Experimental Parameters	57
4.1.2 The MechanoCulture FX Cell Stretching Device.....	58

Table of Contents (Continued)

	Page
4.2 MECHANOTRANSDUCTION	59
4.3 EFFECTS OF STRETCHING VASCULAR SMOOTH MUSCLE CELLS	60
4.4 METHODS, RESULTS, AND DISCUSSION.....	60
4.4.1 Stretching VSMCs on Microstamped Collagen Patterns- Methods	61
4.4.2 Stretching VSMCs on Microstamped Collagen Patterns- Results and Discussion	63
4.4.3 Stretching Stencil Patterned VSMCs (Trial 1) – Methods.....	65
4.4.4 Stretching Stencil Patterned VSMCs (Trial 1) – Results and Discussion	68
4.4.5 Stretching Stencil Patterned VSMCs (Trial 2) – Methods.....	76
4.4.6 Stretching Stencil Patterned VSMCs (Trial 2) – Results and Discussion	77
4.5 CONCLUSIONS AND FUTURE DIRECTION.....	81
4.6 REFERENCES	82
APPENDICES	83
Appendix A: Vascular Smooth Muscle Cell Culture Protocol	84
Appendix B: Counting Cells Protocol	85
Appendix C: Proliferation Assay Protocol	86
Appendix D: Proliferation Assay Standard Curve Protocol	87
Appendix E: Immunocytochemistry (ICC) Staining Protocol.....	89

Table of Contents (Continued)

	Page
Appendix F: Fabrication of Stamp Master Using Photolithography Protocol	91
Appendix G: Fabrication of PDMS Stamps from Master Wafer Protocol	94
Appendix H: Microstamping Collagen Protocol	95
Appendix I: Stencil Patterning Cells Protocol	96
Appendix J: Cell Stretching Protocol	97
Appendix K: Legend of Photomask Stamp Designs.....	99
Appendix L: Results from Microstamping Trials	102
Appendix M: Stretching Programs	103
Appendix N: Proliferation Assay Data from Stretching Experiments.....	105
Appendix O: VSMC Proliferation Assay Standard Curves.....	110
Appendix P: Images of DAPI-Stained VSMCs for Number of Nuclei Analysis.....	112

LIST OF TABLES

Table	Page
2.1 Comparison of Contractile and Synthetic Phenotypes.....	19
3.1 Summary of Vascular Smooth Muscle Cell Micropatterning Studies.....	42
4.1 Program sequence for stretching VSMCs on microstamped collagen patterns.....	62
4.2 Program sequence for stretching VSMCs plated in lines using PDMS stencils	67
4.3 T-tests comparing the proliferation rates of stenciled VSMCs.....	69
4.4 T-tests comparing the proliferation rates of stretched VSMCs	70
4.5 T-tests comparing number of nuclei between control, stretched, stencil-patterned, and non-stenciled VSMCs	72
4.6 Program sequence for stretching VSMCs plated in lines using PDMS stencils	76
4.7 T-tests comparing the proliferation rates of control and Stretched VSMCs.....	77
4.8 T-tests comparing number of nuclei between Day 0 control, Day 1 control, parallel and perpendicularly stretched VSMCs	79

LIST OF FIGURES

Figure	Page
2.1 Blood vessel classification and direction of blood flow	5
2.2 Blood vessel tunics in an artery, vein, and capillary.....	6
2.3 Types of fluid flow in blood vessels	7
2.4 Mechanical forces present in blood vessels	8
2.5 Representative cells of muscle tissue types	9
2.6 Primary porcine VSMCs.....	10
2.7 Primary human umbilical artery smooth muscle cells	11
2.8 Cytoskeletal arrangement of vascular smooth muscle cells.....	12
2.9 Microfilament structure of a vascular smooth muscle cell.....	14
2.10 Organization of thick and thin filaments during relaxation and contraction.....	15
2.11 Smooth muscle cell contraction	16
2.12 Contractile and synthetic phenotypes of vascular smooth muscle cells	17
2.13 Factors promoting synthetic VSMC phenotype in vascular disease development.....	20
2.14 Cell types involved in atherosclerotic fatty streak development.....	21
2.15 Human aortic smooth muscle cells in culture, passage 5.....	23
2.16 ICC staining of VSMCs for cytoskeleton with phalloidin (red) and nuclei with DAPI (blue)	24

List of Figures (Continued)

Figure		Page
2.17	ICC staining of VSMCs for cytoskeleton with ActinGreen 488 and nuclei with DAPI (blue)	24
2.18	ICC staining of VSMCs for collagen type I (green) and nuclei with DAPI (blue)	25
2.19	ICC staining of VSMCs for alpha-smooth muscle actin (green) and nuclei with DAPI (blue)	25
2.20	ICC staining of VSMCs for alpha-smooth muscle actinin (green) and nuclei with DAPI (blue)	25
3.1	Process of photolithography to create a master silicon wafer for both positive and negative photoresists.....	32
3.2	Soft lithography techniques: microfluidic patterning, microstamping, and stencil patterning	33
3.3	Steps of microstamping.....	34
3.4	Steps of microfluidic patterning.....	35
3.5	VSMC circumferential alignment in a blood vessel	40
3.6	SolidWorks drawing of photomask with eleven stamp designs.....	44
3.7	Photolithography results	45
3.8	PDMS stamps.....	46
3.9	Schematic of PDMS stamps.....	46
3.10	Microstructures on PDMS stamps	46
3.11	3D printed stamp handles.....	48
3.12	Schematic of stamp with attached 3D-printed handle	48
3.13	PDMS stamps with handles	48

List of Figures (Continued)

Figure	Page
3.14 Successful collagen microstamping on PDMS gel	49
3.15 Microstamped collagen with Pluronic solution	50
3.16 Schematic of microfluidic patterning mold	52
3.17 Stencils	53
3.18 Stencil patterning of VSMCs stained with phalloidin and DAPI	53
4.1 Mechanisms of 2D uniaxial stretch.....	57
4.2 MechanoCulture FX System.....	59
4.3 Overview of methods of microstamping collagen and stretching VSMCs	61
4.4 MechanoCulture FX cell stretching system.....	63
4.5 Visible collagen patterns.....	63
4.6 VSMCs stained for phalloidin	64
4.7 Overview of methods of stenciling and stretching VSMCs (Trial 1)	65
4.8 Proliferation rates of control and stretched VSMCs plated without a stencil	68
4.9 Proliferation rates of control and parallel or perpendicularly stretched VSMCs plated in a line pattern with a stencil	69
4.10 Proliferation rates of control VSMCs with and without	69
4.11 Proliferation rates of stretched VSMCs	70
4.12 Number of nuclei in VSMCs (Trial 1).....	72

List of Figures (Continued)

Figure	Page
4.13 Control, non-stretched VSMCs (4X)	73
4.14 Control, non-stretched VSMCs (10X)	73
4.15 Stretched VSMCs (4X)	73
4.16 Stretched VSMCs (10X)	74
4.17 Overview of methods of stenciling and stretching VSMCs (Trial 2)	76
4.18 Proliferation rates of control and stretched VSMCs	77
4.19 Proliferation rates of parallel and perpendicular stretched cells	78
4.20 Number of nuclei in VSMCs (Trial 2)	79
4.21 Stencil Patterning: Day 0 Control	80
4.22 Control VSMCs	80
4.23 Stretched VSMCs.....	80

CHAPTER ONE

INTRODUCTION

1.1 MOTIVATION

Vascular smooth muscle cells regulate blood flow by contracting and relaxing blood vessels. Biomechanical signals received from both the topography of the surrounding extracellular matrix, as well as the mechanical forces from blood flow, maintain homeostasis of vascular smooth muscle cells. Micropatterning dictates cellular morphology and functions, with parallel lines promoting a contractile phenotype in vascular smooth muscle cells. Micropatterning techniques, including microstamping, microfluidic patterning, and stencil patterning were implemented to create a microenvironment representative of *in vivo* vascular conditions¹. The goal of micropatterning was to align vascular smooth muscle cells in a way that mimics their circumferential arrangement and contractile functioning in blood vessels.

Cell stretching devices are used to replicate the mechanical forces received by vascular smooth muscle cells. Cell stretching at a physiologically relevant regimen has been shown to promote a contractile phenotype in vascular smooth muscle cells². The combination of micropatterning and stretching is used to promote a more *in vivo*-like phenotype with associated contractile functions. Manipulating the cellular microenvironment allows for control over cellular phenotype and behaviors. The ability to produce vascular smooth muscle cells with a desired phenotype is necessary to create experimental models of both healthy and diseases states. One third of the world's

population suffers from vascular disease, so the ability to more effectively and accurately study pathogenesis and potential therapeutics is essential³. The goal of this study is to investigate phenotypic changes associated with stretching of micropatterned vascular smooth muscle cells.

1.2 RESEARCH AIMS

Aim 1: Optimize micropatterning techniques to align vascular smooth muscle cells.

The first aim of this research project was to optimize a micropatterning technique to create parallel lines of vascular smooth muscle cells. Parallel cell alignment mimics the natural circumferential arrangement of vascular smooth muscle cells in blood vessels, encouraging more *in vivo*-like cell behaviors¹. The extracellular matrix and topographical features of a cell's microenvironment provide biophysical and biochemical cues important in the regulation of cell responses. Therefore, implementing a method to align vascular smooth muscle cells promotes contractile phenotypes.

Aim 2: Analyze phenotype changes by staining micropatterned, stretched cells for actin cytoskeleton and collagen.

Vascular smooth muscle cells were stretched with a regimen physiologically equivalent to the mechanical forces of pulsatile blood flow present in a healthy blood vessel. The majority of healthy vascular smooth muscle cells exhibit a contractile phenotype, so cyclic strain mechanical stimulation was implemented to produce a more natural, contractile phenotype². To analyze the effects of stretching micropatterned

vascular smooth muscle cells, immunocytochemistry staining for contractile elements and collagen was performed. Phalloidin stained actin filaments, a part of the cell's cytoskeleton, allowing for visualization of the phenotype of the cell. Contractile vascular smooth muscle cells secrete minimal extracellular matrix proteins compared to synthetic cells, so quantification of collagen can also reveal cellular behaviors⁴.

Aim 3: Quantify proliferation rates, an indicator of vascular smooth muscle phenotype, by performing a proliferation assay on micropatterned, stretched cells.

Contractile vascular smooth muscle cells have lower proliferation rates compared to synthetic cells, so a proliferation assay was performed to quantify proliferation. Determining proliferation rates is a way to assess the amount of contractile functioning of vascular smooth muscle cells.

1.3 REFERENCES

1. Y. Li, *et al.* "Engineering cell alignment *in vitro*." *Biotechnology Advances*, 32: 347-365, 2014.
2. G. Ye, *et al.* "The role of mechanotransduction on vascular smooth muscle myocytes cytoskeleton and contractile function." *The Anatomical Record*, 297(9): 1758-1769, 2014.
3. T.S. Al-Shehabi, *et al.* "Anti-atherosclerotic plants which modulate the phenotype of vascular smooth muscle cells." *Phytomedicine*, 23: 1068-1081, 2016.
4. S.S.M. Rensen, *et al.* "Regulation and characteristics of vascular smooth muscle cell phenotypic diversity." *Netherlands Heart Journal*, 15(3): 100-108, 2007.

CHAPTER TWO

BLOOD VESSELS AND VASCULAR SMOOTH MUSCLE CELLS

2.1 BLOOD VESSELS

2.1.1 Overview of Vascular Anatomy

The cardiovascular system is made up of the heart, blood vessels, and blood. It is a closed circuit system with the purpose of circulating blood throughout blood vessels to all tissues of the body. This facilitates nutrient and gas exchange while providing a transportation system for cells of the immune system¹. An essential function of the vascular system is to maintain cellular homeostasis throughout the body by promoting nutrient absorption and cellular waste removal through the circulation of blood². Blood vessels are divided into five categories based on lumen diameter and the direction of blood flow: arteries, arterioles, capillaries, venules, and veins (*Figure 2.1*)³. Arteries carry oxygenated blood away from the heart, and a thick muscular layer enables them to withstand high pressures as blood is ejected from the heart. Large arteries, including the aorta, are classified as elastic arteries because they contain many layers of elastin to allow for blood vessel expansion and restriction in response to volume changes³. Small arteries and arterioles are progressively smaller in diameter, and they are considered muscular arteries due to their function in rapid distribution of blood throughout the body². Capillaries are tiny, branching vessels that facilitate direct gas and nutrient exchange with cells³. Deoxygenated blood flows from capillaries into venules, which transition into larger veins to transport blood back to the heart.

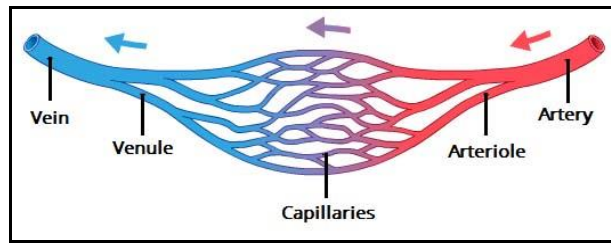


Figure 2.1: Blood Vessel Classification and Direction of Blood Flow⁴

2.1.2 Blood Vessel Structure

Blood vessels vary in structure depending on anatomical location and physiological requirements. Generally, blood vessels are composed of several cell and connective tissue types organized in three layers: the tunica adventitia, tunica media, and tunica intima (*Figure 2.2*)⁵. The tunica adventitia, or tunica externa, is the outermost layer, and it is made up of extracellular matrix (ECM) proteins that allow it to serve as the structural support of the blood vessel^{5,6}. Within the adventitia, fibroblasts and progenitor cells are present. Fibroblasts maintain the ECM scaffolding network, while stem and vascular progenitor cells differentiate into many vascular cell types based on biochemical and mechanical signaling⁵. The tunica media is the muscular middle layer of the blood vessel, and it contains circumferentially arranged vascular smooth muscle cells along with a network of elastin and collagen fibers⁵. The main function of the tunica media is to regulate blood flow by adjusting the blood vessel diameter through the processes of vasoconstriction, or contraction, and vasodilation, or relaxation^{3,6}. The tunica media is the thickest layer of an arterial wall. Up to 75% of the tunica media can contain vascular smooth muscle cells, and due to the presence of high amounts of collagen and elastin fibers, arteries are able to withstand the mechanical forces associated with pulsatile blood flow^{7,8}. The tunica intima is the innermost layer, and it is composed

of a single layer of endothelial cells, along with a basement membrane (sub-endothelial layer) and inner elastic lamina^{3,5}. Endothelial cells line the lumen of blood vessels and have direct contact with blood, controlling the diffusion of nutrients and wastes to maintain cellular homeostasis^{2,9}. The cellular and connective tissue composition dictates the physiological function of each tunic, as well as the blood vessel as a whole.

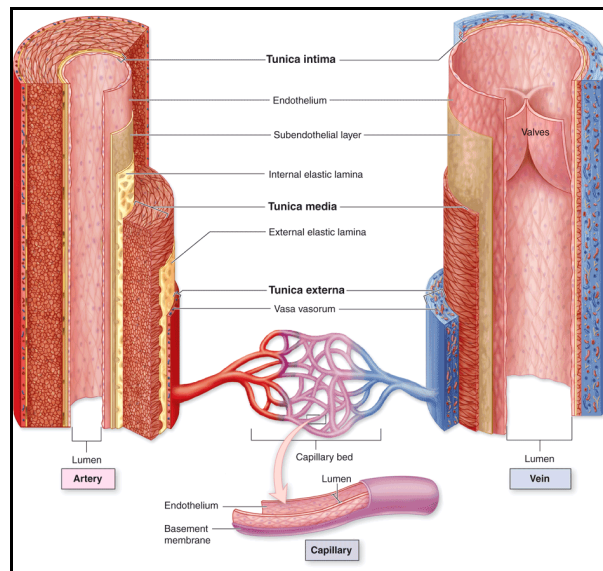


Figure 2.2: Blood Vessel Tunics in an Artery, Vein, and Capillary¹⁰

2.1.3 Mechanical Forces Affecting Blood Vessels

The vascular system is a complex, branching network of vessels influenced by a combination of mechanical forces¹¹. Hemodynamics is the study of the fluid dynamics of blood flow throughout this complex system based on physical factors including blood pressure, cardiac output, and the resistance of a vessel to flow^{12,13,14}. Blood pressure is defined as the force that blood applies to the inside of blood vessel walls, and it accounts for a large portion of the mechanical forces exerted on blood vessels^{7,15,16}. Arterial blood flow is pulsatile due to the constant ejection of blood from the heart, so blood pressure is

much higher in arteries than veins¹⁷. Large arteries, such as the aorta, have circumferentially arranged layers, enabling them to dampen pulsatile blood flow from the heart into a steady, uniform flow as blood enters smaller vessels^{7,17}. The elastic nature of blood vessel walls serves to reduce the blood pressure exerted on subsequent vessels, which is an example of hemodynamic homeostasis¹¹. There are three patterns of blood flow that are recognized in blood vessels: laminar, turbulent, and bolus flow (*Figure 2.3*)¹². Laminar blood flow is found in the majority of vessels in a healthy vascular system, and it occurs under steady flow conditions as blood moves in parallel layers down a blood vessel^{18,19}. Turbulent flow is characterized by the movement of random and chaotic layers, which occurs in either large arterial vessels or diseased vessels¹². Bolus flow occurs in capillaries, where blood cells are required to assemble into a single-file line in order to travel through the vessel¹².

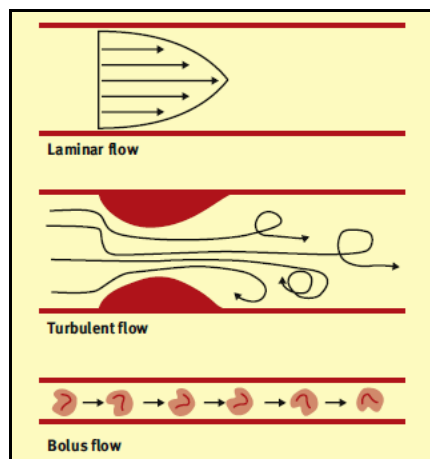


Figure 2.3: Types of Fluid Flow in Blood Vessels¹²

On the macroscopic level, blood vessels are subjected to many mechanical forces: pulsatile blood flow, shear stress, cyclic strain, and hydrostatic pressure (*Figure 2.4*)²⁰. Shear stress can be defined as the frictional force generated by blood flow acting parallel

to the blood vessel wall^{14,19}. The endothelial lining is in direct contact with blood, and the mechanical force associated with the shear stress of blood flow is necessary for endothelial cell homeostasis¹⁹. Cyclic strain is due to circumferential stretch that occurs when pulsatile blood flow is present in the vascular system¹⁴. Hydrostatic pressure is a normal stress that acts perpendicularly to the blood vessel wall¹⁹. Changes in these mechanical forces due to anatomical changes in the vascular system play an important role in the development of vascular diseases¹⁷. The combination of these naturally occurring mechanical forces maintain and regulate vascular and cellular homeostasis¹⁶.

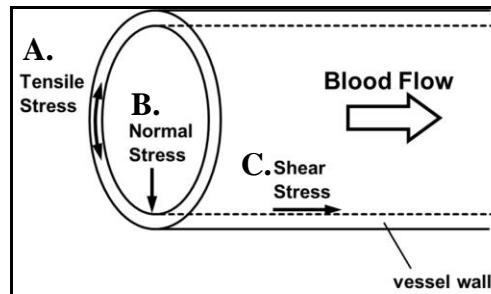


Figure 2.4: Mechanical Forces Present in Blood Vessels, A. Tensile stress (cyclic strain) from circumferential stretch, B. Normal stress from hydrostatic pressure, and C. Shear stress from unidirectional blood flow¹⁹

2.2 VASCULAR SMOOTH MUSCLE CELLS

2.2.1 Characteristics of Smooth Muscle

There are three types of muscle tissue: skeletal, cardiac, and smooth (*Figure 2.5*). Skeletal muscle cells, or fibers, are multinucleated and contain sarcomeres, visible as an alternating, striated pattern of thick and thin microfilaments which are responsible for muscle contraction. Skeletal muscles include axial and appendicular muscles, and contraction is voluntary due to innervation by the somatic nervous system⁷. The muscular

wall of the heart is composed of individual cardiac muscle cells, which are striated in appearance and connect to surrounding muscle cells with intercalated discs. Cardiac muscle is stimulated by the autonomic nervous system, so contraction is involuntary⁷. Smooth muscle tissue is found in visceral organs, including the stomach and intestines, as well as in hollow passageways, such as blood vessels. Smooth muscle is important in the movement of materials throughout the body; propelling blood through blood vessels is one example. Smooth muscle cells have a single, central nucleus and are described as fusiform, elongated, and spindle-shaped, with a wider middle and narrowed ends⁷. Cells are relatively small, with lengths ranging from 50 to 200 μm and diameters of 5 to 10 μm ⁷. Smooth muscle differs from skeletal and cardiac muscle in that it is not striated; while thick and thin filaments are present in smooth muscle, they are not organized as a sarcomere. Additionally, smooth muscle contraction is involuntary, has a slow contraction speed, and is resistant to fatigue due to lower ATP requirements compared to skeletal muscle.

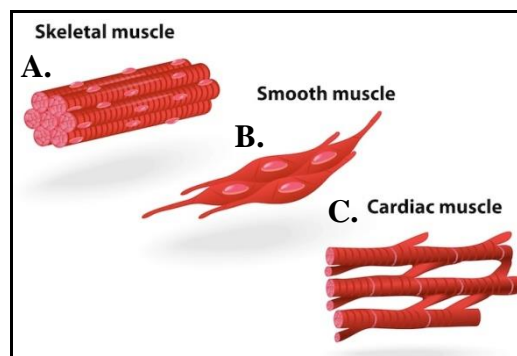


Figure 2.5: Representative cells of muscle tissue types, A. Bundle of multinucleated skeletal muscle fibers, B. Fusiform smooth muscle cells with central nuclei, and C. Cardiac muscle cells²¹

2.2.2 Structural Characteristics of Vascular Smooth Muscle Cells

Vascular smooth muscle cells (VSMCs) are the most abundant type of cell found in blood vessels²². Similar to other types of smooth muscle cells, they are spindle-shaped and have a central nucleus. Additionally, vascular smooth muscle cells are aligned next to each other in a staggered, parallel fashion. VSMCs are usually arranged circumferentially in blood vessels, with their alignment dependent upon shear stress in the location of the vessel²³. *In vitro*, the phenotype displayed by vascular smooth muscle cells depends on the artery of origin, as well as duration of time in culture^{24,25} (Figures 2.6-2.7). The main physical elements of the cell include: the basal lamina, mitochondria, caveolae, sarcoplasmic reticulum, cytoskeleton, and the contractile apparatus (Figure 2.8)⁵.

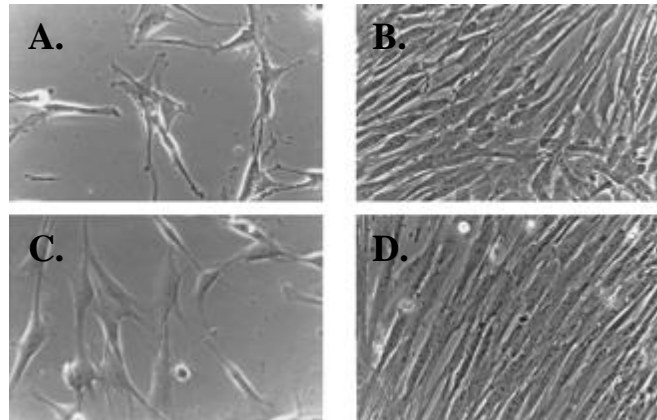


Figure 2.6: Primary porcine VSMCs (100X), A. Aortic SMCs (2 days), B. Aortic SMCs (10 days), C. Iliac Artery SMCs (2 days), D. Iliac Artery SMCs (10 days) [modified from ref. 23]

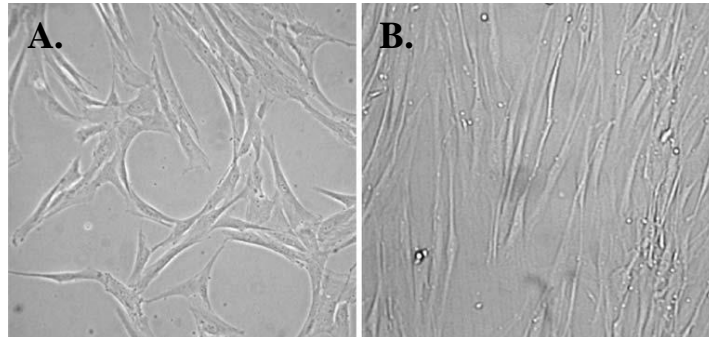


Figure 2.7: Primary human umbilical artery smooth muscle cells, A. 10 days, B. 17 days, (100X)
[modified from ref. 24]

Vascular smooth muscle cells produce their own reticular network of ECM protein fibers, including elastin and collagen types I and III²⁶. These ECM proteins form an outer layer, termed the basal lamina, that surrounds the sarcolemma, or cell membrane, of individual smooth muscle cells. The basal lamina provides unity and attachment among neighboring cells²⁶. As such, vascular smooth muscle cells are attached to neighboring cells by either indirect ECM assemblies or direct cell-cell contacts through desmosomes. The mitochondrion is a mighty organelle responsible for generating the ATP necessary for cellular functions⁵. Some studies show that mitochondria in vascular smooth muscle cells might also play a role in cell signaling²⁶. Caveolae are indentations in the sarcolemma, vital in cell signaling pathways as well as vascular contraction. The sarcoplasmic reticulum (SR) is an organelle made of intricate tubules, noted for its role in calcium storage, release, and uptake⁵. The function of the sarcoplasmic reticulum depends on its location: the peripheral SR maintains calcium homeostasis through calcium release, while the central SR supplies calcium to initiate smooth muscle contraction⁵.

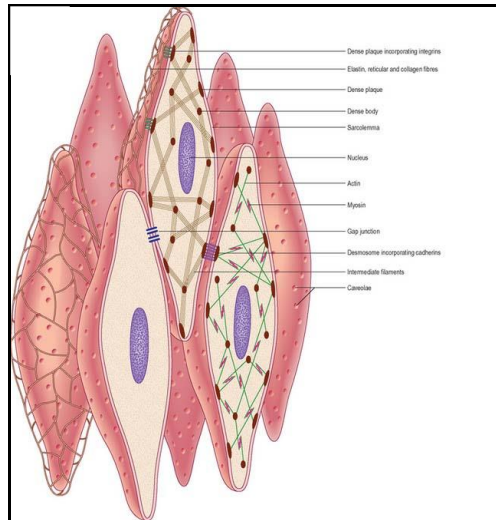


Figure 2.8: Cytoskeletal Arrangement of Vascular Smooth Muscle Cells [modified from ref. 25]

The arrangement of structural components throughout vascular smooth muscle cells forms two main entities: the scaffolding cytoskeleton and the contractile apparatus²⁶. The cytoskeleton does not simply provide shape and structure to the cell, but it is also important in protecting organelles and promoting cellular activities. Cytoskeletal proteins must constantly reorganize and adapt to cellular activities as well as changing external conditions. The cytoskeleton of the cell is composed of three fibers: microtubules, intermediate filaments, and microfilaments⁵. Microtubules are the largest, made from alpha and beta tubulin polymers, and they are important in not only maintaining cell shape but also intracellular transport^{5,27}. The main role of the intermediate filament network is to provide structural support and organization for the cell²⁶. Desmin and vimentin are proteins that form intermediate filament bundles, and larger arteries express a higher vimentin/desmin ratio than smaller arteries²⁷. Intermediate filament bundles run longitudinally or diagonally through the cell, and they are connected by either cytoplasmic dense bodies or submembranous dense plaque structures²⁶. Dense bodies are

distributed throughout the cytoplasm, and they serve as an attachment or anchoring site, connecting the intermediate filament network²⁸. Dense plaques are found below the sarcolemma, and they anchor intermediate filaments to the extracellular matrix surrounding the cell. Cell-cell contacts occur between dense plaques from adjacent cells, forming a desmosome structure²⁶.

Microfilaments are the thinnest fibers, and they include thick filaments (myosin) and thin filaments (actin)²⁸. Smooth muscle myosin is composed of two heavy and two light chains, and it is involved in regulating smooth muscle contraction²⁷. Several isoforms, or protein variants, of actin are located in smooth muscle: α - smooth muscle actin, γ -smooth muscle actin, β -non-muscle actin, and γ -non-muscle actin (*Figure 2.9*)²⁷. Smooth muscle actin is associated with myosin for contractile functions, and large arteries contain about 60% α - smooth muscle actin²⁷. Together, actin and myosin form the contractile apparatus, or contractile unit, of the cell, forming a network by inserting into dense bodies and dense plaques along with the intermediate filaments. In this way, dense bodies and plaques are analogous to Z-lines in the sarcomere of a skeletal muscle fiber²⁸. Therefore, some cytoskeletal components serve as structural support for maintaining cell shape, while the microfilaments function as the contractile apparatus of the cell.

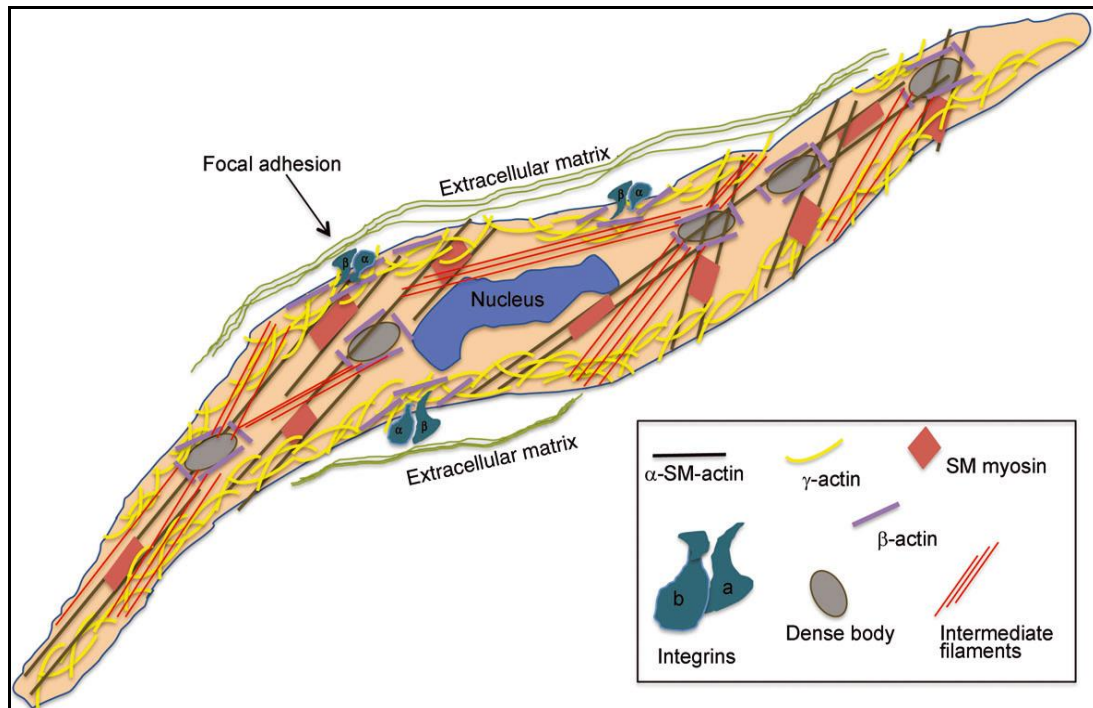


Figure 2.9: Microfilament Structure of a Vascular Smooth Muscle Cell²⁷

2.2.3 Functions of Vascular Smooth Muscle Cells

Maintaining vascular homeostasis is the main function of vascular smooth muscle cells, and this is achieved by the contraction and relaxation of blood vessels. Altering the diameter of the blood vessel lumen enables vascular smooth muscle cells to regulate blood pressure, blood flow/ distribution, and blood vessel tone^{22,29}.

The contractile apparatus system is responsible for generating the tension to contract smooth muscle⁵. Smooth muscle contraction is stimulated by both biochemical and mechanical signals, including stretch from the cell itself³⁰. Calcium ions serve as the initiator of smooth muscle contraction. After a stimulus occurs, the sarcoplasmic reticulum releases stored calcium into the cytoplasm, and simultaneously calcium ions enter the cell through calcium channels in the sarcolemma³⁰. Together, these mechanisms

increase the concentration of cytosolic calcium. Next, calcium ions interact with the regulatory protein calmodulin, which causes the myosin light chain to be phosphorylated by the enzyme myosin kinase³¹. Phosphorylation of myosin allows myosin heads to interact with the actin of thin filaments (*Figure 2.10*).

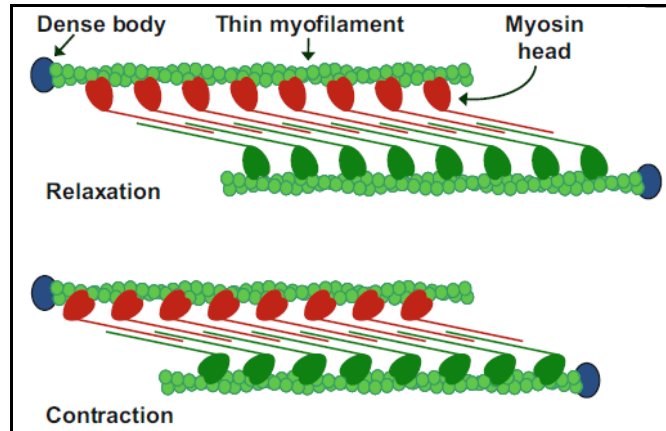


Figure 2.10: Organization of thick and thin filaments during relaxation and contraction [modified from ref. 5]

Since thin filaments are anchored to dense bodies in both the cytoplasm and on the sarcolemma, the movement of the thin and thick filaments sliding past each other pulls on the entire cytoskeletal network of the cell, including the intermediate filaments also attached to the same dense bodies³⁰. This process causes the entire cell to contract, as seen in *Figure 2.11*. Calcium sensitization occurs to prolong the contractile force produced by the cell, and this process is regulated by the RhoA/ Rho kinase pathway³⁰. Finally, smooth muscle relaxation occurs as excess calcium ions are removed through several mechanisms, including calcium uptake by the sarcoplasmic reticulum and calcium transport to extracellular fluid by sodium-calcium exchanger channels in the cell membrane³⁰.



Figure 2.11: Smooth muscle cell contraction, A. Relaxed muscle cell, B. Contracted muscle cell³¹

2.2.4 Vascular Smooth Muscle Cell Phenotypes

While the previous section describes the general structural characteristics and contractile functioning of vascular smooth muscle cells, it is important to note that there is phenotypic diversity among vascular smooth muscle cells. While phenotypes range across a spectrum, two characteristic phenotypes can be identified: contractile and synthetic²⁹. These two phenotypes are associated with specific morphologies along with differing cellular functions. Vascular smooth muscle cells are highly differentiated, but not terminally differentiated: they are capable of transitioning reversibly between phenotypes³². The process of vascular smooth muscle cells switching between phenotypes is termed “phenotypic modulation”²⁹. This plasticity allows vascular smooth muscle cells to adapt to the conditions of their local environment. Contractile VSMCs function to contract, while synthetic VSMCs are less contractile and have higher proliferation rates. Cell-cell and cell-extracellular matrix interactions, mechanical stimuli, and chemical cues are all factors that affect VSMC phenotype³³. *Figure 2.12* shows the physical appearance of the two phenotypes, as well as the cues that can promote each phenotype³³.

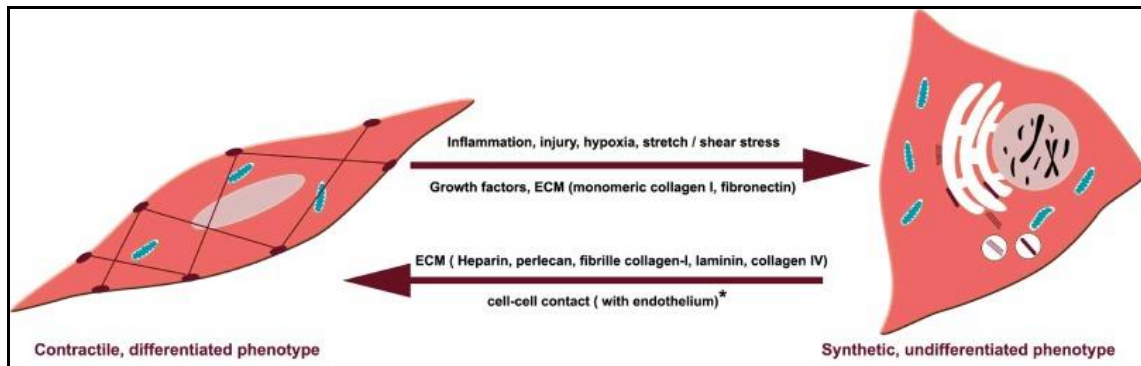


Figure 2.12: Contractile and synthetic phenotypes of vascular smooth muscle cells [modified from ref. 32]

Contractile, or differentiated, VSMCs make up the majority of smooth muscle cells located in healthy adult blood vessels, contracting in order to regulate blood flow and pressure^{29,32}. Contractile VSMCs have limited proliferation and migration, and they are described as quiescent yet active³⁴. They secrete only small amounts of extracellular matrix proteins²⁹. Contractile VSMCs adhere to the spindle-shaped morphology and have an abundance of contractile filaments to support their main function of contraction and relaxation²⁹. The contractile phenotype can be confirmed through staining for various cell marker proteins: α - smooth muscle actin, SM22 α , SM-calponin, smoothelin, and N-cadherin²⁹. The first four markers listed are associated with actin or the cytoskeleton, enabling visualization of the contractile elements specific to smooth muscle cells. N-cadherin is a cell-cell adhesion molecule important in cell signaling among vascular smooth muscle cells³⁵.

To note, it has been found that *in vivo* phenotypes can be maintained *in vitro* despite the differing environmental conditions³⁴. Desired phenotypes can be purposefully manipulated using a variety of methods, including the addition of serum or growth

factors, choice of cell culture substrate, or the application of mechanical signals^{34,36}. In fact, it has been shown that mechanical strain induces the contractile phenotype in vascular smooth muscle cells²⁹. Additionally, studies have shown that endothelial cells play a role in regulating and maintaining the contractile phenotype of surrounding vascular smooth muscle cells³². The contractile phenotype is more likely to be expressed *in vitro* when cells are seeded at a higher density and there are increased cell-cell contacts, as well as when cells are plated in a more *in-vivo* like arrangement²². Also, studies have shown that both substrate stiffness and the properties of the extracellular matrix environment affects the phenotype of vascular smooth muscle cells^{22,37}.

Vascular smooth muscle cells in the synthetic phenotype are termed dedifferentiated, and they exhibit a triangular or rhomboid shape^{29,32}. The number of protein synthesis organelles increase in the synthetic phenotype, allowing the cells to produce more extracellular matrix proteins, including elastin and collagen. Synthetic VSMCs are also characterized by increased proliferation and migratory rates and decreased contractility²⁹. There are not many protein markers specific to the synthetic phenotype, so traditionally staining for contractile markers along with proliferation and migration data is used to confirm phenotype³². Synthetic VSMCs are typically associated with vascular disease and injury²². *Table 2.1* summarizes the common characteristics of the two phenotypes.

Table 2.1: Comparison of Contractile and Synthetic Phenotypes^{29,32,38}

Contractile Phenotype	Synthetic Phenotype
Mature, differentiated	Dedifferentiated
Elongated, spindle-shaped	Rhomboid, triangular shaped
Low rates of proliferation and migration	High rates of proliferation and migration
Secrete minimal amounts of ECM proteins	Secrete large amounts of ECM proteins
Contract, regulate blood flow	Minimal contractile function
Express contractile protein markers	Do not express contractile protein markers

2.3 CLINICAL SIGNIFICANCE

The leading cause of death both worldwide and in the U.S. is heart disease³⁹. Heart disease includes stroke, arrhythmias, and cardiovascular diseases, such as atherosclerosis, hypertension, and restenosis³⁹. Worldwide, approximately one in three deaths are attributed to cardiovascular disease³⁸. The main risk factors for cardiovascular disease are smoking, hypertension (high blood pressure), diet, lifestyle and exercise³⁸. Atherosclerosis is a vascular disease characterized by the accumulation of plaque and lipids in blood vessels, leading to vessel occlusion and more serious consequences such as myocardial infarction or stroke⁴⁰. Restenosis is the narrowing of a blood vessel that occurs in response to a vascular injury received during a surgical procedure, such as an angioplasty³². Abnormal vascular smooth muscle cells contribute to the development of these cardiovascular diseases²⁷.

The characteristic proliferative and migratory functions of synthetic vascular smooth muscle cells contribute to the development of many cardiovascular diseases, including atherosclerosis, hypertension, and restenosis. The current paradigm for cardiovascular disease development is based on VSMC plasticity and the ability for cells to switch to the synthetic phenotype and remodel the extracellular matrix¹¹. It has also

been suggested that the activation of vascular stem cells present in the tunica media coupled with VSMC dedifferentiation could contribute to the development of cardiovascular disease¹¹. Mechanical forces in blood vessels can be altered due to various factors, including hypertension, and this leads to the development of vascular smooth muscle cell pathophysiology²³. On a cellular level, phenotypic switching of VSMCs to the synthetic phenotype is characteristic of the development of atherosclerosis in blood vessels³⁷. Additionally, diseased vessels have changing mechanical signaling, cellular interactions, growth factors, and biochemical and inflammatory signals, which promote the synthetic phenotype (*Figure 2.13*)^{37,36}. Synthetic VSMCs are able to synthesize more extracellular matrix proteins, leading to arterial stiffening and plaque accumulation in vessels¹¹.

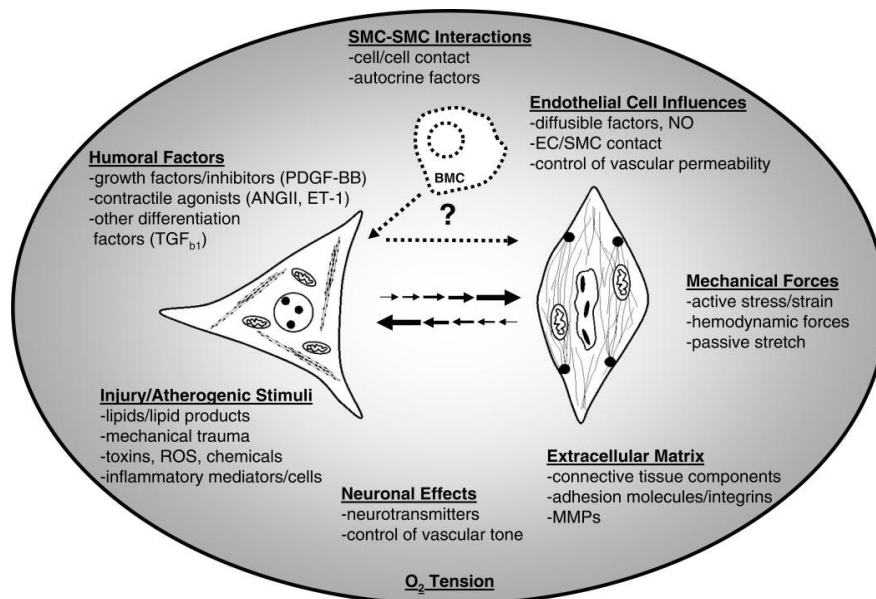


Figure 2.13: Factors Promoting Synthetic VSMC Phenotype in Vascular Disease Development³⁶

The cellular pathology associated with the development of atherosclerosis is endothelial cell dysfunction and vascular smooth muscle cell phenotypic modulation³⁸.

Atherosclerotic lesion development involves several cell types including endothelial cells, macrophages, platelets, lymphocytes, and vascular smooth muscle cells (*Figure 2.14*). In brief, endothelial cell dysfunction allows a lipid layer to accumulate, attracting macrophages that transition into foam cells. This leads to the formation of a lipid core in the intimal layer of the blood vessel, eventually inducing phenotypic modulation of vascular smooth muscle cells to the synthetic phenotype³⁸. The combination of these mechanical, biochemical, and cellular interactions causes VSMCs to dedifferentiate into the synthetic phenotype. Synthetic VSMCs then produce enough extracellular matrix proteins to form the fibrous cap of a plaque in a diseased vessel³². In restenosis, VSMCs either undergo trauma or the surrounding endothelial cells are destroyed^{32,40}. Then, VSMCs will migrate, proliferate, and secrete ECM proteins, contributing to the intimal lesions associated with restenosis³². Unfortunately, in the presence of certain risk factors and biochemical signals, vascular smooth muscle cells adopt functions that further the development of vascular disease⁴⁰. In conclusion, the development of vascular diseases demonstrates the complexity associated with the vascular environment and cellular regulation³².

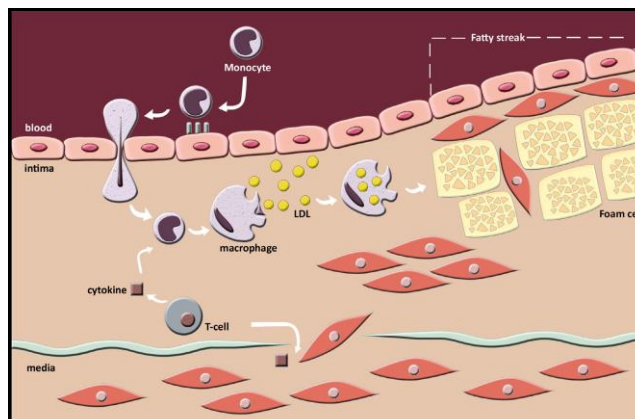


Figure 2.14: Cell types involved in atherosclerotic fatty streak development³⁸

2.4 MATERIALS AND METHODS

2.4.1. Vascular Smooth Muscle Cell Culture

Adult Human Aortic Vascular Smooth Muscle cells (HAOSMCs) were purchased from Cell Applications, Inc. (Cat. 354pk-05a). HAOSMCs were cultured in polystyrene flasks in standard cell culturing conditions (37°C, 5% CO₂), using smooth muscle cell growth medium (Cell Applications, Inc.). First, frozen cells were thawed by warming a cryogenic vial of frozen cells retrieved from a liquid nitrogen tank. The frozen cell suspension was centrifuged with warmed media in a 15 mL centrifuge tube at 1,000 rpm for 5 minutes, and a cell pellet formed at the bottom of the tube. The supernatant was removed, cells were vortexed with 1 mL of media, and cells were then plated. Cells were passaged by first removing media and adding 0.25% Trypsin (Mediatech, Inc.) for 5-7 minutes to allow the cells to detach from the flask surface. An equal amount of media was added to the trypsin/ cell solution to counteract the toxic effects of trypsin. The trypsin/media solution was centrifuged for 5 minutes at 1,000 rpm, leaving a cell pellet at the bottom of the centrifuge tube. The supernatant was then removed, and remaining cell pellet was vortexed with 1 mL media. To count cells, 20 µL of the original 1 mL cell suspension and 20 µL of Trypan blue dye solution (Sigma) were added to 160 µL of media. 20 µL of the dye solution was added to a hemocytometer, and cells were counted using the hemocytometer grid. Images of cells were taken using an Olympus CKX41 microscope with Q-Imaging Software (*Figure 2.15*). Detailed cell culture protocols are available in *Appendix A-B*.

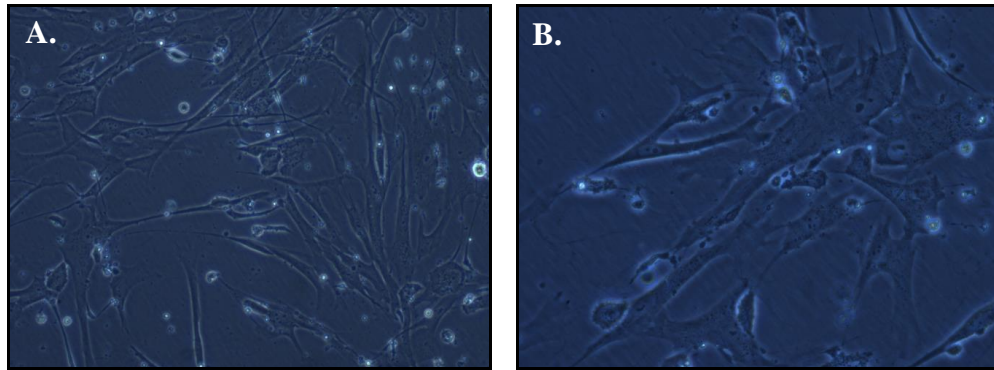


Figure 2.15: Human Aortic Smooth Muscle Cells in culture, passage 5, A. 10X, B. 20X

2.4.2. Immunocytochemistry Staining

Immunocytochemistry staining is performed to stain a specific protein or cellular product using monoclonal primary antibodies that bind to the desired antigen. A fluorescent secondary antibody is then able to bind to the primary antibody to allow for visualization of the stain using a fluorescent microscope. Staining was performed separately for the following primary antibodies: Collagen Type 1 (*Figure 2.18*), alpha-smooth muscle actin (*Figure 2.19*), and alpha-smooth muscle actinin (*Figure 2.20*). Additionally, phalloidin staining was performed to visualize the actin cytoskeleton of the cell using either Alexa Fluor Phalloidin 568 (Invitrogen) or ActinGreen 488 (Life Technologies), (*Figures 2.16- 2.17*). Finally, the nucleus of the cell was stained with DAPI (Invitrogen).

In brief, cells were fixed with a 4% formaldehyde (Sigma), 0.1% glutaraldehyde (Polysciences, Inc.) solution at room temperature for 20 minutes. Cells were permeabilized with a 0.1% Triton X-100 (Sigma) solution at room temperature for 15 minutes. Cells were then blocked in a 2% BSA (Rockland), 3% goat serum (MP Biomedicals) blocking solution at room temperature for 30 minutes. Cells were rinsed 3

times with 1X PBS (Alfa Aesar) between every solution change. Next, the monoclonal primary antibody diluted in the goat serum blocking solution was added and incubated at 4°C overnight. Mouse anti-collagen type 1 (Sigma) was added at a dilution of 1:500, mouse anti-alpha smooth muscle actin (Sigma) was added at a dilution of 1:200, and mouse anti-alpha smooth muscle actinin (Hybridoma Bank) was added at a dilution of 3 µg/mL. The secondary antibody, goat anti-mouse Alexa Fluor 488 (Invitrogen, green) was added at a concentration of 4 µL/mL for 2 hours at room temperature. Alexa Fluor 568 Phalloidin (Invitrogen, red) was added at a concentration of 2.5% in 1X PBS for 20 minutes at room temperature. 300 nM DAPI (Invitrogen, blue) was added for 5 minutes at room temperature. Images were taken using an EVOS fluorescent microscope.

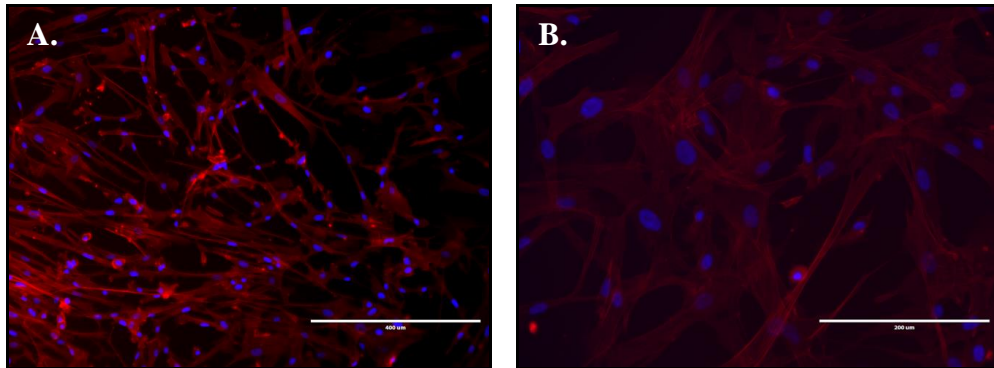


Figure 2.16: ICC staining of VSMCs for cytoskeleton with phalloidin (red) and nuclei with DAPI (blue), A. 10X, B. 20X

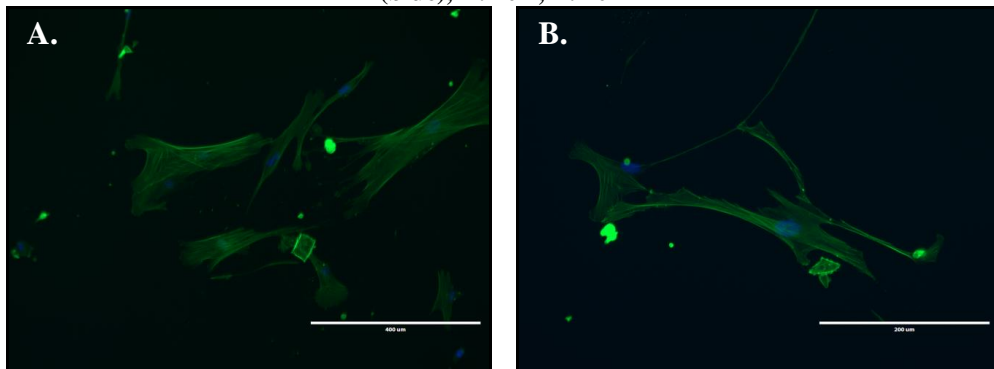


Figure 2.17: ICC staining of VSMCs for cytoskeleton with ActinGreen 488 and nuclei with DAPI (blue), A. 10X, B. 20X

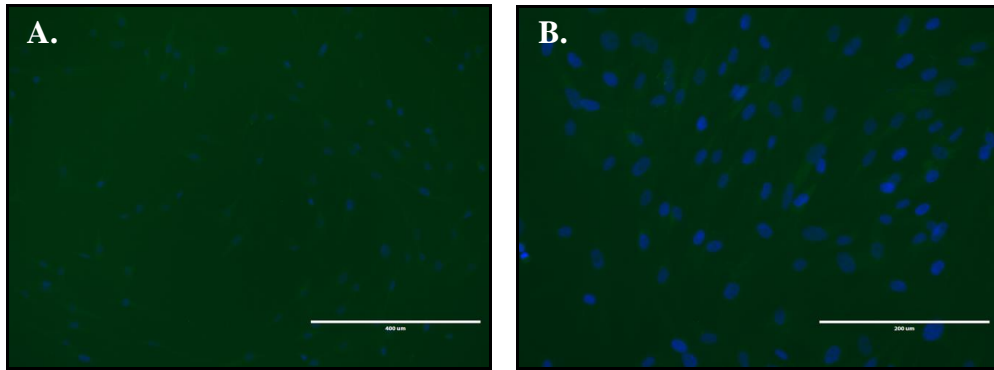


Figure 2.18: ICC staining of VSMCs for Collagen Type 1 (green) and nuclei with DAPI (blue), A. 10X, B. 20X

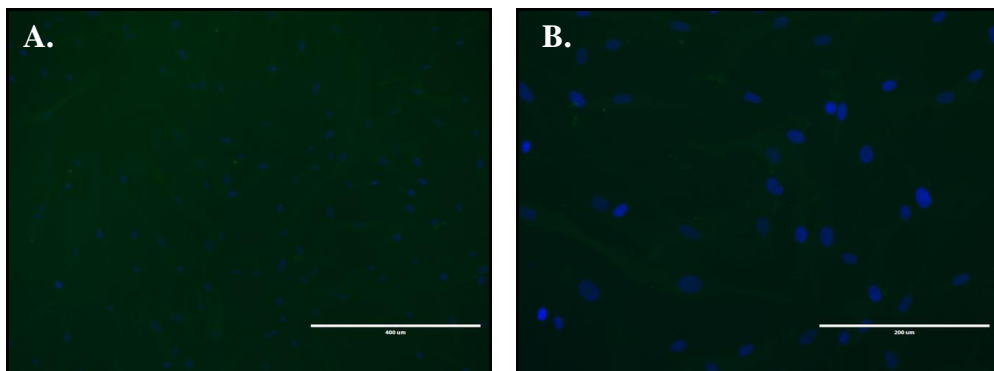


Figure 2.19: ICC staining of VSMCs for alpha-smooth muscle actin (green) and nuclei with DAPI (blue), A. 10X, B. 20X

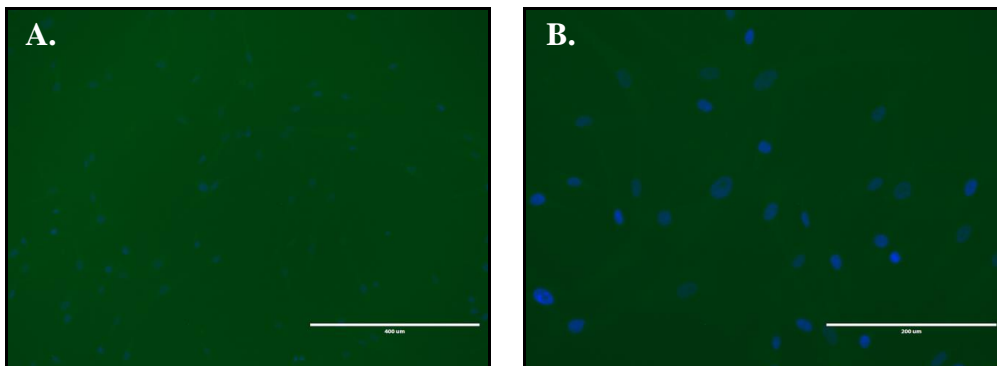


Figure 2.20: ICC staining of VSMCs for alpha-smooth muscle actinin (green) and nuclei with DAPI (blue), A. 10X, B. 20X

2.5 REFERENCES

1. J.A. Eble, *et al.* “The Extracellular Matrix of Blood Vessels.” *Current Pharmaceutical Design*, 15(12): 1385-1400, 2009.
2. M.K. Pugsley, *et al.* “The Vascular System: An overview of Structure and Function.” *Journal of Pharmacological and Toxicological Methods*, 44: 333-340, 2000.
3. S.I. Fox. *Human Physiology*, ed. 14. McGraw-Hill Education, 2016.
4. D. Rogers, *et al.* “Overview of the Vessels Involved in Blood Circulation.” *TeachMeAnatomy, The TeachMe Series*. December 22, 2017.
5. Y. Gao. *Biology of Vascular Smooth Muscle: Vasoconstriction and dilatation*. Springer Nature. 2017.
6. W.D. Tucker, *et al.* “Anatomy, Blood Vessels.” *National Institutes of Health, StatPearls Publishing*. December 15 2017.
7. M.P. McKinley, *et al.* *Human Anatomy*, ed. 4. McGraw-Hill Education, 2015.
8. H. Gray, *et al.* *Gray’s Anatomy: The Anatomical Basis of Clinical Practice*, ed. 41. Elsevier Health Sciences, 2015.
9. B. Alberts, *et al.* “Blood Vessels and Endothelial Cells.” *Molecular Biology of the Cell*, ed. 4. National Institutes of Health, Garland Science, 2002.
10. L.W. Janson, *et al.* “The Cardiovascular System.” *The Big Picture: Medical Biochemistry*. The McGraw-Hill Companies, 2016.
11. P. Lacolley, *et al.* “Vascular Smooth Muscle Cells and Arterial Stiffening: Relevance in Development, Aging, and Disease.” *Physiological Reviews*, 97: 1555-1617, 2017.
12. A.S. Patel, *et al.* “Cardiovascular haemodynamics and shock.” *Surgery*, 27(11): 459-464, 2009.
13. J. Sandham. “Haemodynamics.” *EBME and Clinical Engineering*. May 2011.
14. E.A.V. Jones. “Mechanical factors in the development of the vascular bed.” *Respiratory Physiology & Neurobiology*, 178: 59-65, 2011.

15. "Blood Pressure." *PubMed Health Glossary, National Institute of Diabetes and Digestive and Kidney Diseases*. Web. 2018.
16. L.E. Mantella, *et al.* "Variability in vascular smooth muscle cell stretch-induced responses in 2D culture." *Vascular Cell*, 7(7): 1-9, 2015.
17. B. Thomas, *et al.* "Blood Flow in Human Arterial System-A Review." *Procedia Technology*, 24: 339-346, 2016.
18. R.E. Klabunde. "Laminar Flow." *Cardiovascular Physiology Concepts*. Web. 2018.
19. H.J. Hsieh, *et al.* "Shear-induced endothelial mechanotransduction: The interplay between reactive oxygen species (ROS) and nitric oxide (NO) and the pathophysiological implications." *Journal of Biomedical Science*, 21(3), 2014.
20. M.A. Gimbrone, *et al.* "The Critical Role of Mechanical Forces in Blood Vessel Development, Physiology and Pathology." *Journal of Vascular Surgery*, 29(6):1104-1151, 1999.
21. "Types of Muscle Tissues." *Science Learn, Curious Minds*. Web. June 21, 2007.
22. K.E. Steucke, *et al.* "Vascular smooth muscle cell functional contractility depends on extracellular mechanical properties." *Journal of Biomechanics*, 48(12): 3044-3051, 2015.
23. J. Qiu, *et al.* "Biomechanical regulation of vascular smooth muscle cell functions: from *in vitro* to *in vivo* understanding." *Journal of the Royal Society Interface*, 11, 2014.
24. S. Patel, *et al.* "Characteristics of Coronary Smooth Muscle Cells and Adventitial Fibroblasts." *Circulation*, 101: 524-232, 2000.
25. E. Cairrão, *et al.* "Isolation and culture of human umbilical artery smooth muscle cells expressing functional calcium channels." *In Vitro Cellular and Developmental Biology*, 45: 175-184, 2009.
26. R. Yamin, *et al.* "Deciphering actin cytoskeletal function in the contractile vascular smooth muscle cell." *The Journal of Physiology*, 590(17): 4145-4154, 2012.
27. M. Bond, *et al.* "Dense bodies and actin polarity in vertebrate smooth muscle." *The Journal of Cell Biology*, 95: 403-413, 1982.

28. S.S.M. Rensen, *et al.* "Regulation and characteristics of vascular smooth muscle cell phenotypic diversity." *Netherlands Heart Journal*, 15(3): 100-108, 2007.
29. R.C. Webb. "Smooth Muscle Contraction and Relaxation." *Advances in Physiology Education*, 27(4): 201-206, 2003.
30. "Smooth Muscle." *OpenStaxCollege, Pressbooks*. Web. 2016.
31. E.M. Rzucidlo, *et al.* "Regulation of vascular smooth muscle cell differentiation." *Journal of Vascular Surgery*, 45(25): 25-32, 2007.
32. B.N. David-Dusenbery, *et al.* "Micro-managing vascular smooth muscle cell differentiation and phenotypic modulation." *Arteriosclerosis, Thrombosis, and Vascular Biology*, 31(11): 2370-2377, 2011.
33. A. Huber, *et al.* "Phenotypic changes in cultured smooth muscle cells: Limitation or opportunity for tissue engineering of hollow organs?" *J. Tissue Eng Regen Med*, 6(7): 505-511, 2012.
34. Z. Sun, *et al.* "N-cadherin, A vascular smooth muscle cell-cell adhesion molecule: Function and signaling for vasomotor control." *Microcirculation*, 21: 208-218, 2014.
35. G.K. Owens, *et al.* "Molecular Regulation of Vascular Smooth Muscle Cell Differentiation in Development and Disease." *Physiological Reviews*, 84: 767-801, 2004.
36. O.V. Sazonova, *et al.* "Cell-cell interactions mediate the response of vascular smooth muscle cells to substrate stiffness." *Biophysical Journal*, 101: 622-630, 2011.
37. T.S. Al-Shehabi, *et al.* "Anti-atherosclerotic plants which modulate the phenotype of vascular smooth muscle cells." *Phytomedicine*, 23: 1068-1081, 2016.
38. "Heart Disease: Scope and Impact." *The Heart Foundation*. Web. 2018.
39. D.M. Milewicz, *et al.* "Genetic variants promoting smooth muscle cell proliferation can result in diffuse and diverse vascular diseases: Evidence for a hyperplastic vasculomyopathy." *Genetics in Medicine*, 12(4): 196-203, 2010.

CHAPTER THREE

MICROPATTERNING TECHNIQUES AND CELLULAR RESPONSES

3.1 MICROPATTERNING TECHNIQUES

3.1.1 Microfabrication

Microfabrication is the process of manufacturing structures on the micrometer scale, allowing for precision and incredible detail¹. Originally used in microelectronic applications, microfabrication techniques have since been adapted to create systems and structures used in biological and cellular studies^{1,2}. Using micro-electromechanical systems (MEMS) in combination with biological and molecular elements allows for developments such as biomolecular sensors that are able to recognize and respond to chemical changes, cell-based assays, and controlled drug delivery devices that release therapeutic drugs based on environmental signals^{1,2}.

3.1.2 Micropatterning

Micropatterning is a microfabrication technique specifically focused on the controlled localization of biomolecules to create a patterned substrate for cell adhesion^{1,3}. The first cell patterning took place in the 1960's by S.B. Carter's lab, with the intent of manipulating cellular environments to perform more controlled experiments in studying cell motility^{4,5}. The general purpose of micropatterning is to develop a local microenvironment that promotes cell adhesion in a desired geometry¹. Cell behavior is guided by elements of the surrounding environment: the substrate material, extracellular matrix proteins, and even neighboring cells¹. These chemical, biological, and physical

parameters alter internal cell signaling pathways, influencing the resulting cellular responses⁶. Therefore, guiding cells into a particular orientation or pattern allows for the manipulation of cellular processes and interactions⁶.

Micropatterning is beneficial in that it enables studies on cellular interactions with their environment¹. Patterned configurations can represent various environmental conditions, which allows for analysis of single-cell, multi-cell, and *in vivo*-like configurations¹. Single cell micropatterning offers insights to cytoskeletal and organelle organization, individual cellular processes, and even cell-cell communication³. Additionally, micropatterning allows microscale studies on cellular behavior and cell-cell interactions with limited external factors. Successful micropatterning is characterized not only by cell adhesion onto the patterned biomolecule, but also by minimal cell adhesion on the non-patterned surface³. A variety of micropatterning techniques, including photolithography and soft lithography, are employed to create a desired two-dimensional cellular microenvironment. It should be noted that due to constraints and requirements, substrate, biomolecule, and cell type choices must be optimized for their specific application, as there is no universal protocol³.

3.1.3 Photolithography

Photolithography is a process used to transfer images from a photomask to a rigid surface using UV light exposure². A photomask is a transparent sheet made of glass or plastic, with high resolution patterns represented by the opaque and transparent regions². During photolithography, geometric patterns are transferred to a silicon wafer serving as the master to form topographical features from a photoresist polymer (*Figure 3.1*)¹. First,

a light sensitive photoresist polymer is spin-coated onto the wafer¹. The wafer is baked to allow for hardening of the photoresist. To transfer the pattern, the wafer is exposed to UV light through the transparent regions of photomask, allowing select patterns to be irradiated^{1,2}. The photoresist-covered wafer is baked again and undergoes a development process to remove excess photoresist¹. The photoresist will either become soluble or insoluble after being illuminated with UV light⁶. Positive photoresist becomes soluble when exposed to UV light and can be removed with photoresist developer, leaving structures representative of the transparent pattern of the photomask². Conversely, negative photoresist becomes crosslinked and insoluble upon exposure to UV light, remaining as raised structures on the wafer as the photoresist developer removes the unexposed photoresist and producing the inverse of the photomask pattern². The most widely used photoresist in photolithography applications is SU-8, a negative photoresist, by MicroChem Corporation². An advantage of using photolithography is that high resolution patterns can be achieved, and patterned silicon wafers can be stored long-term^{2,6}. However, photolithography requires expensive materials as well as processing in a clean room environment^{2,6}.

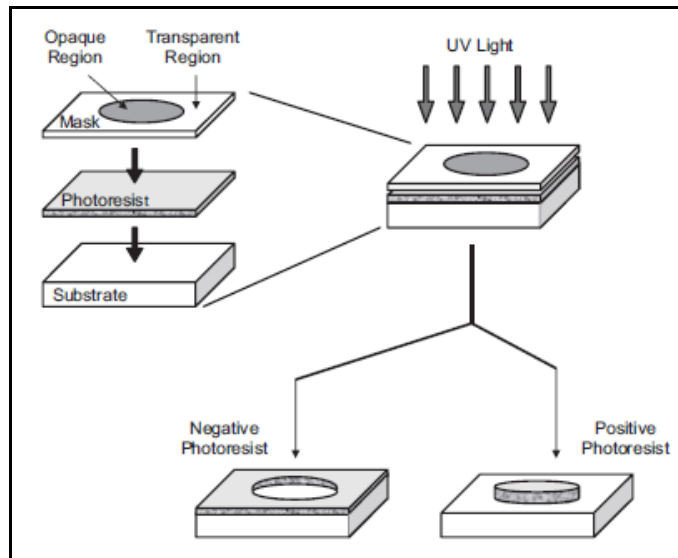


Figure 3.1: Process of photolithography to create a master silicon wafer for both positive and negative photoresists²

3.1.4 Soft Lithography

Adapted from photolithography, soft lithography is a process that uses an elastomeric, or “soft”, material to transfer patterns to a surface². Generally, an elastic stamp or mold is created from a master silicon wafer produced by photolithography. An elastomeric polymer is cast over the master wafer, is cured or hardened, and the desired stamps can then be removed from the master¹. PDMS, or poly(dimethyl)-siloxane, is the most commonly used polymer to make elastomeric stamps, molds, and stencils, although other siloxanes can also be used¹. PDMS is hydrophobic, transparent, biocompatible, and possesses good thermal and mechanical characteristics. PDMS is low cost and easy to use, making it a strong stamp material choice^{5,7}. The stamps or molds can then be used to pattern biomolecules onto a receiving surface⁶. The three most commonly used soft lithography techniques are microstamping, microfluidic patterning, and stencil patterning (Figure 3.2)².

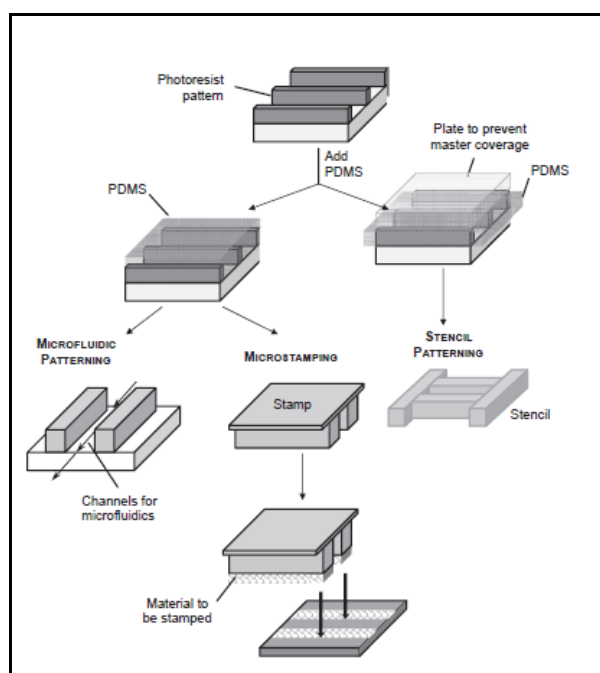


Figure 3.2: Soft lithography techniques: microfluidic patterning, microstamping, and stencil patterning²

3.1.5 Microstamping

Microstamping, or micro-contact printing (μ CP), is the most commonly used micropatterning method for cell patterning applications¹. Microstamping is based on the contact-transfer of biomolecules or organic molecules from stamps onto a receiving surface². Biomolecules are first “inked” onto the surface of a PDMS stamp and are then “stamped” or “printed” onto the receiving surface through the process of surface adsorption^{2,6}. A “backfilling” procedure can be performed to restrict cell adhesion to the pattern and reduce cell spreading (*Figure 3.3*)¹. Backfilling prevents protein absorption by modifying the surface chemistry of the substrate through the addition of a molecule or chemical to become non-reactive. Advantages of microstamping are ease of use, low cost, and the ability to customize and reuse stamps¹. Limitations of this method are pattern size constraints as well as the tendency for cell spreading despite backfilling³.

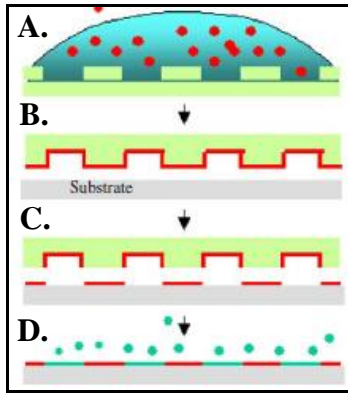


Figure 3.3: Steps of microstamping: A, “Inking”, B, “Stamping”, C. Stamp removal, and D. Backfilling [modified from ref. 1]

3.1.6 Microfluidic Patterning

Microfluidic patterning uses a PDMS mold with microchannels to form the desired pattern². The mold is created from a master wafer to create a substrate with microchannels¹. The mold adheres to the receiving surface due to the self-sealing properties of PDMS, and a biomolecule solution is flooded into the mold, with capillary forces drawing the solution through the channels^{5,6}. The biomolecules will form a pattern in the regions where the PDMS substrate does not contact the surface (*Figure 3.4*)¹. An advantage of this method is that parallel microchannels allow for patterning of several biomolecules simultaneously, enabling complex studies on cellular interactions with varied molecules¹. However, patterns are limited to open network, continuous geometries which must be large enough to allow for fluid flow underneath the mold^{2,6}.

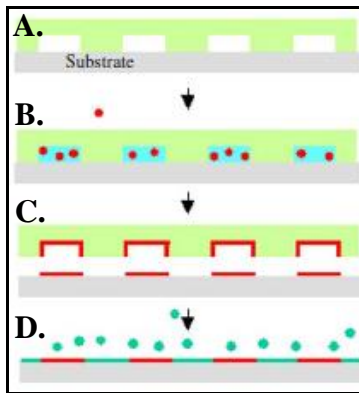


Figure 3.4: Steps of microfluidic patterning: A. Mold placed on substrate, B. Biomolecules flow through microchannels of the mold, C. Mold removal, D. Backfilling [modified from ref. 1]

3.1.7 Stencil Patterning

Stencil patterning uses a template or stencil so that cells can be seeded directly onto the receiving surface in the desired pattern⁵. PDMS stencils can be produced from a master wafer, with the pattern representing the inverse of the master⁸. Laser ablation can be used to create precise geometric stencils from a polymer film⁹. Generally the stencil is placed onto the substrate, cells are seeded, and the stencils are removed once cells have adhered to the surface⁹. An alternative method is plasma stenciling, which is based on surface activation to produce hydrophilic, cell-adhesive regions¹⁰. Plasma stenciling employs a PDMS stencil to direct plasma activation of the substrate surface, creating the hydrophilic regions for preferential cell adhesion¹⁰. Stencil patterning has been shown to produce more controlled, localized patterns of cell alignment compared to other micropatterning techniques⁹. Advantages of this method include ease of use, stencil biocompatibility, and a range of possible pattern designs⁸. Additionally, cells can be directly seeded onto the substrate without a protein pattern or backfilling procedure.

3.1.8 Considerations for Soft Lithography

“Backfilling” is an additional process used to prevent cells from adhering to the background regions of a micropatterned surface¹. After biomolecules are patterned and the remaining surface is backfilled, cells can be plated onto the substrate. Backfilling is achieved by using nontoxic, anti-adhesive molecules, such as Pluronics, to reduce unwanted cell adhesion and spreading¹¹. Pluronics are triblock surfactants that prevent protein adsorption on a hydrophobic surface¹². ECM protein patterns can become compromised when exposed to cells in a culture medium¹³. Proteins in the culture medium adsorb to a substrate surface, allowing non-specific cell adhesion and rendering the patterned proteins irrelevant^{13,14}. Further, a study showed that culturing cells on collagen results in increased cell spreading due to cell-ECM interactions, confirming the necessity of a more effective anti-adhesive method¹². Pluronics mitigate this issue by preventing both protein adsorption and cell adhesion on non-patterned hydrophobic surfaces¹². Pluronics are commonly used because they are effective and low cost, although they might require additional surface chemistry procedures and are only stable for short-term storage³.

Soft lithography is an advantageous process because of its immense flexibility in substrate and molecule selections. Many molecules can be patterned, including extracellular matrix proteins (collagen, laminin, fibronectin), peptides, polysaccharides, lipids, and antibodies². Additionally, stamps and molds are reusable, easy to produce, and less expensive than photolithography methods¹. However, most soft lithography methods still require a master produced by photolithography². There are size and resolution

constraints depending on the method used, as well as limited pattern geometries¹. Depending on the cell type, cells are capable of attaching to backfilled or passivated regions of the substrate, although in lower quantities than in the protein-covered patterns³. Cells are also able to detach from protein patterns, thus remodeling or degrading the protein pattern. Overall, optimization of soft lithography methods is required for successful patterning based on experimental specifications³.

3.2 THE EXTRACELLULAR MATRIX AND CELLULAR RESPONSES

3.2.1 Cellular Microenvironments and the Role of the Extracellular Matrix

The microenvironment of a cell is imperative for regulation and homeostasis of cellular processes: cells sense and respond to the signals in their environment^{7,15}. The extracellular matrix (ECM) forms the non-cellular, structural framework on which cells adhere and establish tissue organization^{7,15}. The ECM has both physical characteristics (topographical features, mechanical stiffness) and molecular organization (ECM protein composition) that provide signaling cues to cells⁷. ECM proteins have both nanometer and micron-level structures that influence various aspects of cellular behavior¹⁶. Contact guidance describes the phenomenon in which cells respond to the external signals received from interactions with the ECM¹⁶.

Common fibrous ECM proteins are collagen, elastin, laminin, and fibronectin; each contributes to specific cellular behaviors¹⁷. Collagen is the most abundant ECM protein in the body, and it is important in providing structural support¹⁸. Collagen fibers are highly organized, with a triple helix of collagen molecules forming the fibrils that are

intertwined to form functional fibers¹⁸. Collagen provides tensile strength throughout tissues, and it plays a role in regulating cell adhesion and migration¹⁵. Elastin provides elastic recoil in tissues that experience constant deformation, allowing tissues to stretch and recover without permanent damage or impairment^{15,18}. Fibronectin is an adhesive protein that not only organizes the matrix but also enables cell adhesion and attachment^{15,18}. Laminin is a fibrous protein important in connecting the plasma membrane to the surrounding ECM network, facilitating cell signaling¹⁹.

3.2.2 Cellular Responses to Micropatterning

Micropatterning allows for precise construction of an extracellular matrix that mimics the native microenvironment⁷. Replicating the unique structure of a cell's ECM facilitates studies on the interactions between a cell and its environment, providing insight on cell behaviors, cell mechanics, and the internal cell processes of apoptosis and division⁷. Most cells, including vascular smooth muscle cells, are anchorage-dependent, requiring attachment to either an ECM surface or neighboring cells for survival⁷. Thus, it is important to understand how cells are affected by the contact guidance provided by the ECM.

Cell alignment is defined as the spatial arrangement of cells, and it affects many cellular functions including cell morphology, adhesion, migration, and proliferation¹³. Micropatterning allows for customized cell alignment. Depending on anatomical location and orientation, a specific pattern is chosen to construct an *in vivo*-like microenvironment⁷. For example, parallel lines mimic vascular smooth muscle cell alignment, while a diamond or lattice pattern provides a more natural arrangement for

cardiomyocytes and cardiac fibroblasts²⁰. Integrins are a cellular structure important in cell-ECM interactions, and the arrangement of the ECM influences the distribution of integrins throughout the cell⁷. Integrin quantity and placement can alter the organization of cytoskeletal elements, leading to overall changes in the morphology and structure of the cell⁷. A trend exhibited in many studies is that cells aligned on grooved topographies orient themselves in the direction of the groove, exhibiting an elongated phenotype due to altered microtubule and microfilament organization²¹.

Cell migration is almost entirely dependent on signals from the environment: a motogen induces cell migration to occur in a particular direction. ECM patterns can direct cell migration by changing the orientation of the internal cytoskeleton and motility structures⁷. Many cell types patterned in grooves or lines have displayed migration in the direction of alignment, along with increased migration rates¹⁶. Cell proliferation refers to the rate of increase of cell number. A trend seen in patterned cells is a decrease in proliferation rates, perhaps due to cytoskeletal structure or phenotype changes^{13,16}. Additionally, patterning has been shown to alter gene expression, which can be used to manipulate cell differentiation¹⁶. It should be noted that cellular responses depend on many factors, including the size and geometry of ECM features as well as the cell type itself.

3.3 RESPONSE OF VASCULAR SMOOTH MUSCLE CELLS TO MICROPATTERNING

3.3.1 Native Microenvironments of Vascular Smooth Muscle Cells

In a native blood vessel, vascular smooth muscle cells are circumferentially oriented in the tunica media layer¹³. VSMCs are surrounded by a dense ECM network composed of collagen fibers and helical bands of elastin (*Figure 3.5*)¹³. VSMCs are highly organized, and although they exhibit phenotype plasticity, they typically display a contractile phenotype with an elongated morphology²². In a healthy blood vessel, the contractile phenotype is associated with low proliferation rates²². The mechanical forces associated with blood flow induce the alignment of vascular smooth muscle cells as blood vessels form during angiogenesis¹³. The arrangement of VSMCs reflects their contractile function: the circumferential alignment allows for maximal contraction and relaxation with minimal fatigue¹³. It is likely that the native microenvironment, ECM arrangement, and tightly packed circumferential alignment of surrounding VSMCs enforces the contractile phenotype in a healthy vascular system^{23,24}.

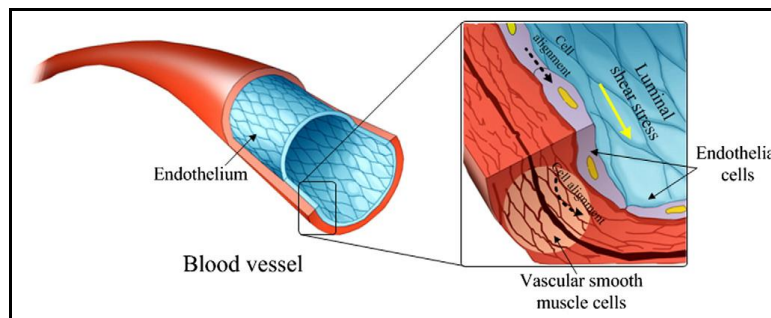


Figure 3.5: VSMC circumferential alignment in a blood vessel [modified from ref. 13]

3.3.2 Motivation for Micropatterning Vascular Smooth Muscle Cells

The majority of VSMCs *in vitro* display a synthetic phenotype, with random organization and minimal alignment²³. Additionally, the synthetic phenotype becomes more prevalent at higher passage numbers²³. VSMCs at a higher seeding density are capable of switching to a contractile phenotype²⁵. Understanding ECM-cell and cell-cell interactions in a micropatterned environment is important in regulating VSMC phenotype²⁵. Micropatterning can be used as a method to control VSMC phenotype by mimicking an *in vivo* environment²⁶. This will allow for more controlled and uniform studies, as the two phenotypes are associated with two different sets of functions that could significantly affect experimental results²². Micropatterning methods can be used to explore how VSMC phenotypes and cell behaviors can be manipulated and maintained. This is essential in studying cell biology, disease states and progression, as well as in blood vessel tissue engineering applications²³. Understanding how to promote phenotypes is important in establishing more controlled and accurate studies of vascular smooth muscle cells.

3.3.3 Responses of Vascular Smooth Muscle Cells to Micropatterning

Despite a variety of micropatterning methods and specifications, there are several established trends noticed in micropatterned vascular smooth muscle cells. Micropatterning VSMCs has been shown to regulate cell morphology and shape, proliferation rates, phenotypic display, and cell spreading. Generally, micropatterning induces a more *in vivo*-like phenotype in VSMCs. VSMCs become more elongated, possibly due to the alignment mimicking their native environment²³. Proliferation rates

also decrease, possibly due to the limited ability to spread in the patterned environment²². Overall, the topography of the micropatterned surface can promote cell alignment and regulate many cellular functions. Studies have shown that patterning onto topographical grooves elicits the same response as micropatterned ECM proteins, suggesting the physical structures of the environment are responsible for phenotype changes in VSMCs. However, ECM proteins provide both physical and chemical cues that might enhance these phenotypic trends. *Table 3.1* summarizes several studies investigating responses of vascular smooth muscle cells to micropatterning.

Table 3.1: Summary of Vascular Smooth Muscle Cell Micropatterning Studies

Author	Cell Type	Patterning Method	Specifications	Results
²² Thakar, et al. 2003	Bovine aortic SMCs	Microfluidic patterning	20 µm collagen lanes	Decreased cell shape index, spreading area, and proliferation rates
²³ Williams, et al. 2011	Rabbit common carotid SMCs	Microcontact printing	20 µm comb polymer lanes	Decreased cell shape index, increased elongation and alignment
²⁵ Cao, et al. 2010	Human aortic SMCs	Microchannel Scaffolds	300 µm wide microchannels	Decreased ECM protein production, increased contractile protein expression
²⁴ Goessl, et al. 2000	Rat vascular SMCs	Plasma Lithography	5 x 5 µm ² to 60 X 60 µm ² squares	Maintained cell alignment, control of cell shape and size
²⁷ Thakar, et al. 2009	Human aortic SMCs	Microcontact printing	10 µm fibronectin lanes	Elongated morphology, decreased cell shape index, cell spreading, and proliferation rates
²⁸ Shen, et al. 2006	Rat aortic SMCs	Micro-patterning of polymeric grooves	40- 160 µm microchannels	Spindle-shape morphology, increased contractile protein expression and alignment

3.4 METHODS, RESULTS, DISCUSSION, AND FUTURE IMPROVEMENTS

The following section includes the methods and results for each step of the micropatterning process. A photomask was designed, which was used in photolithography to fabricate a master wafer. The master was then used in soft lithography processes to create stamps and molds. Three micropatterning processes were implemented: microstamping, microfluidic patterning, and stencil patterning. Results for each method are discussed, and recommendations for future improvements are included.

3.4.1. Photomask Design

A photomask was designed using SolidWorks and was produced on high resolution transparency film by CAD/Art Services. Several design factors were considered when designing the photomask, including master wafer and stamp size requirements, as well as pattern sizes and geometries dictated by the vascular smooth muscle cell type. Eleven stamp designs were produced on the photomask, and they were arranged in a circular layout with a diameter less than 7 cm to fit onto the silicon wafer during photolithography (*Figure 3.6*). The outer dimensions of each stamp design were set as 6 X 6 mm in order to fit into the 8 X 8 mm area of the cell stretcher well plates. Five patterns were parallel lines, and six patterns were diamonds. All lines were spaced 300 μm apart to ensure sufficient spacing for cell alignment and to prevent cell crossover. Parallel lines were designed with varying widths: 10, 30, 50, 100, and 300 μm . Diamonds were designed with varied widths (30 or 100 μm) and angles of intersection (45°, 60°, and 90°). A legend of the photomask stamp designs along with the final proof is available in *Appendix K*.

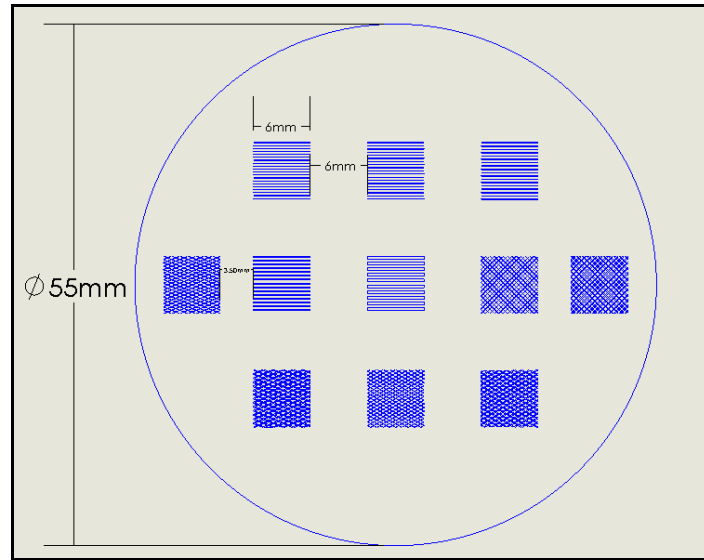


Figure 3.6: SolidWorks drawing of photomask with eleven stamp designs

3.4.2. Photolithography

Photolithography was used to fabricate the master wafer by transferring the patterns on the photomask to a photoresist-covered wafer using UV light exposure. Photolithography was performed in a clean room environment. In brief, a silicon wafer (University Wafer) was preheated on a hot plate at 95°C for 5 minutes, cleaned with isopropyl alcohol (IPA), and blown dry with nitrogen gas. The silicon wafer was placed on a spin-coater, and the vacuum was turned on to hold the wafer in place. SU-8 photoresist (MicroChem Corp.) was added to the center of the wafer in an even layer. The photoresist was spin-coated onto the wafer at 500 rpm for 10 seconds, 3,000 rpm for 30 seconds, and 500 rpm for 10 seconds to produce a photoresist thickness of 5 μm . The photoresist-coated wafer was soft baked at 95°C for 2 minutes. The UV controller and mask aligner were powered on, and the UV arc lamp was allowed to warm up for 10 minutes. The UV exposure system was calibrated, and the intensity and exposure time were set on the UV controller. The photomask and wafer were placed into the mask

holder of the UV exposure system, which was secured in place. The wafer was exposed to UV light for a specified amount of time, baked at 95°C for 3 minutes, and allowed to cool. The photoresist was developed by rinsing the wafer with SU-8 developer (MicroChem Corp.). The wafer was rinsed with IPA, alternating between developer and IPA until excess photoresist was removed. Finally, the wafer was hard baked at 150°C for 30 minutes to crosslink the remaining photoresist features. *Appendix F* describes the full protocol of using photolithography to fabricate the master wafer.

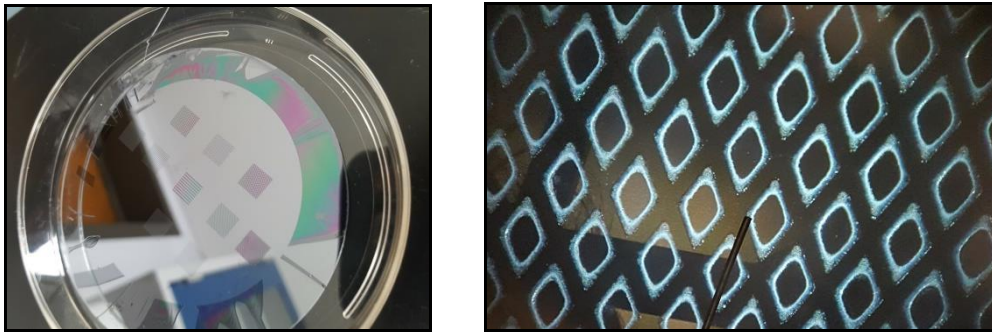


Figure 3.7: Photolithography results, A. Master silicon wafer, B. Diamond microstructures on wafer

The photolithography process was successful at transferring the stamp patterns onto the silicon wafer. *Figure 3.7B* shows the diamond microfeatures of the photoresist on the wafer.

3.4.3. Soft Lithography

Before stamp fabrication, the master wafer was silanized. 50 μL of octyl(trichlorosilane) was added to a petri dish and placed inside a vacuum desiccator along with the master. The vacuum to the dessicator was applied for 20 minutes, and the master was stored in the desiccator overnight. To fabricate stamps, PDMS was prepared by mixing a Sylgard 184 base and curing agent in a 10:1 ratio for 10 minutes. The mixed

polymer was cast over the master in a petri dish and placed in a desiccator for 10 minutes to remove air bubbles. The master was baked on a hot plate for 1 hour at 70°C to allow the PDMS to fully harden. The PDMS was allowed to cool and was carefully removed from the petri dish and master wafer using a scalpel. The individual stamps were then cut from the PDMS sheet and stored pattern side-up (*Figure 3.8, 3.9, and 3.10*).

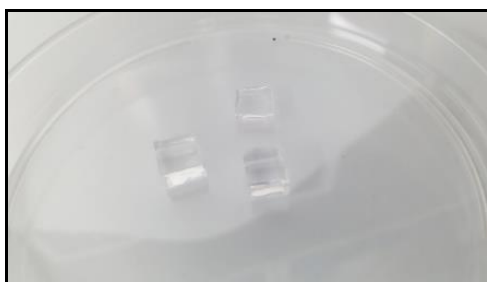


Figure 3.8: PDMS stamps

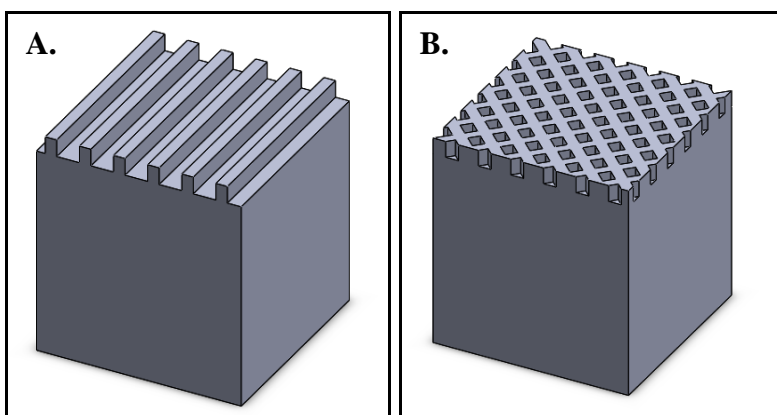
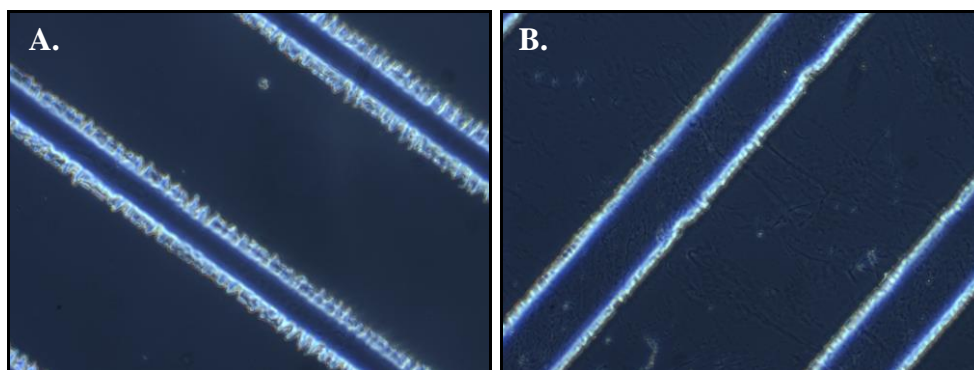


Figure 3.9: Schematic of PDMS stamps, A. Line pattern, B. Diamond pattern (not shown to scale)



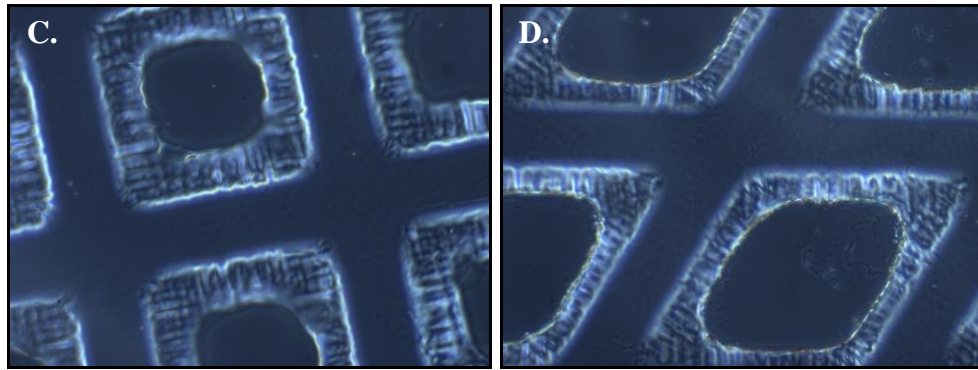


Figure 3.10: Microstructures on PDMS stamps, A. 30 μm lines, B. 100 μm lines, C. 100 μm , 90° diamonds, D. 100 μm 45° diamonds (10X)

PDMS stamps with handles were fabricated for ease of use in patterning. 2 X 2 X 20 mm handles were designed in SolidWorks and 3D printed at the Watt Center MakerSpace. A compatible stamp holder was printed to hold the stamps with handles upside-down during the “inking” process of microstamping. A thin layer of PDMS was cast over the master and allowed to cure. Another layer of PDMS was cast over the initial layer, and the handles were arranged on top of the master patterns. The second layer of PDMS was allowed to cure, and the individual stamps were cut out. While some handles were aligned, it was difficult to accurately position the handles directly above each pattern. Additionally, handles did not stand upright in the liquid PDMS, and thus did not dry completely upright. As a result, stamping was inefficient due to the unequal contact of the stamp to the surface. Efforts to attach handles to the PDMS stamps separately included hot glue, super glue, and liquid PDMS, but all were unsuccessful at providing a secure, durable attachment for both sterilization and stamping procedures. In the future, a system that directly aligns and holds the handles in place above the wafer would be effective in positioning the handles in the PDMS. Handles would allow for easier handling of stamps during the stamping process (*Figures 3.11, 3.12, and 3.13*).



Figure 3.11: 3D-printed stamp handles

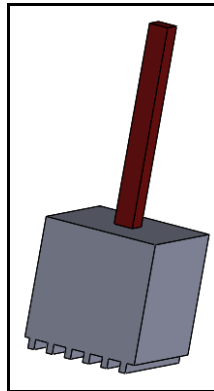


Figure 3.12: Schematic of stamp with attached 3D-printed handle (not shown to scale)

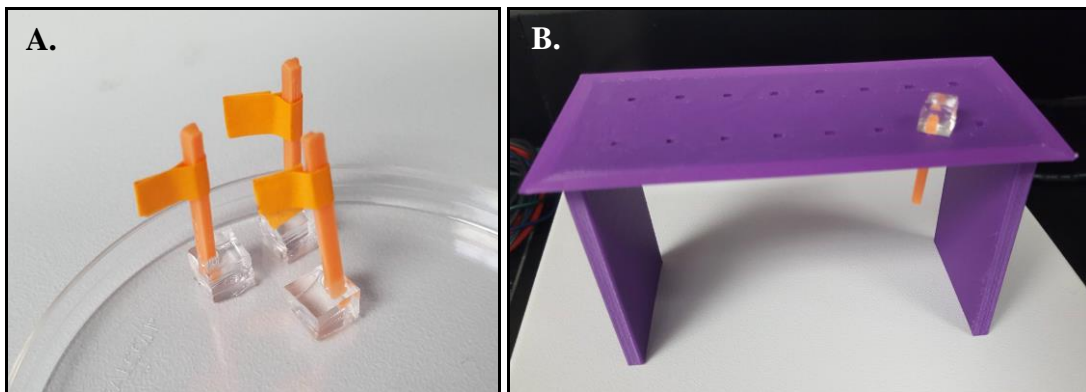


Figure 3.13: PDMS stamps with handles, A. Stamp and handle assembly, B. Stamp holder

3.4.4. Microstamping

Successful microstamping was achieved through optimization of various parameters, including the duration of “inking” and “stamping”, method of collagen removal after “inking”, drying of collagen, substrate materials, and weight applied to the

stamp. A successful protocol is described in *Appendix H* and is summarized here. PDMS stamps were sterilized in 100% ethanol and sonicated for 15 minutes in an ultrasonic cleaner (VWR International). Stamps were rinsed with ethanol and allowed to dry. Stamps were “inked” for 1 hour by adding 100 μ L of 100 μ g/mL collagen to the patterned side of the stamp. At the same time, the stamping substrate, either the silicone-based well plate for the cell stretcher or a PDMS gel, was placed in a UV-ozone chamber for 15 minutes. The collagen was removed from the stamp, and the stamp was rinsed twice with 1X PBS and allowed to dry completely. The rinse and dry method produced better collagen edges with minimal distortion compared to drying the collagen with a nitrogen gun. The stamps were then placed onto the stamping substrate for 30 minutes. Best results were seen when only the edges of the stamp were pressed gently with tweezers to ensure initial contact, with no additional pressure placed on the stamp (*Figure 3.14*). Images of collagen patterns were taken using an Olympus CKX41 microscope. Images of unsuccessful stamping trials are in *Appendix L*.

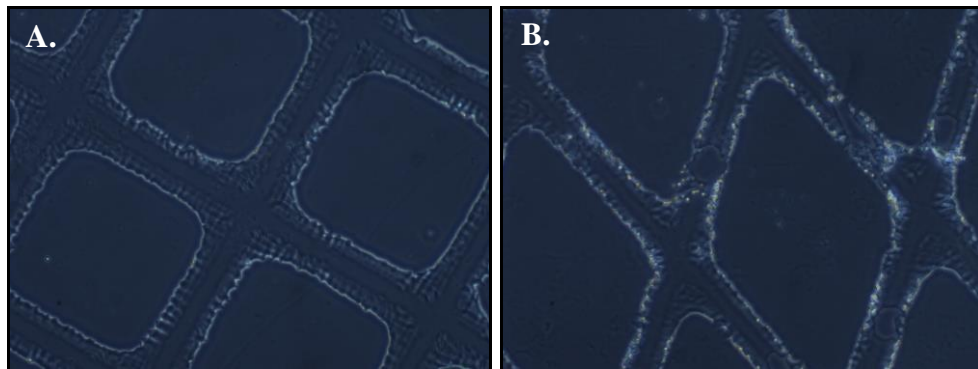
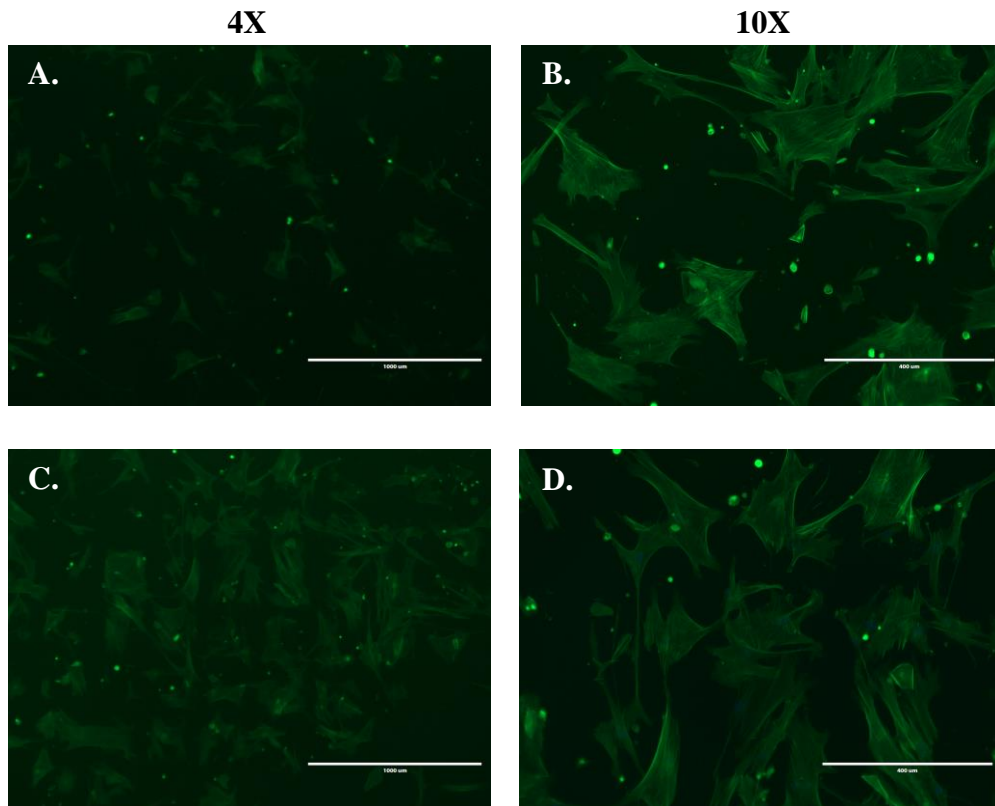


Figure 3.14: Successful collagen microstamping on PDMS gel, A. 90°, B. 60° diamonds (10X)

3.4.5 Pluronic Solutions to Eliminate Non-Specific VSMC Adhesion

A Pluronic solution was employed to promote cell adhesion specifically on the collagen while reducing cell spreading off of the pattern. A 1% Pluronic-125 (Sigma) solution was made in millipore water. The Pluronic solution was added either before or after microstamping and was incubated at room temperature for 1 hour. The surface was rinsed 3 times with 1X PBS. VSMCs were plated and incubated for 24 hours. VSMCs were fixed in a 4% formaldehyde (Sigma), 0.1% glutaraldehyde (Polysciences, Inc.) solution for 20 minutes, followed by a 0.1% Triton X-100 (Sigma) solution for 15 minutes to permeabilize the cells. ActinGreen 488 (Life Technologies) was added for 30 minutes to stain the cytoskeleton, and 300 nM DAPI (Invitrogen) was added for 5 minutes to stain the nuclei.



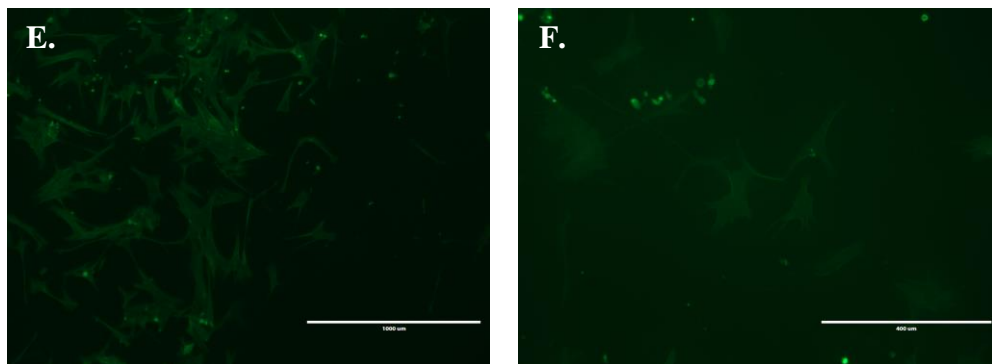


Figure 3.15: Microstamped collagen with Pluronic solution, A, B. Control, C, D. Pluronic added before stamping, E, F. Pluronic added after stamping

Figure 3.15 A-B show the control VSMCs randomly oriented with no preferential attachment to the collagen pattern. When the Pluronic solution was added before microstamping, the collagen pattern was preserved (*Figure 3.15 C-D*). Significant cell spreading and overlapping of lanes still occurred. When the Pluronic solution was added after microstamping, it possibly altered the collagen pattern, leaving groupings of cell adhesion (*Figure 3.15 E-F*). The addition of the Pluronic solution did decrease cell adhesion directly to the petri dish, although there was still some undesired cell spreading. The Pluronic solution did not promote cell alignment onto the pattern significantly compared to the control. Overall, the Pluronic solution did not provide the parallel cell alignment desired.

3.4.6 Microfluidic Patterning

PDMS stamps with parallel lines used for microstamping were modified to have open channels on two opposite sides, thus forming a mold with microchannels (*Figure 3.16*). The molds were placed pattern-down onto a petri dish so the pattern made direct contact with the substrate, leaving 300 μm gaps. A cell suspension was then flooded through the channels to promote cell adhesion along the open surface left by the

microchannels. Cells did adhere to the petri dish, but not many cells were able to travel through the microchannels. It is possible that the height of the mold was not tall enough to allow for proper fluid flow through the microchannels, or that the cell suspension was not properly flushed through the channels. In the future, a mold with taller features would likely be more successful at aligning cells, which could be achieved by molding PDMS to a master with taller photoresist features.

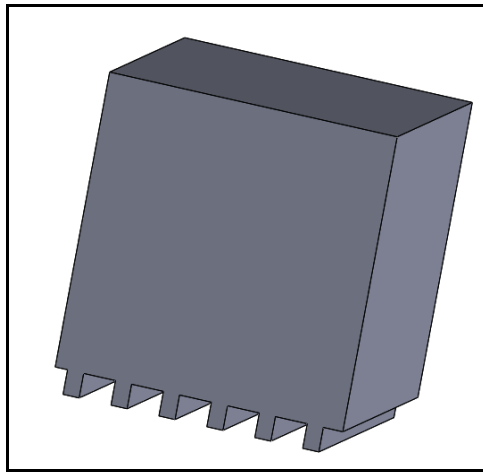


Figure 3.16: Schematic of microfluidic patterning mold (not shown to scale)

3.4.7 Stencil Patterning

The next type of micropatterning attempted was stencil patterning. As a proof of concept, 7 X 7 mm stencils were cut from a cured PDMS sheet approximately 2 mm thick. Two 1-mm channels were cut to form the negative space of the stencil (*Figure 3.17*). Stencils were firmly pressed against a petri dish surface, and cells were seeded and allowed to incubate for 24 hours. Cells were fixed, permeabilized, and stained with Alexa Fluor 568 Phalloidin (Thermo Fisher Scientific) for the cytoskeleton and DAPI (Invitrogen) for the nuclei.

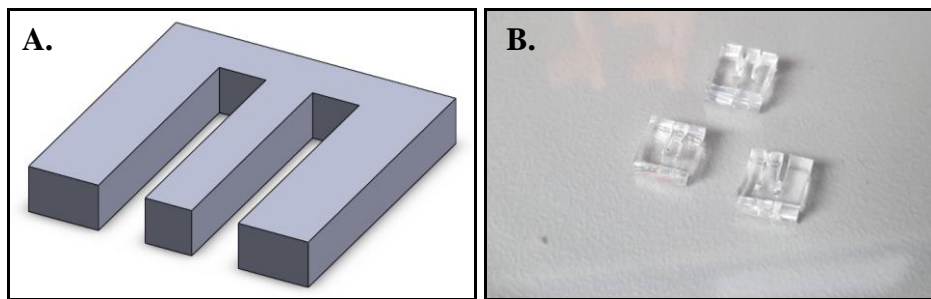


Figure 3.17: Stencils: A, Schematic of stencil patterning stencil template (not drawn to scale), B. PDMS stencils

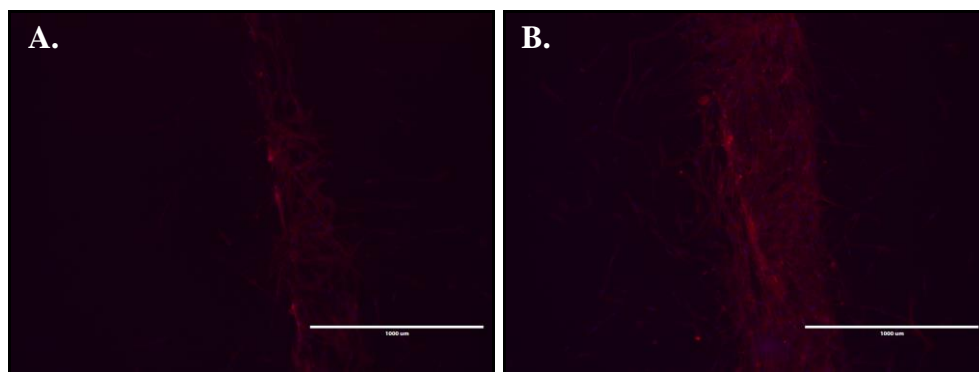


Figure 3.18: A, B. Stencil patterning of VSMCs stained with Phalloidin (red) and DAPI (blue) (4X)

Stencil patterning was successful in aligning VSMCs. Cells adhered to the negative space of the stencil, although there was some cell spreading underneath the stencil (*Figure 3.18*). This could be improved by more precisely fabricating the stencils to have completely flat surfaces. Stencil patterning onto the silicone surfaces seemed to be the most effective micropatterning method for VSMC alignment.

3.5 REFERENCES

1. D. Falconnet, *et al.* "Surface engineering approaches to micropattern surfaces for cell-based assays." *Biomaterials*, 27: 3044-3063, 2005.
2. T. Betancourt, *et al.* "Micro-and nanofabrication methods in nanotechnological medical and pharmaceutical devices." *International Journal of Nanomedicine*, 1(4): 483-495, 2006.
3. J. Fink, *et al.* "Comparative study and improvement of current cell micro-patterning techniques." *Lab on a Chip*, 7: 672-680, 2007.
4. S.B. Carter. "Principles of cell motility: The direction of cell movement and cancer invasion." *Nature*, 208(5016): 1183-1187, 1965.
5. A. Folch, *et al.* "Microengineering of Cellular Interactions." *Annual Review of Biomedical Engineering*, 2: 227-256, 2000.
6. C.A. Goubko, *et al.* "Patterning multiple cell types in co-cultures: A review." *Materials Science and Engineering C*, 29: 1855-1868, 2009.
7. M. Nikkhah, *et al.* "Engineering microscale topographies to control the cell-substrate interface." *Biomaterials*, 33: 5230-5246, 2012.
8. J. Wu, *et al.* "Patterning cell using Si-stencil for high-throughput assay." *RSC Advances*, 1: 746-750, 2011.
9. J.J. Messner, *et al.* "Laser-fabricated cell patterning stencil for single cell analysis." *BMC Biotechnology*, 17(89), 2017.
10. J.P. Frimat, *et al.* "Plasma stencilling methods for cell patterning." *Analytical and Bioanalytical Chemistry*, 395: 601-609, 2009.
11. J.L. Tan, *et al.* "Simple Approach to Micropattern Cells on Common Culture Substrates by Tuning Substrate Wettability." *Tissue Engineering*, 10(5): 865-872, 2004.
12. J.M. Corey, *et al.* "Patterning N-type and S-type Neuroblastoma Cells with Pluronic F108 and ECM Proteins." *Journal of Biomedical Materials Research Part A*, 93(2): 673-686, 2011.

13. Y. Li, *et al.* "Engineering cell alignment *in vitro*." *Biotechnology Advances*, 32: 347-365, 2014.
14. J.M. Walz, *et al.* "Methodology of the Microcontact Printing of Fibronectin and Blocking with Pluronic to Control Cell Adhesion." Stanford, 2005.
15. C. Frantz, *et al.* "The extracellular matrix at a glance." *Journal of Cell Science*, 123(24): 4195-4200, 2010.
16. C.J. Bettinger, *et al.* "Engineering Substrate Micro- and Nanotopography to Control Cell Function." *Angewandte Chemie International Edition in English*, 48(30): 5406-5415, 2009.
17. J.K. Mouw, *et al.* "Extracellular Matrix Assembly: A Multiscale Deconstruction." *Nature Reviews Molecular Cell Biology*, 15(12): 771-785, 2015.
18. K.C. Dee, *et al.* *An Introduction to Tissue-Biomaterial Interactions*. John Wiley & Sons. 2003.
19. M. Aumailley. "The laminin family." *Cell Adhesion & Migration*, 7(1): 48-55, 2013.
20. P. Camelliti, *et al.* "Microstructured Cocultures of Cardiac Myocytes and Fibroblasts : A Two-Dimensional In Vitro Model of Cardiac Tissue." *Microscopy and Microanalysis*, 11: 249-259, 2005.
21. E. Martínez, *et al.* "Effects of artificial micro- and nano-structured surfaces on cell behaviour." *Annals of Anatomy*, 191: 126-135, 2009.
22. R.G. Thakar, *et al.* "Regulation of vascular smooth muscle cells by micropatterning." *Biochemical and Biophysical Research Communications*, 307: 883-890, 2003.
23. C. Williams, *et al.* "The use of micropatterning to control smooth muscle myosin heavy chain expression and limit the response to transforming growth factor β 1 in vascular smooth muscle cells." *Biomaterials*, 32: 410-418, 2011.
24. A. Goessl, *et al.* "Control of shape and size of vascular smooth muscle cells in vitro by plasma lithography." *Journal of Biomedical Materials Research*, 57(1): 15-24, 2001.

25. Y. Cao, *et al.* "Regulating orientation and phenotype of primary vascular smooth muscle cells by biodegradable films patterned with arrays of microchannels and discontinuous microwalls." *Biomaterials*, 31: 6228-6238, 2010.
26. J.S. Choi, *et al.* "Circumferential alignment of vascular smooth muscle cells in a circular microfluidic channel." *Biomaterials*, 35: 63-70, 2014.
27. R.G. Thakar, *et al.* "Cell-shape regulation of smooth muscle cell proliferation." *Biophysical Journal*, 96: 3423-3432, 2009.
28. J.Y. Shen, *et al.* "Three-dimensional microchannels in biodegradable polymeric films for control orientation and phenotype of vascular smooth muscle cells." *Tissue Engineering*, 12(8): 2229-2240, 2006.

CHAPTER FOUR

STRETCHED TO THE LIMIT: CELL STRETCHING

4.1 CELL STRETCHING DEVICES

4.1.1 Device Specifications and Experimental Parameters

Cell stretching devices are research tools employed in studying the effects of mechanical conditions on cell behaviors¹. The development of cell stretching devices that realistically represent healthy or pathological conditions is important to accurately represent the mechanical environment cells experience *in vivo*¹. There are many types of cell stretching devices, ranging from commercially available to custom-made. Commercially available devices include the Flexcell (Flexcell International), ElectroForce (Bose), Strex (B-Bridge International), and MechanoCulture FX (CellScale)². Both 2D and 3D stretching environments are available, and *Figure 4.1* shows the possible mechanisms of stretch for 2D uniaxial devices.

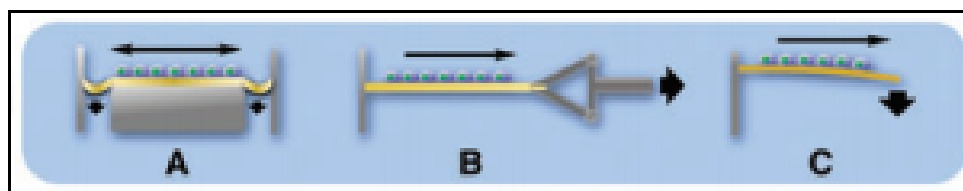


Figure 4.1: Mechanisms of 2D uniaxial stretch: A, Pneumatic, B. Electromechanical clamp-arm, C. Cantilever bending [modified from ref. 2]

Cell stretching devices have many adjustable parameters, including stress/ strain magnitude, rate of force application, stretch direction/orientation, stretch regimen, frequency, and duration^{1,2}. The stretch regimen can be uniaxial, biaxial, or radial stretching, each of which have characteristic effects on cells¹. For example, uniaxial

stretching has been shown to align cells in a specific orientation¹. Surface and EMC interactions with the tested cell type can affect the overall results². Additionally, patterning cells may cause variations in the amount of strain applied to the substrate and subsequently received by the cells². While commercially available cell stretching devices have limited customizable parameters, they are very useful because they have known properties, strain profiles, and stretch regimens. The inherent differences between devices and the settings used can have great effects on mechanical cues the tested cells actually receive, so it is important to use a well-characterized device². Using commercial stretching devices provides a uniform way to study mechanical conditions, generating scientific results that can be compared more easily.

4.1.2 The MechanoCulture FX Cell Stretching Device

The MechanoCulture FX by CellScale is a mechanical stimulation system that produces cyclic uniaxial stretch across a well plate using a clamp-arm system³ (*Figure 4.2*). Customizable test parameters include linear or sinusoidal velocity, stretch magnitude (percent axial strain), frequency, rest periods, repetitions, and duration of the stretching program³. A specialized silicone well plate is utilized by the MechanoCulture FX to provide uniform axial stretch to each well. Further, the device components can be sterilized with UV light or autoclave methods, ensuring sterility and compatibility with cell culture environments. The MechanoCulture FX has been used to study the effects of cyclic strain on cell and ECM fiber alignment^{4,5}.

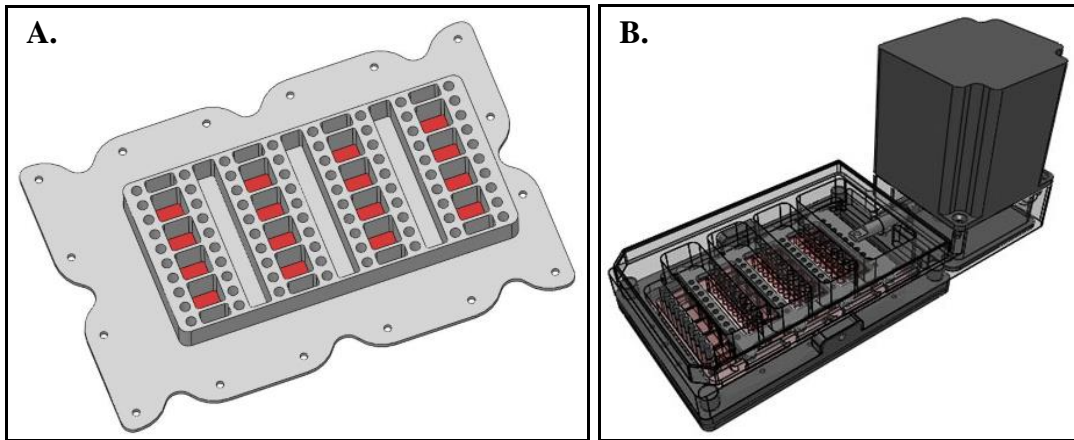


Figure 4.2: MechanoCulture FX System, A. Specialized well plate, B. Cell Stretching Device³

4.2. MECHANOTRANSDUCTION

Mechanotransduction is the process by which external, mechanical signals are converted to biochemical signals that influence intracellular responses⁶. External mechanical stimuli induce a cascade of cellular processes imperative for the regulation of a cell's homeostatic activities¹. Mechanical signaling regulates many cellular functions, including differentiation, migration, gene expression, and adhesion⁷. The cytoskeleton of a cell is viscoelastic, capable of withstanding mechanical forces, and it is heavily involved in distributing the mechanical signals enforced upon the cell. Mechanoreceptors, including integrins and protein kinases, are found in both the cytoskeleton and cell membrane, and they are the receptors that convert the initial physical stimulus into a biochemical signal⁸.

4.3 EFFECTS OF STRETCHING VASCULAR SMOOTH MUSCLE CELLS

VSMCs are constantly exposed to mechanical signaling from the shear stress and pressure on the blood vessel wall caused by the pulsatile flow of blood through vasculature. Continuous mechanical signaling is necessary to maintain the healthy, contractile functioning of VSMCs⁹. Abnormal mechanical forces are associated with the transition of contractile VSMCs to the synthetic phenotype. The presence of synthetic VSMCs is indicative of many vascular diseases, including atherosclerosis and hypertension^{9,10}. Understanding how mechanical forces influence tissue and cell behavior will advance clinical therapeutics and diagnostics, as well as lead to a better general understanding of vascular pathology at the cellular level. Cell stretching devices are used to not only study the effects of mechanical forces on the pathogenesis of VSMCs, but also to create disease state models to test potential therapeutics for vascular disease⁷.

4.4 METHODS, RESULTS, AND DISCUSSION

Three stretching experiments were performed to determine the effect of a physiologically relevant stretching regimen on aligned vascular smooth muscle cells:

- 1) VSMCs on microstamped collagen patterns
- 2) Stencil patterned VSMCs (Trial 1)
- 3) Stencil patterned VSMCs (Trial 2)

The methods and results for each of these three experiments are discussed below.

4.4.1 Stretching VSMCs on Microstamped Collagen Patterns – Methods

To determine the effect of cyclic stretching on cell phenotype, VSMCs were plated onto microstamped collagen patterns using PDMS stamps. The MechanoCulture FX Mechanical Stimulation System, Version 1, by CellScale was used as the cell stretching system.

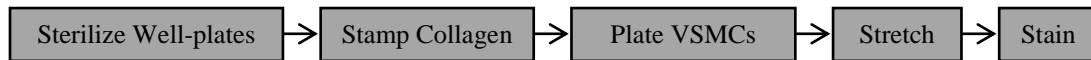


Figure 4.3: Overview of methods of microstamping collagen and stretching VSMCs

Specialized silicone well plates custom for the MechanoCulture FX System were sterilized in 100% ethanol and UV light for 30 minutes (*Figure 4.4*). PDMS stamps were sterilized in 100% ethanol by sonicating for 15 minutes in an ultrasonic cleaner (VWR International). The experimental plate was secured in the well plate holder of the sterilized cell stretching system. Collagen was stamped onto the well plates using both line and diamond patterns (stamps #2, 5, 7, and 8, as seen in *Table K-1*), following the methods described in *Chapter 3.4.4*. VSMCs were passaged using 0.25% Trypsin (Mediatech, Corning) and plated at a density of 20,000 cells per well. VSMCs were removed after 30 minutes to improve cell adhesion directly onto the collagen pattern. The MechanoCulture FX control box was programmed with a set of pre-conditioning steps along with a stretch representative of normal blood vessel physiology for a duration of 24 hours (*Table 4.1*). A stretch regimen of 5% axial strain at 1 Hz was used to represent healthy vascular physiology. Complete programming screen display of the MechanoCulture FX software is available in *Appendix M*. The control box was

programmed, plugged into a power source, and connected to the cell stretching system in the incubator. To begin cell stretching, the button on the control box was pressed once.

After the stretching sequence was completed, VSMCs were stained. First, cells were fixed with a 4% formaldehyde (Sigma), 0.1% glutaraldehyde (Polysciences, Inc.) solution at room temperature for 20 minutes. Cells were permeabilized with a 0.1% Triton X-100 (Sigma) solution at room temperature for 15 minutes. Alexa Fluor 568 Phalloidin (Thermo Fisher Scientific) was added at a concentration of 2.5% in PBS for 20 minutes at room temperature to stain for the actin cytoskeleton of the cell. 300 nM DAPI (Thermo Fisher Scientific) was added for 5 minutes at room temperature to stain for cell nuclei. Cells were rinsed three times with 1X PBS (Alfa Aesar) between every solution change. 1X PBS was added to the stained wells for storage. Images were taken using the EVOS microscope.

Table 4.1: Program sequence for stretching VSMCs on microstamped collagen patterns

Step of Program Sequence	Strain (%)	Stretch Displacement (mm)	Frequency (Hz)	Stretch/ Recovery Duration (s)	Total Step Duration (s)
Initial Stretch	-	0.5	-	10.0/ 0.0	10
Pre-Conditioning	1	0.1333	0.1	5.0/ 5.0	900
Pre-Conditioning	1	0.1333	0.5	1.0/ 1.0	900
Pre-Conditioning	1	0.1333	1	0.5/ 0.5	900
Pre-Conditioning	2.5	0.3333	1	0.5/ 0.5	900
Heart Physiology	5	0.6666	1	0.5 /0.5	86,400

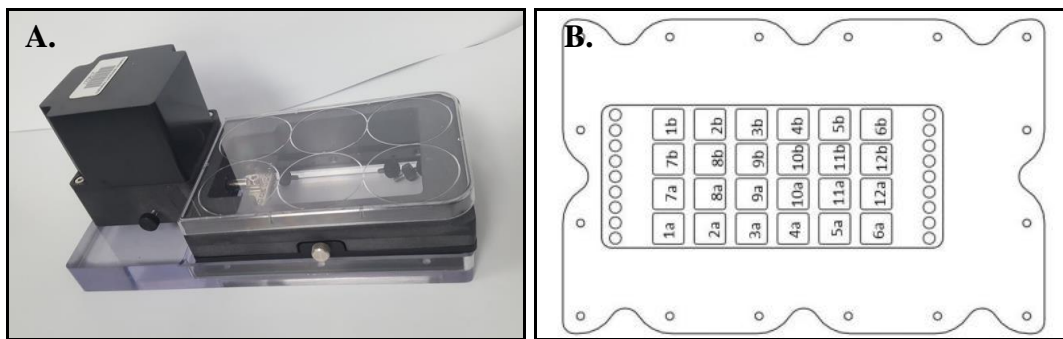


Figure 4.4: MechanoCulture FX cell stretching system A. Well plate holder, B. Specialized silicone 24- well plate for the MechanoCulture FX³

4.4.2 Stretching VSMCs on Microstamped Collagen Patterns – Results and Discussion

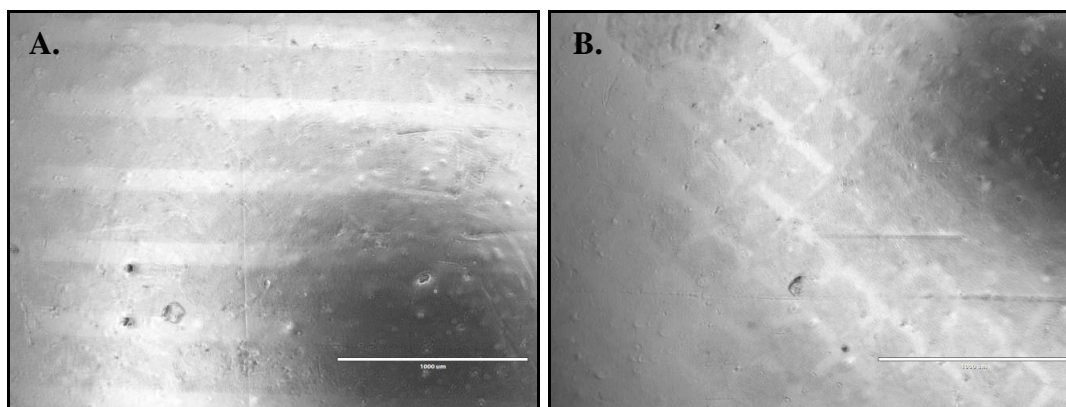


Figure 4.5: Visible collagen patterns (4X), A. 100 µm collagen lines (stamp #5) B. 30 µm collagen diamonds (stamp #7)

Under light microscopy, collagen patterns are visible on the silicone well plate. *Figure 4.5A* shows 100 µm collagen lines patterned using Stamp #5, and *Figure 4.5B* shows 30 µm collagen diamonds patterned using Stamp #7. While the collagen patterns are visible, the silicone well plate does not allow for visualization of VSMCs due to their naturally thin, flattened structure.

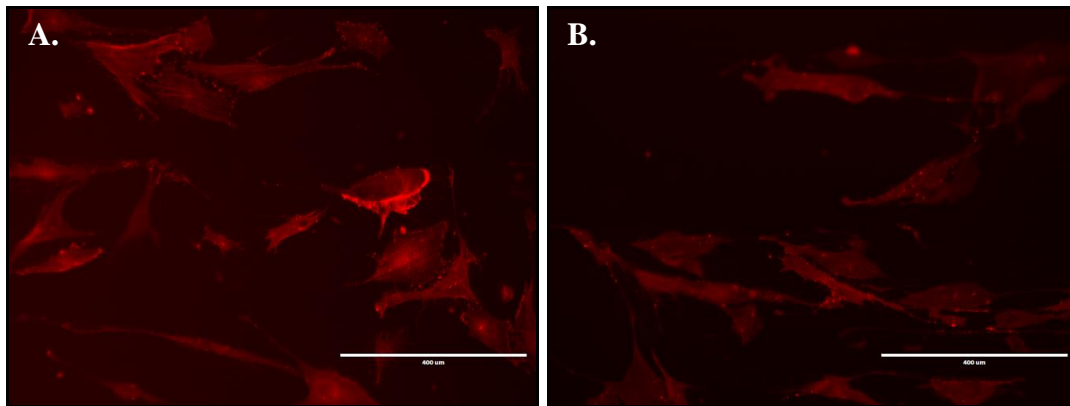


Figure 4.6: VSMCs stained for phalloidin (10X), A. Control VSMCs, B. Stretched VSMCs

VSMCs did not appear to adhere specifically to the collagen patterns, but instead were able to adhere to both the collagen patterns as well as the untreated area of the silicone well plate. While some cells did adhere to the collagen only, the ability of the cells to attach to the well plate allowed significant cross over among the patterned lines. In *Figure 4.6A*, control VSMCs did not form into a specific pattern. The Pluronic solutions were not able to effectively eliminate non-specific binding of VSMCs on micropatterned surfaces (as described in *Chapter 3.4.5*). Overall, microstamping collagen onto the silicone well plates did not promote significant cell adhesion in the desired patterns. To combat this issue in future experiments, stencil patterning was performed to produce better alignment of VSMCs for stretching.

Figure 4.6B shows VSMCs after they received the stretching regimen. The cells demonstrated a more elongated phenotype while adhering to collagen in a line resembling the original collagen pattern. This finding supports literature that states vascular smooth muscle cells exhibit a more contractile phenotype when stretched. The transition to a contractile phenotype could be due to the presence of extracellular matrix cues from the micropatterned collagen in combination with the mechanical forces applied to the cells.

4.4.3 Stretching Stencil Patterned VSMCs (Trial 1) – Methods

To determine the effect of cyclic stretching on cell phenotype and proliferation rate, VSMCs were plated in line patterns using PDMS stencils. The MechanoCulture FX Mechanical Stimulation System, Version 1, by CellScale was used as the cell stretching system.

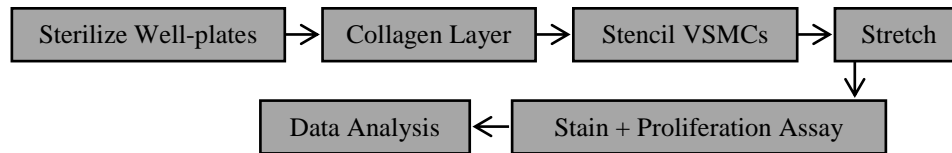


Figure 4.7: Overview of methods of stenciling and stretching VSMCs (Trial 1)

First, specialized silicone well-plates were sterilized with 100% ethanol for 1 hour and UV light for 45 minutes. The ethanol was removed, and the plates were allowed to dry. The experimental plate was secured in the well plate holder of the sterilized cell stretching system. A thin layer of collagen (Discovery Labware Inc., Corning) was added to each well at a concentration of 100 $\mu\text{L}/\text{mL}$ and allowed to incubate overnight to provide a better surface for cell adhesion. After 24 hours, collagen was removed from the well plates and allowed to dry. PDMS stencils were sterilized by sonicating for 15 minutes in 100% ethanol. Dried stencils were placed in well-plates in either a parallel or perpendicular direction (following the methods described in *Chapter 3.4.7*). VSMCs were passaged using 0.25% Trypsin (Mediatech, Corning) and plated at a density of 50,000 cells per well. VSMCs were removed after 10 minutes to improve cell adhesion. After 24 hours, the stencils were removed from the well-plates, and media was replaced in each well. The five experimental groups of cells were: control without a stencil,

control with a stencil, stretched without a stencil, stretched with a parallel stencil, and stretched with a perpendicular stencil.

The MechanoCulture FX control box was programmed with a set of pre-conditioning steps along with a stretch representative of normal blood vessel physiology for a duration of 24 hours (*Table 4.2*). Complete programming screen display of the MechanoCulture FX software is available in *Appendix M*. The control box was programmed, plugged into a power source, and connected to the well plate holder of the cell stretching system in the incubator. To begin cell stretching, the button on the control box was pressed once. After the stretching sequence was completed, either a proliferation assay was performed or the VSMCs were fixed for immunocytochemistry staining.

To begin the proliferation assay, proliferation assay solution (CellTiter 96, Promega) was added to the wells in a 1:5 ratio with media. CellTiter 96 is a colorimetric proliferation assay that quantifies formazan produced by cells in response to the assay solution in order to determine the number of viable cells present¹¹. Well plates were incubated for 1 hour, and the combined assay/ media solution was transferred to a 96-well plate. Absorbance values were measured using a Synergy 4 Microplate Reader (BioTek) with Gen 5 1.11 Microplate Data Collection & Analysis Software. A two-tailed student's t-test with unequal variance was performed to determine if there is a statistically significant difference between the proliferation rates of each sample group.

Table 4.2: Program sequence for stretching VSMCs plated in lines using PDMS stencils

Step of Program Sequence	Strain (%)	Stretch Displacement (mm)	Frequency (Hz)	Stretch/Recovery Duration (s)	Total Step Duration (s)
Initial Stretch	-	1.5	-	10.0/ 0.0	10
Pre-Conditioning	1	0.1333	0.1	5.0/ 5.0	900
Pre-Conditioning	1	0.1333	0.5	1.0/ 1.0	900
Pre-Conditioning	1	0.1333	1	0.5/ 0.5	900
Pre-Conditioning	2.5	0.3333	1	0.5/ 0.5	900
Heart Physiology	5	0.6666	1	0.5 /0.5	86,400

Cells were fixed using a 4% formaldehyde (Sigma), 0.1% glutaraldehyde (Polysciences, Inc.) solution at room temperature for 20 minutes. Cells were permeabilized with a 0.1% Triton X-100 (Sigma) solution at room temperature for 15 minutes. Cells were blocked with a 2% BSA (Rockland), 3% goat serum (MP Biomedicals, LLC) blocking solution. Finally, monoclonal mouse anti-collagen Type 1 primary antibody (Sigma) in the blocking solution at a concentration of 1:500 was added to the wells and allowed to incubate at 4°C overnight. Goat anti-mouse Alexa Fluor 488 was used as the secondary antibody at a concentration of 4 µL/mL, and it was incubated at room temperature for 2 hours. Alexa Fluor 568 Phalloidin (Thermo Fisher Scientific) was added at a concentration of 2.5% in PBS for 20 minutes at room temperature to stain for the actin cytoskeleton of the cell. 300 nM DAPI (Thermo Fisher Scientific) was added for 5 minutes at room temperature to stain for cell nuclei. Cells were rinsed three times with 1X PBS (Alfa Aesar) between every solution change. 1X PBS was added to the stained wells for storage. Images were taken using the EVOS microscope. Images were taken at 4X and 10X, and phenotypes were qualitatively compared among groups. Additionally, 4 images were taken of the DAPI-stained nuclei at representative areas of

each well, and the number of nuclei for each image were counted. Images of control wells were selected randomly, and images of the stretched and patterned wells were selected in the patterned regions only (*Appendix P*).

4.4.4 Stretching Stencil Patterned VSMCs (Trial 1) – Results and Discussion

Proliferation assay data, demonstrated as the comparison of the number of viable cells, is shown in *Figures 4.8- 4.11* and *Tables 4.3- 4.4*. Viable cell number is represented as an absorbance value as received by the well plate reader. Proliferation rate data is supplemented with analysis of the number of nuclei, which is shown in *Figure 4.12* and *Table 4.5*. Immunocytochemistry staining images are shown in *Figures 4.13- 4.16*.

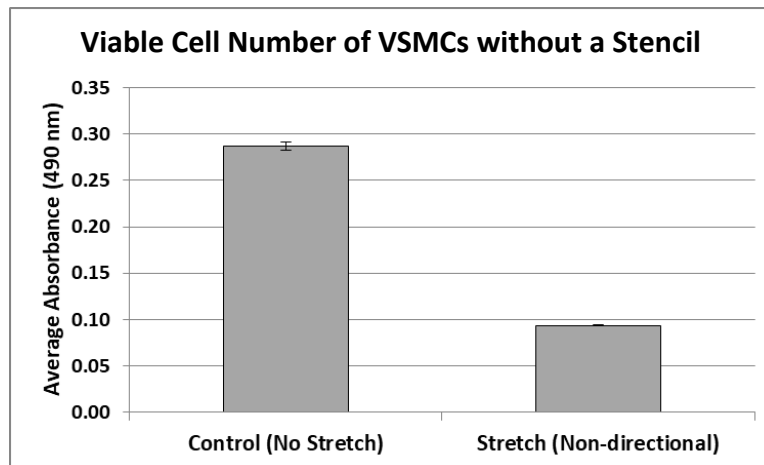


Figure 4.8: Viable cell number of control and stretched VSMCs plated without a stencil, p-value (2.03 E-16) indicates that there is a statistically significant difference

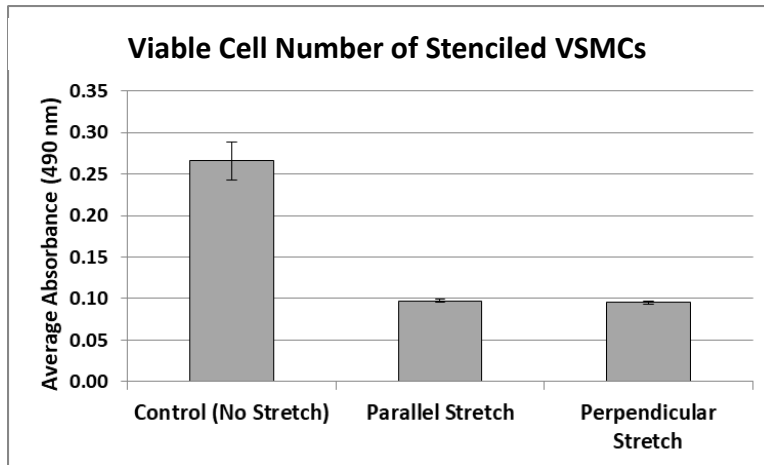


Figure 4.9: Viable cell number of control and parallel or perpendicularly stretched VSMCs plated in a line pattern with a stencil

Table 4.3: T-Tests comparing the viable cell numbers of stenciled VSMCs; p-values indicate that there is a statistically significant difference between all sample groups

T-Tests for Stenciled VSMCs	Control (No Stretch)	Parallel Stretch	Perpendicular Stretch
Control (No Stretch)			
Parallel Stretch	2.05 E-13		
Perpendicular Stretch	1.60 E-13	1.08 E-2	

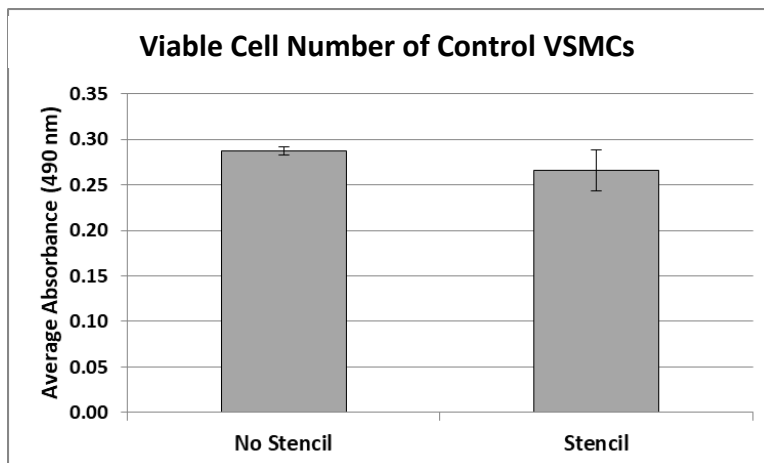


Figure 4.10: Viable cell number of control VSMCs with and without a stencil, p-value (0.044) indicates that there is a statistically significant difference

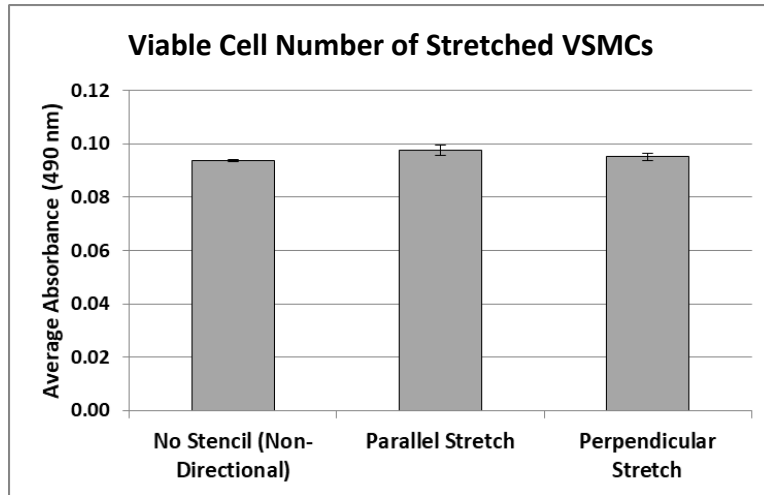


Figure 4.11: Viable cell number of stretched VSMCs, either non-directional without a stencil or those plated with a stencil in parallel or perpendicular directions

Table 4.4: T-Tests comparing the viable cell numbers of stretched VSMCs; p-values indicate that there is a statistically significant difference between all sample groups

T-Tests for Stretched VSMCs	No Stencil (Non-Directional)	Parallel Stretch	Perpendicular Stretch
No Stencil (Non-directional Stretch)			
Parallel Stretch	0.001		
Perpendicular Stretch	0.029	0.011	

Based on absorbance values from the proliferation assay, the number of viable cells of control VSMCs is higher than that of the stretched VSMCs, for both samples plated without stencils (*Figure 4.8*) and those with stencils (*Figure 4.9*). This data supports literature that states stretched VSMCs become more contractile, as seen by the lower viable cell number. *Figure 4.8* shows that stretched VSMCs have significantly lower viable cell numbers than their control counterparts, which is characteristic of contractile VSMC functions. As seen in *Figure 4.9*, both parallel and perpendicularly stretched stencil-patterned VSMCs have a lower viable cell number than control stencil-

patterned VSMCs. *Table 4.3* confirms that there is a statistically significant difference between control and stretched pattern-stenciled VSMCs, as well as between the parallel and perpendicularly stretched, stencil-patterned VSMCs. The viable cell number of VSMCs stenciled parallel to the stretch direction was slightly higher than that of the perpendicularly stenciled VSMCs. This could be due to a decreased ability to proliferate when the cytoskeleton of the cell was arranged perpendicular to stretch.

Figures 4.10 and 4.11 demonstrate the effect of stencil patterning on VSMC viable cell number. It is expected that the wells without stencils will have a higher absorbance value, and thus cell number, due to the greater available surface area for cell adhesion. *Figure 4.10* shows that the viable cell number of stencil-patterned VSMCs is statistically significantly lower than that of non-stenciled VSMCs. This is expected due to the decreased surface area caused by the stencil placement in the well. *Figure 4.11* demonstrates a different trend with stretched VSMCs: the stenciled VSMCs actually had higher viable cell numbers than the non-stenciled VSMCs. This could be due to an inconsistency in stencil size, shape, and well placement. Conflicting trends could also be due to the high seeding density of cells, so this was adjusted in the next experiment.

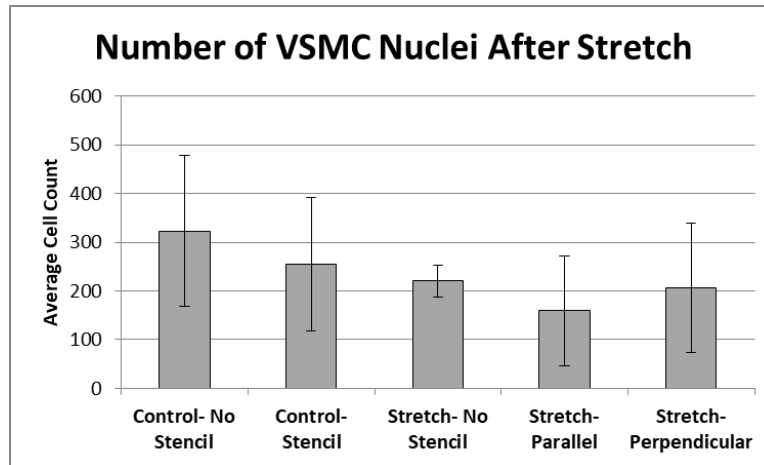


Figure 4.12: Number of Nuclei in VSMCs (Trial 1)

Table 4.5: T-Tests comparing number of nuclei between control, stretched, stencil-patterned, and non-stenciled VSMCs

T-Tests	Control- No Stencil	Control- Stencil	Stretch- No Stencil	Stretch- Parallel	Stretch- Perpendicular
Control- No Stencil					
Control- Stencil	0.532				
Stretch- No Stencil	0.241	0.637			
Stretch- Parallel	0.139	0.322	0.343		
Stretch- Perpendicular	0.294	0.624	0.842	0.613	

The number of nuclei represents the cell density of VSMCs in a particular region of the pattern. There is not a statistically significant difference between any of the experimental groups, which is likely due to the high variability present in each group (*Table 4.5*). The variability of nuclei number could be due to the inconsistency of cell spreading throughout the wells. However, some trends are seen that support the proliferation assay data. Both control groups have a larger number of nuclei than stretched cells.

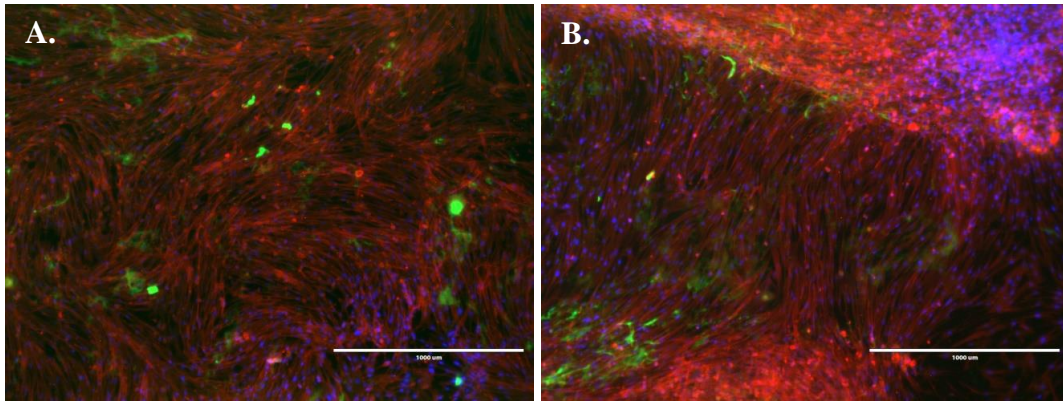


Figure 4.13: Control, non-stretched VSMCs, A. No stencil, B. Stencil-patterned (4X)

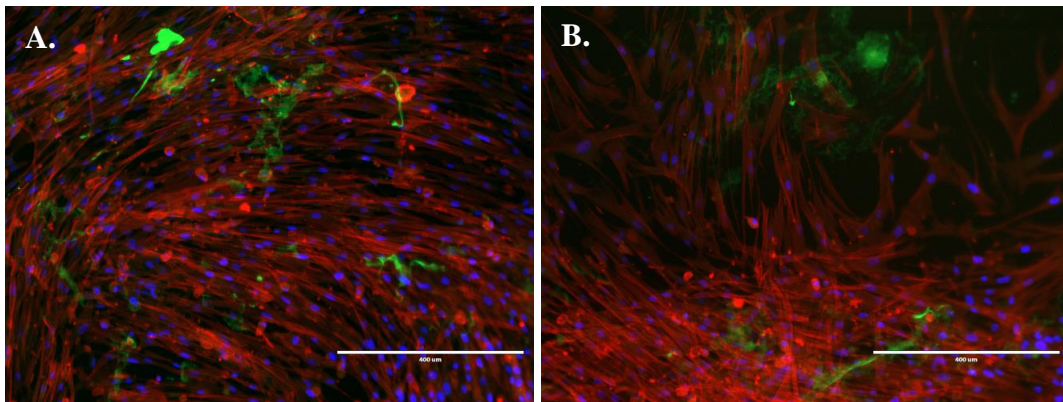
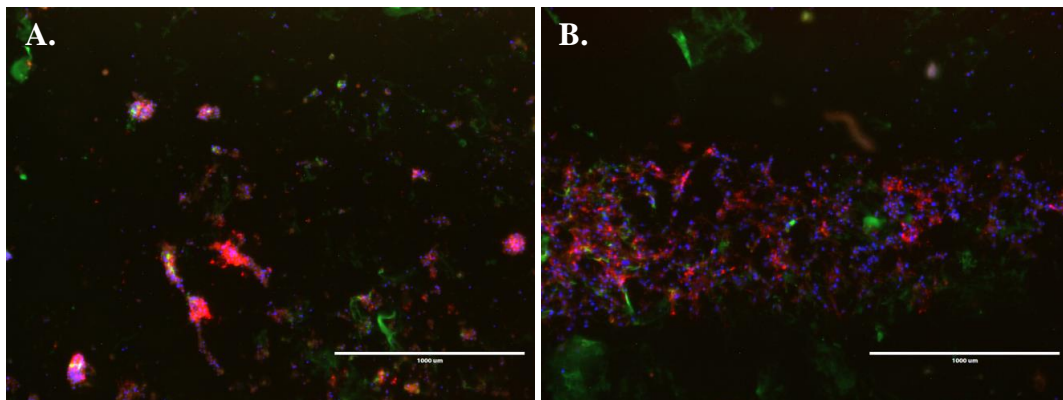


Figure 4.14: Control, non-stretched VSMCs, A. No stencil, B. Stencil-patterned (10X)



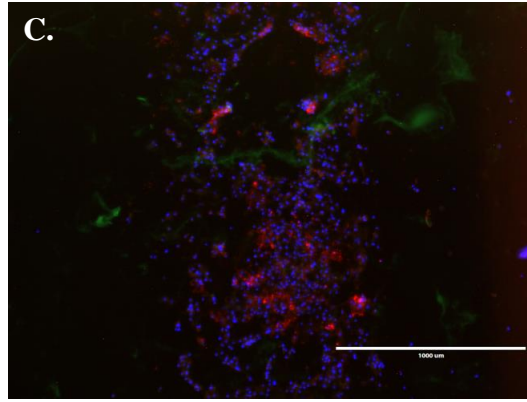


Figure 4.15: Stretched VSMCs, A. No stencil, B. Parallel stencil, C. Perpendicular stencil (4X)

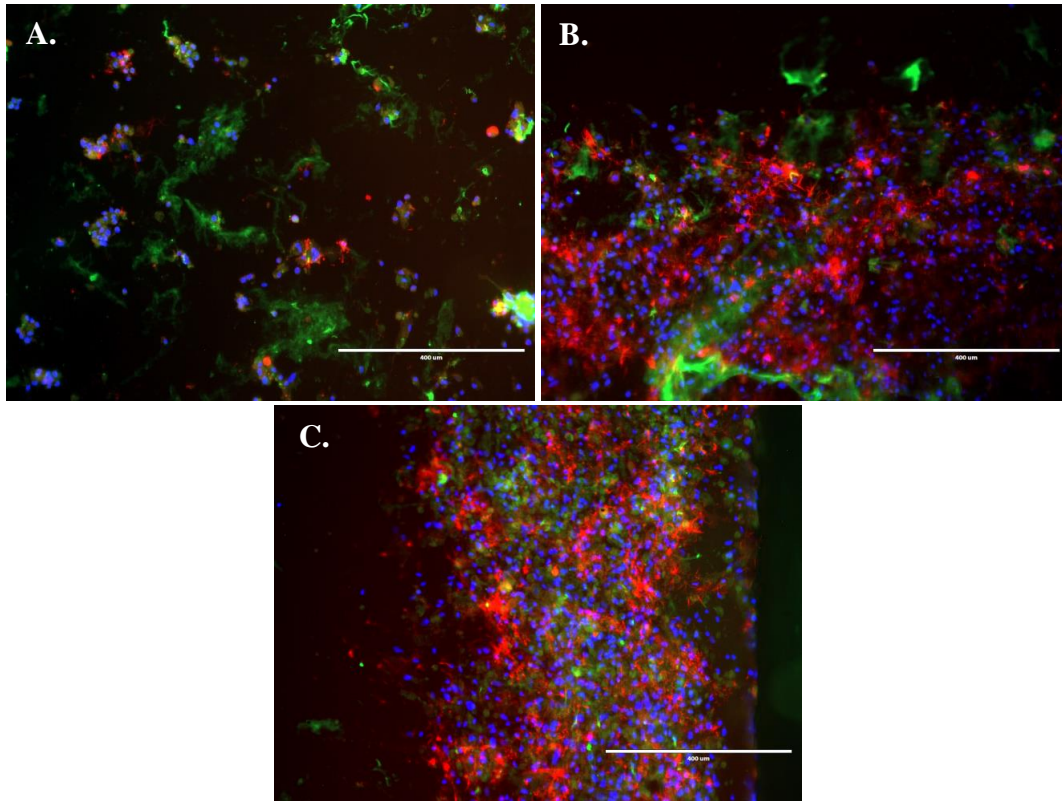


Figure 4.16: Stretched VSMCs, A. No stencil, B. Parallel stencil, C. Perpendicular stencil (10X)

The efficacy of the stencil patterning technique was revealed through staining and imaging. *Figure 4.13* shows both control and stencil-patterned non-stretched VSMCs. While non-patterned VSMCs exhibit random arrangement and cell spreading (*Figure 4.13A*), the stencil-patterned VSMCs are more aligned. However, the high seeding

density along with an allotted 24 hours to migrate and proliferate after the stencil was removed allowed for a high amount of cell spreading between the two patterned lines seen in *Figure 4.13B*. *Figure 4.14* supports this trend, with cell spreading from the original stencil outline visible in *Figure 4.14B*. Successful cell stenciling with minimal spreading was also demonstrated with stretched VSMCs (*Figures 4.15- 4.16*). Cell spreading could be reduced by using a more precisely fabricated stencil with sharper edges and corners that will adhere to the well plate.

Stretched VSMCs exhibit significant phenotype changes compared to control cells. As seen in *Figure 4.15 and 4.16*, stretched VSMCs appear to be more round and less adhered to the well plate surface. There are several hypotheses for the cause behind this phenotype. First, it is possible that the initial pre-stretching step of 1.5 mm (*Table 4.2*) caused too much displacement of the well plate, disrupting cell adhesion. The subsequent stretching regimen then might have prevented the cells from forming strong new attachments to the well plate after the initial disruption, leading to the small, rounded phenotype displayed. Another hypothesis is that the specialized well plate was placed in tension in its position in the well plate holder of the cell stretching system. When it was removed from the well plate holder for staining, the tension in the well plate was released, perhaps disrupting the cell attachment to the surface. Additionally, the collagen layer on the well plate could affect cell interactions and mechanics, leading to the cells not fully adhering to the surface.

4.4.5 Stretching Stencil Patterned VSMCs (Trial 2) – Methods

To determine the effect of cyclic stretching without the initial pre-conditioning stretch step, VSMCs were plated in line patterns using PDMS stencils. The MechanoCulture FX Mechanical Stimulation System, Version 1, by CellScale was used as the cell stretching system.

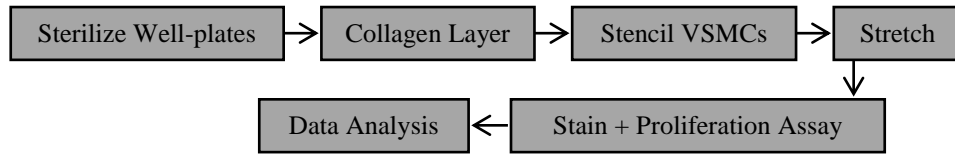


Figure 4.17: Overview of methods of stenciling and stretching VSMCs (Trial 2)

The same methods described for Trial One (as described in *Chapter 4.4.3*) were followed for Trial Two, with a few changes as specified. VSMCs were plated at a density of 10,000 cells per well and were not removed following plating. Due to well plate limitations, VSMCs were only stencil-patterned. However, a Day 0 control group was added to analyze phenotypic and proliferation changes over time. The four experimental groups of cells were: Day 0 control, Day 1 control, parallel stretched (Day 1), and perpendicularly stretched (Day 1). The cell stretching program sequence was adjusted to remove any initial stretching, as seen in *Table 4.6*. Finally, a proliferation assay and immunocytochemistry staining were performed.

Table 4.6: Program sequence for stretching VSMCs plated in lines using PDMS stencils

Step of Program Sequence	Strain (%)	Stretch Displacement (mm)	Frequency (Hz)	Stretch/Recovery Duration (s)	Total Step Duration (s)
Pre-Conditioning	1	0.1333	0.1	5.0/ 5.0	900
Pre-Conditioning	1	0.1333	0.5	1.0/ 1.0	900
Pre-Conditioning	1	0.1333	1	0.5/ 0.5	900
Pre-Conditioning	2.5	0.3333	1	0.5/ 0.5	900
Heart Physiology	5	0.6666	1	0.5 /0.5	86,400

4.4.6 Stretching Stencil Patterned VSMCs (Trial 2) – Results and Discussion

Proliferation assay data, demonstrated as the comparison of the number of viable cells, is shown in *Figures 4.18- 4.19* and *Table 4.8*. Viable cell number is represented as an absorbance value as received by the well plate reader. Proliferation rate data is supplemented with analysis of the number of nuclei, which is shown in *Figure 4.20* and *Table 4.9*. Immunocytochemistry staining images are shown in *Figures 4.21- 4.23*.

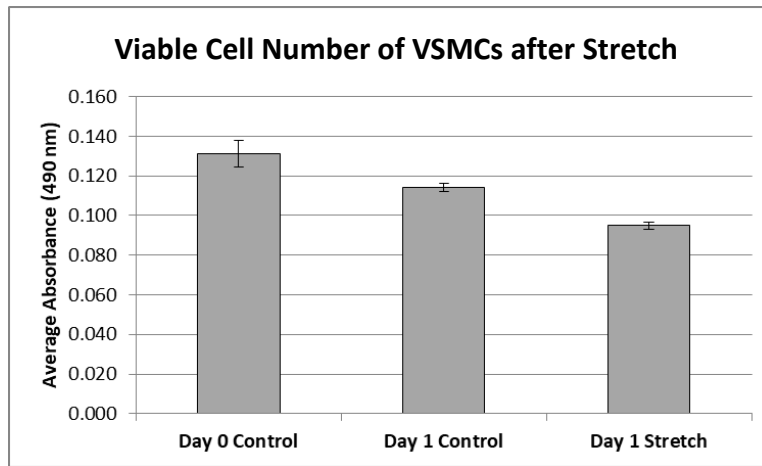


Figure 4.18: Viable cell number of control and stretched (combined parallel and perpendicular) VSMCs

Table 4.7: T-Tests comparing the viable cell numbers of control and stretched VSMCs; p-values indicate that there is a statistically significant difference between all sample groups

T-Tests	Day 0 Control	Day 1 Control	Stretch
Day 0 Control			
Day 1 Control	1.104 E-4		
Stretch	1.893 E-9	2.602 E-13	

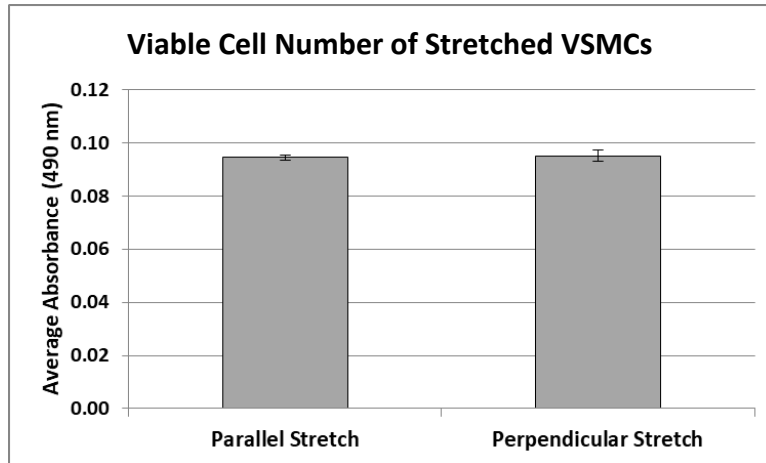


Figure 4.19: Viable cell number of parallel and perpendicular stretched cells, p-value (0.493) indicates that there is not a statistically significant difference

Results from Trial 2 mirrored that of Trial 1: the viable cell number of stretched VSMCs were lower than that of the control counterparts (*Figure 4.18*). Decreased viable cell number, representative of proliferation rate, are characteristic of a contractile phenotype. Additionally, it was seen that viable cell number of control VSMCs decreased from Day 0 to Day 1. This suggests that the well plate environment might not have been sufficient for prolonged cell growth. In the future, VSMCs can be seeded at a lower density, or different extracellular matrix proteins, such as fibronectin, could be used as a surface layer to promote increased cell proliferation. *Figure 4.19* indicates that there is not a statistically significant difference between parallel and perpendicularly stretched cells.

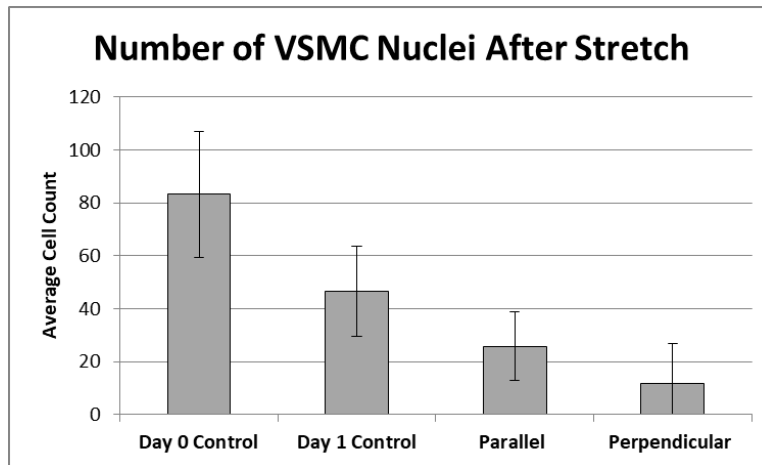


Figure 4.20: Number of Nuclei in VSMCs (Trial 2)

Table 4.8: T-Tests comparing number of nuclei between Day 0 control, Day 1 control, parallel and perpendicularly stretched VSMCs

T-Tests	Day 0 Control	Day 1 Control	Parallel	Perpendicular
Day 0 Control				
Day 1 Control	0.01173			
Parallel	0.00040	0.03834		
Perpendicular	0.00536	0.07861	0.79165	

Analysis of the number of DAPI-stained nuclei in selected representative images supports proliferation assay data. The number of nuclei is greater in the control than in the stretched VSMCs (*Figure 4.20*). Further, the number of nuclei is less in the Day 1 control compared to the Day 0 control, complementing the associated proliferation rates. There is not a statistically significant difference between the parallel and perpendicularly stretched VSMCs, possibly due to similar mechanical conditions or similar limited surface areas (*Table 4.8*). The large variability in each group could be due to the variability of cell spreading.

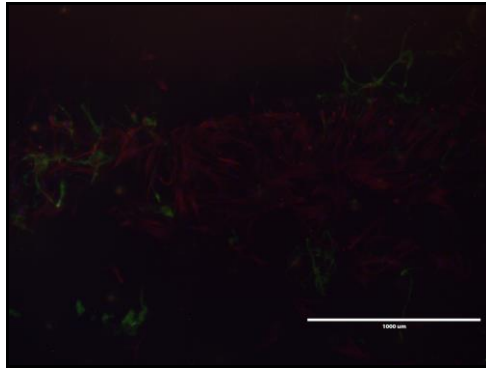


Figure 4.21: Stencil Patterning: Day 0 Control (4X)

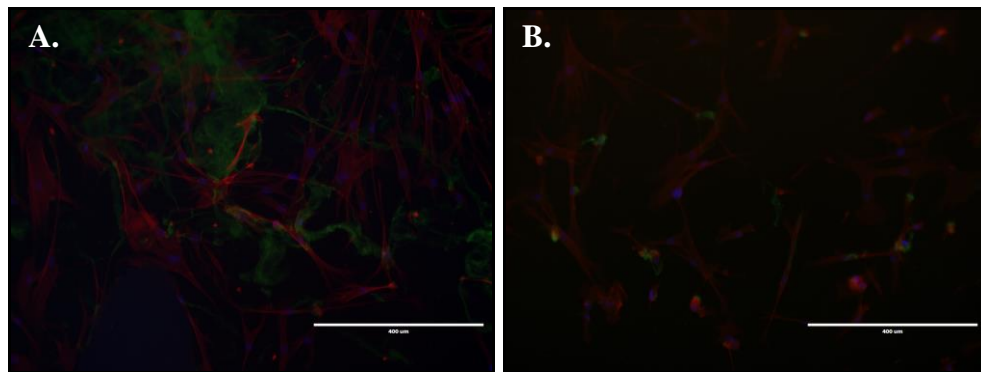


Figure 4.22: Control VSMCs, A. Day 0 Control, B. Day 1 Control (10X)

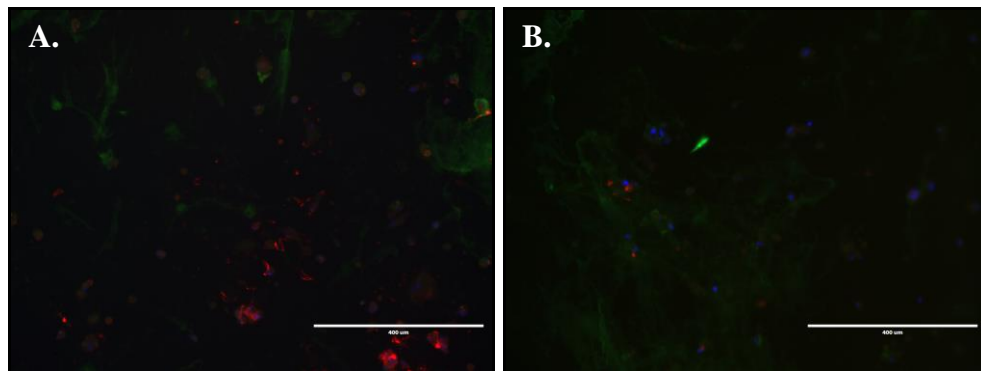


Figure 4.23: Stretched VSMCs, A. Parallel stencil, B. Perpendicular stencil (10X)

Stencil patterning was shown to be effective at aligning VSMCs into parallel lines (Figure 4.21). Day 0 control VSMCs were found to be more confluent than Day 1 control VSMCs, suggesting that there was a secondary cause for the decreased proliferation rates (Figure 4.22). Further, stretched VSMCs exhibited significant phenotype changes

compared to both day 0 and 1 control cells. The same hypotheses suggested for Trial 1 apply to this experiment as well.

4.5 CONCLUSIONS AND FUTURE DIRECTION

Overall, stencil patterning was the most effective way to align VSMCs on the silicone well plates for cell stretching experiments. Stencil patterned VSMCs exhibited a much more aligned arrangement with reduced cell spreading and random attachment compared to VSMCs plated on micropatterned collagen. Improvements to the stencil patterning method include creating uniform stencils with a standardized size and shape. Laser cutting PDMS stencils would be a better fabrication method that would allow for higher quality, better performing stencils. PDMS stencils could also be produced using a master with taller photoresist features.

While cell stretching promoted a more contractile phenotype when VSMCs were plated on microstamped collagen, some additional modifications in the stencil patterning experiments led to the display of a rounded, unattached phenotype. Future stretching experiments would not include an initial stretching step, and the stretched well plate would remain in the well plate holder of the cell stretching system for staining and imaging to prevent disruption of the cell attachments to the well plate.

4.6 REFERENCES

1. H. Kamble, *et al.* “Cell stretching devices as research tools: engineering and biological considerations.” *Lab on a Chip*, 16: 3193-3203, 2016.
2. B.D. Riehl, *et al.* “Mechanical Stretching for Tissue Engineering: Two-Dimensional and Three-Dimensional Constructs.” *Tissue Engineering: Part B*, 18(4): 288-300, 2012.
3. MechanoCulture FX Manual, version 1.2. *CellScale*. 2018.
4. K. Chen, *et al.* “Role of boundary conditions in determining cell alignment in response to stretch.” *Proceedings of the National Academy of Sciences*, 115(5): 986-991, 2017.
5. D. Gaspar, *et al.* “Tenogenic phenotype maintenance and differentiation using macromolecular crowding and mechanical loading.” *Bioengineering Biotechnology Conference Abstract: 10th World Biomaterials Congress*, 2016.
6. M. Nikkhah, *et al.* “Engineering microscale topographies to control the cell-substrate interface.” *Biomaterials*, 33: 5230-5246, 2012.
7. F.J. Alenghat, *et al.* “Mechanotransduction: All Signals Point to Cytoskeleton, Matrix, and Integrins.” *Science Signaling*, 119, 2002.
8. K.G. Shyu. “Cellular and molecular effects of mechanical stretch on vascular cells and cardiac myocytes.” *Clinical Science*, 116: 377-389, 2009.
9. J. Qiu, *et al.* “Biomechanical regulation of vascular smooth muscle cell functions: from *in vitro* to *in vivo* understanding.” *Journal of the Royal Society Interface*, 11, 2014.
10. L.E. Mantella, *et al.* “Variability in vascular smooth muscle cell stretch-induced responses in 2D culture.” *Vascular Cell*, 7(7), 2015.
11. “CellTiter 96 AQueous One Colution Cell Proliferation Assay.” *Promega Corporation*. Technical Bulletin. December, 2012.

APPENDICES

Appendix A

Vascular Smooth Muscle Cell Culture Protocol

Materials:

1. Smooth muscle cell growth medium (Cell Applications, Inc., Cat. No. 311-500)
2. 0.25% Trypsin, 2.21 mM EDTA, 1X sodium bicarbonate (Mediatech, Inc., a Corning subsidiary, REF 25-053-CI)

Passaging Cells Procedure:

1. Remove media from cell culture flask.
2. Add thawed Trypsin to flask to cover the surface, (5 mL for T-75 flask, 10 mL for T-160 flask).
3. Incubate for 5-7 minutes, until cells become detached from the flask surface.
4. Add equal amount of warmed media to the flask.
5. Transfer the media/trypsin solution to a 15 mL centrifuge tube.
6. Centrifuge media/trypsin solution at 1,000 rpm for 5 minutes.
7. Cell pellet will form at bottom of centrifuge tube.
8. Remove supernatant from cell pellet.
9. Add 1 mL of media and vortex to evenly distribute cells throughout the solution.
10. Plate cells into cell culture flask or well plate.

Thawing Cells Procedure:

1. Remove cryogenic vial of frozen cells from the liquid nitrogen tank.
2. Thaw cryogenic vial as quickly as possible, placing in water bath as necessary.
3. Transfer cell suspension into a 15 mL centrifuge tube with 5 mL of warmed media.
4. Centrifuge solution at 1,000 rpm for 5 minutes.
5. Cell pellet will form at bottom of centrifuge tube.
6. Remove supernatant from cell pellet.
7. Add 1 mL of media and vortex to evenly distribute cells throughout the solution.
8. Plate cells into cell culture flask or well plate.

Notes: All cell culture procedures are sterile and performed in a standard laminar flow hood. Smooth muscle cell growth medium is light sensitive and is stored as such.

References: “Protocol for Passaging Adherent Cells”, Gibco Cell Culture Basics, Thermo Fisher Scientific. Web. 2018. <https://www.thermofisher.com/us/en/home/references/gibco-cell-culture-basics/cell-culture-protocols/subculturing-adherent-cells.html#4>

Appendix B

Counting Cells Protocol

Materials:

1. Trypan blue dye solution, 0.4% (Sigma, T8154)
2. Bright-Line hemocytometer (Hausser Scientific)
3. Smooth muscle cell growth medium (Cell Applications, Inc., Cat. No. 311-500)

Procedure:

1. Passage cells, leaving a 1 mL suspension of cells in media.
2. In a 1 mL centrifuge tube, add 160 μ L media, 20 μ L of cell suspension, and 20 μ L of Trypan blue dye solution.
3. Vortex the combined solution to mix.
4. Add 20 μ L of the combined cell/dye solution to a hemocytometer.
5. Count the number of cells present in the 5 marked squares in the hemocytometer grid shown in *Figure B-1*:

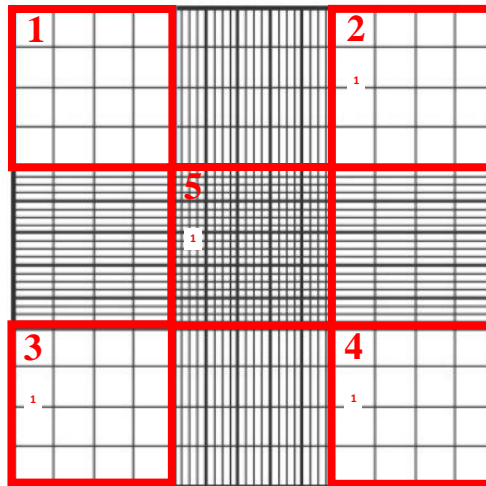


Figure B-1: Counting cells using a hemocytometer grid

6. Determine the number of cells per mL of original cell suspension with the following equation:

$$\text{Total \# of Cells/ mL} = (\text{COUNT}/5) \times 10 \times (10^4)$$

7. Determine the number of cells needed for plating with the following equation:

$$\text{Amount of Solution Needed } (\mu\text{L}) = (\# \text{ of Cells Needed} / \text{Total \# of Cells/mL}) \times 1000$$

References: “Counting cells using a hemocytometer”, Abcam. Web. 2018.

<http://www.abcam.com/protocols/counting-cells-using-a-haemocytometer>.

Appendix C

Proliferation Assay Protocol

Materials:

1. CellTiter 96 AQueous One Solution Cell Proliferation Assay (Promega Corporation, REF G3581)
2. Smooth muscle cell growth medium (Cell Applications, Inc., Cat. No. 311-500)

Procedure:

Begin Assay Incubation

1. Remove media from the wells.
2. Add fresh media to each well.
3. Add proliferation assay to each well.
1:5 Ratio for Assay: Media
4. Incubate for 1 hour at 37°C.

Read Absorbance Using Well Plate Reader

1. Remove 120 µL of the combined assay/media solution and transfer to a 96-well plate, repeating until well is depleted
2. Repeat for each well
3. Read absorbance values using the Synergy 4 Microplate Reader by BioTek
4. On Gen 5 1.11 Microplate Data Collection & Analysis Software, click the following:
Read a Plate
Instrument Selection > Synergy 4 > Ok
Procedure > Plate Type: 96 WELL PLATE
Read > Set "Absorbance" to 490 nm > Ok
Description: Read: (A) 490
Plate 1 Reading > READ
Name and Save the file
5. After "Place plate on carrier" notification appears, load the well plate onto the tray, remove the lid, and click Ok
6. Tray will automatically close and read the plate
7. When reading is complete, on "Plate 1" tab, select "490" from the "Data" selection tab to show the absorbance readings
8. Export the data to Excel for analysis
9. Remove the well plate, close the tray, and turn off the well plate reader

References: "CellTiter 96® AQueous Non-Radioactive Cell Proliferation Assay Technical Bulletin", Promega, Promega Corporation. Web. 2018.

<https://www.promega.com/resources/protocols/technical-bulletins/0/celltiter-96-aqueous-nonradioactive-cell-proliferation-assay-protocol/>

Appendix D

Proliferation Assay Standard Curve Protocol

Materials:

1. CellTiter 96 AQueous One Solution Cell Proliferation Assay (Promega Corporation, REF G3581)
2. Smooth muscle cell growth medium (Cell Applications, Inc., Cat. No. 311-500)

Procedure:

Plate Cells

1. Passage and count cells.
2. Plate cells in triplicates in a 24- well plate for the following seeding densities (*Figure D-1*):
1,000; 2,500; 5,000; 10,000; 25,000; 50,000; 100,000; 200,000

Note: Higher seeding densities can be added depending on seeding density used in experiments.

3. Add 1 mL of media per well.
4. Incubate for 4-6 hours at 37°C.

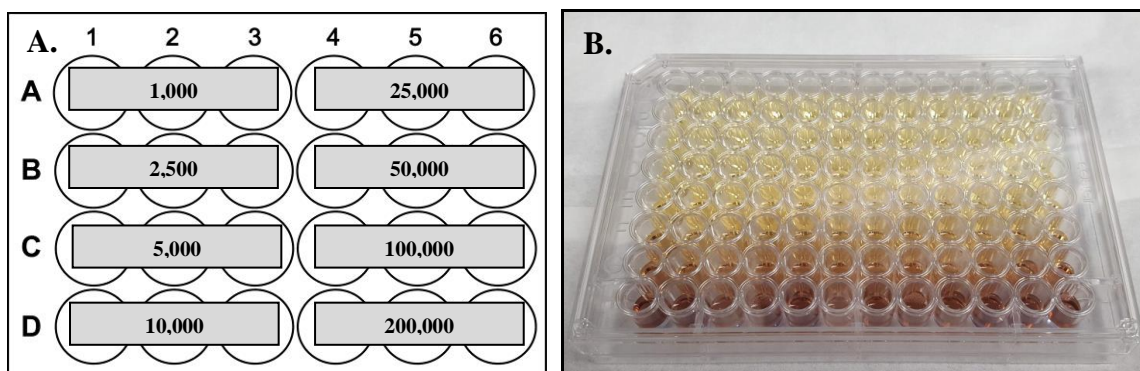


Figure D-1. Well Plate Layout, A. Culturing Cells in 24- Well Plate, B. Proliferation Assay Solution in 96- Well Plate

Begin Assay Incubation

1. Remove media from the wells.
2. Add fresh media to each well (333.3 uL).
3. Add proliferation assay to each well (66.7 uL).
1:5 Ratio for Assay: Media
4. Incubate for 1 hour at 37°C.

Read Absorbance Using Well Plate Reader

Follow steps as described in *Appendix C*.

Create Standard Curve in Excel

1. Find average absorbance for each seeding density
2. Plot Absorbance vs. Cell Number as a scatterplot, including the trendline
3. The equation for the trendline is the standard curve equation that can be used to determine an approximate cell number based on the absorbance readings:

$$\text{CELL NUMBER} = m (\text{ABSORBANCE}) - b$$

References: “*CellTiter 96® AQueous Non-Radioactive Cell Proliferation Assay Technical Bulletin*”, Promega, Promega Corporation. Web. 2018.

<https://www.promega.com/resources/protocols/technical-bulletins/0/celltiter-96-aqueous-nonradioactive-cell-proliferation-assay-protocol/>

Appendix E

Immunocytochemistry (ICC) Staining Protocol

Purpose: ICC Staining allows for specific staining of a protein or cellular product using a primary antibody to bind to the desired antigen. A fluorescent secondary antibody binds to the primary antibody to allow for visualization of the stain using a fluorescent microscope.

Materials:

1. Phosphate-buffered saline (PBS), 1X (Alfa Aesar, J61196)
2. 37% Formaldehyde Solution in H₂O (Sigma, F8775)
3. 8% EM Grade Glutaraldehyde (Polysciences, Inc., 07710)
4. Triton X-100 (Sigma, 234729)
5. Bovine Serum Albumin (Rockland, BSA-50)
6. Goat Serum (MP Biomedicals, LLC, 191356)
7. Alexa Fluor 568 Phalloidin (Invitrogen by Thermo Fisher Scientific, A12380)
8. DAPI: 4',6-diamidino-2-phenylindole, dihydrochloride (Invitrogen by Thermo Fisher Scientific, D21490)

Procedure:

Day 1 Primary Staining:

1. Fix cells using a 4% formaldehyde, 0.1% glutaraldehyde solution in 1X PBS for 20 minutes at room temperature.
2. Rinse gently 3 times with 1X PBS.
3. Permeabilize cells with a 0.1% Triton X-100 solution in 1X PBS for 15 minutes at room temperature.
4. Rinse gently 3 times with 1X PBS.
5. Block cells using a 2% BSA, 3% goat serum solution in 1X PBS for 30 minutes at room temperature.
6. Add primary antibody diluted in blocking solution, and incubate overnight at 4°C.

Primary Antibody: Mouse Anti-Collagen Type 1, monoclonal (Sigma Life Science, REF: C2456)

Day 2 Secondary Staining:

1. Save primary antibody for future uses.
2. Rinse gently 3 times with 1X PBS.
3. Add fluorescent secondary antibody at a concentration of 4 µL/mL in 1X PBS.

Secondary Antibody: Alexa Fluor 488 (green) Goat Anti-Mouse IgG H+L (Thermo Fisher Scientific, Cat. #: A-11001)

4. Rinse gently 3 times with 1X PBS.
5. Add 2.5% Alexa Fluor 568 Phalloidin (red) in 1X PBS for 20 minutes at room temperature.
6. Rinse gently 3 times with 1X PBS.

7. Add 300 nM DAPI solution (blue) in 1X PBS for 5 minutes at room temperature.
8. Rinse gently 3 times with 1X PBS and store in PBS to image.
9. Image with EVOS fluorescent microscope.

Appendix F

Fabrication of Stamp Master Using Photolithography Protocol

Purpose: Photolithography is used to transfer patterns from a high-resolution photomask onto the photoresist-covered silicon wafer used as the stamp master.

Materials:

1. Photoresist: SU-8 2005 (Microchem Corp.)
2. Substrate: 3'' Diameter Polished Silicon Wafer (University Wafer)
3. Isopropyl Alcohol
4. SU-8 Developer (Microchem Corp.)

Procedure:

Protocol Preparation:

Ensure proper Clean Room PPE is worn.

Turn on nitrogen gas tanks to UV lamp and nitrogen gun.

UV Exposure Calibration (Part One)

1. Ensure that N₂ is connected to both the mask aligner and UV controller, and turn on 'nitrogen' switch to ensure proper arc lamp cooling.
 - Required UV controller pressure = 1.5 bar
 - Required Mask aligner pressure = 2.0 bar
2. Turn on power for both UV controller and mask aligner.
3. On the UV controller, press the green button to ignite the UV arc lamp.
 - Allow the arc lamp to warm up for at least 10 min to avoid damaging the lamp. After ignition, the display will decrease to ~150 W, and then slowly increase and stabilize at ~197 W.

Substrate (Silicon Wafer) Preparation:

1. Preheat hot plate (in chemical hood) to 95°C.
2. Spray silicon wafer with isopropyl alcohol (IPA), and blow dry with nitrogen gas.
3. Place wafer directly onto the hot plate for 2-5 min, and cover with petri dish to prevent dust contamination.

Photoresist Spin-coating:

1. In order to prevent contamination by dust/debris, blow silicon wafer with nitrogen gas.
2. Turn vacuum on, turn blue valve (pressure around 22).
3. Place wafer on spin-coater chuck (in chemical hood), and apply vacuum.
4. Add 1 mL SU8-2005 for every inch in diameter of wafer (~2 mL total, enough to cover desired area of wafer. Apply an even coat with no bubbles).

5. Close the lid of the spin-coater, and spin-coat slide with photoresist using the following settings:
 - 500 rpm for 10 seconds
 - 3000 rpm for 30 seconds
 - 500 rpm for 10 seconds
 - Film Thickness: 5 μm(To do this, Select Program, Change Settings, F1 when done, Run to begin.)
6. If other film thicknesses are needed, refer to the manufacturer specification sheet to find appropriate spin-coating settings.

Soft Bake:

1. Place coated wafer on a 95°C hotplate for 2 minutes.
2. Remove wafer from hotplate, and store in a container protected from light.

Photomask Preparation:

1. Cut the photomask to fit on the wafer.
2. Use tape to secure the border of the photomask to the wafer without covering the photomask pattern.

UV Exposure Calibration (Part Two)

1. Press the 'display' button to change the display units to mW/cm^2
2. Press the 'channel' button to change to the desired channel, and press the 'set' button to display the channel settings:
 - Channel 1: Intensity $\sim 2.93 \text{ mW}/\text{cm}^2$, OR
 - Channel 2: Intensity $\sim 4 \text{ mW}/\text{cm}^2$
3. Calculate the desired exposure time: ~ 31 seconds
 - $\text{Time (s)} = \text{Dose (mJ}/\text{cm}^2) / \text{Intensity (mW}/\text{cm}^2)$
 - For 5 μm thickness, recommended dose = 90-105 mJ/cm^2
4. On the mask aligner control panel, turn the dial knob to the desired exposure time, and adjust the time units using the center knob.

UV Exposure

1. Use nitrogen gas to remove any excess debris from the photomask and glass-backing.
2. Pull out the metal mask holder from the exposure system, invert the photomask and glass-backing, and align with the metal mask holder.
3. Press the 'mask vacuum' button to hold the mask and glass-backing in place.
4. Slide the mask holder in place, and use the 2 black knobs to secure the mask holder.
5. Use nitrogen gas to remove any excess debris from the photoresist-coated wafer.
6. Pull out the substrate holder on the right side of the mask aligner, place photoresist-coated wafer on the holder, and slide holder back into place.

7. Press the 'separation' lever backwards on the bottom-left side of the mask aligner, and slide the 'contact' lever upwards and counterclockwise until the photomask and substrate are in contact.
 - When wafer is in contact with the mask, rainbow rings will be seen on mask
8. Press the 'vacuum chamber' button on the mask aligner control panel.
9. Press the green button on mask aligner control panel in order to open the arc lamp shutter.
 - Avoid looking at UV light/reflection during exposure.
10. After exposure, turn the 'contact' knob completely clockwise to release the photomask and substrate.

Post-Exposure Bake (PEB):

1. Immediately place wafer on a 95°C hotplate for 3 minutes.
2. Remove wafer from the hotplate and allow to cool to room temperature while protected from light.

Photoresist Development:

1. In a fume hood, rinse exposed wafer with SU-8 developer in all directions for approximately 1 minute.
 - Hold slide with tweezers, and avoid contact with developer.
2. Rinse wafer with isopropyl alcohol (IPA)
 - While still covered in IPA, inspect the wafer under an upright microscope for the presence of undeveloped photoresist. If black particles remain present between features, continue to rinse wafer with SU-8 developer until particles are removed.
3. Carefully dry the developed wafer dry using nitrogen gas.
4. Inspect the dried wafer under a microscope to ensure the integrity of the features.

Hard Bake:

1. Place wafer on a 150°C hotplate for 30 minutes to completely cross-link photoresist.
2. Dispose of developer/IPA waste in a waste container in back of hood.
3. Turn off all equipment and nitrogen tanks outside the lab when finished.

References:

"Karl Suss MJB3 UV400 Mask Aligner Standard Operating Procedure." Version 1.0. Nanotechnology Research Center, University of Texas at Arlington. February, 2014.

Appendix G

Fabrication of PDMS Stamps from Master Wafer Protocol

Materials:

1. Octyl (trichlorosilane) (Sigma)
2. Sylgard 184 Silicone Elastomer Base and Elastomer Curing Agent (Dow Corning, 4019862)

Procedure:

Master Silanization:

1. Place master in a vacuum desiccator.
2. In a fume hood, add 50 uL octyl(trichlorosilane) to a plastic petri dish, and place dish in the desiccator.
3. Place the lid on the desiccator, connect the desiccator to the house vacuum, and turn on house vacuum for 20 minutes to evacuate the chamber.
4. Store master in the sealed desiccator overnight (12-16 hours) to allow vapor deposition to occur.

Note: Masters should be re-silanized approximately every 10 uses.

Poly(dimethylsiloxane) (PDMS) Preparation:

1. Weigh desired amount of Sylgard 184 base into a weigh boat.
2. Add Syglard 184 curing agent at a 10:1 ratio (base:curing agent)
3. Mix the polymer for 10 minutes using a clean glass stir rod.

Note: Prepared PDMS may be stored at 4°C for 1-2 weeks.

Negative-patterned Stamp Fabrication:

1. Place master inside a plastic petri dish and add PDMS for the desired stamp thickness.
2. Place inside a vacuum desiccator.
3. Place the lid on the desiccator, connect the desiccator to the house vacuum, and turn on vacuum for 10 minutes to remove air bubbles from PDMS.
 - After degassing is complete, close the desiccator valve, disconnect house vacuum, and slowly allow air back into the desiccator.
4. Bake for at least 30 minutes to 1 hour on a 70°C hot plate, or until fully hardened.
5. After baking is complete, allow master to cool to room temperature.
6. Slowly peel PDMS layer away from master, using a scalpel or forceps as necessary.
7. Cut stamps from PDMS layer based on the pattern design, and store stamps in ethanol.

References: “Sylgard® 184 Silicone Elastomer”. Dow Corning, Dow Corning Corporation. April 2, 2014.

Appendix H

Microstamping Collagen Protocol

Materials:

Collagen Type I, Rat Tail, 4.04 mg/mL (Discovery Labware, Inc., Corning, REF 354236)

Ultrasonic Cleaner (VWR International, Model 75HT)

Procedure:

Stamp Preparation:

1. Sterilize stamps by sonicating in 100% ethanol for 15 minutes.
2. In laminar hood, rinse stamps 3X with 100% ethanol.
3. Allow stamps to dry completely.

Stamping:

1. “Ink” the stamp by adding 100 μ L of 100 μ g/mL collagen to the patterned side of the stamp for 1 hour.
2. Place stamping substrate in UV-ozone chamber for 15 minutes.
3. Remove the collagen from the stamp and rinse 2X with 1X PBS.
4. Allow the stamps to air dry completely.
5. With tweezers, “stamp” by placing the stamps pattern-down onto the stamping substrate for 30 minutes.

Note: Press down on the corners of the stamp to ensure the stamp is in contact with the surface, but do not press down.

6. Remove the stamps to reveal the final collagen pattern.

Clean Stamps to Reuse:

1. Rinse stamps ~10 times with 100% ethanol.
2. Sonicate in 100% ethanol for 15 minutes.
3. Store stamps in ethanol with the pattern side facing up.

Appendix I

Stencil Patterning Cells Protocol

Materials:

Collagen Type I, Rat Tail, 4.04 mg/mL (Discovery Labware, Inc., Corning, REF 354236)

Ultrasonic Cleaner (VWR International, Model 75HT)

Procedure:

Substrate and Stencil Preparation:

1. Coat substrate surface with 100 µg/mL collagen and incubate at 37°C overnight.
2. Remove collagen and allow to dry completely.
3. Sterilize stencils by sonicating in 100% ethanol for 15 minutes.
4. In laminar hood, rinse stencils 3X with 100% ethanol.
5. Allow stencils to dry completely.

Stencil Patterning:

1. Place PDMS stencils on collagen-coated substrate surface, pressing firmly to ensure the stencil is completely adhered to the surface.
2. Plate cells and allow to adhere for 24 hours.
3. Remove the stencils and replace media.

Clean Stencils to Reuse:

1. Rinse stencils ~10 times with 100% ethanol.
2. Sonicate in 100% ethanol for 15 minutes.
3. Store stencils in ethanol.

Appendix J

Cell Stretching Protocol

Materials:

1. Well Plate Carrier Assembly (CellScale)
2. Silicone Well Plate (CellScale)
3. Programming Control Box (CellScale)
4. Power Supply, USB Cable, and Box/Stretcher Connection Cable (CellScale)

Procedure:

Develop Cell Stretching Sequence Using Software:

1. Install MechanoCulture Software.
2. After connecting the Control Box to the power supply, connect to the computer using USB cable, ensuring the screen displays “Connected”.
3. Develop a Testing Sequence by clicking “Insert Above” or “Insert Below” to add a test step to the program.
4. Adjust test parameters (control function, stretch magnitude, time units, stretch duration, hold duration, recovery duration, rest duration, and repetitions) by double clicking on each step.
5. Program the Control Box by clicking “Program”.
6. Verify the test sequence has been correctly programmed by clicking “Read”.

Prepare well plate:

1. Modify silicone well plate by making cuts as demonstrated by the red lines in *Figure J-1* to create more uniform axial strains (*Tables J-1 and J-2*, modified from CellScale user manual).
2. Sterilize by filling wells with 100% ethanol for 1 hour, followed by 30 minutes of UV light exposure.

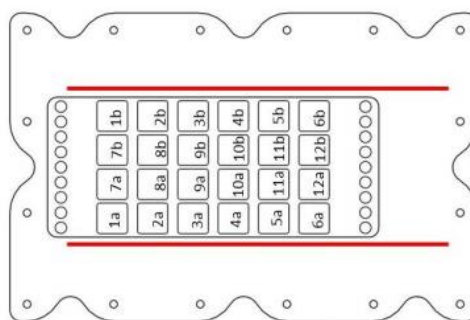


Figure J-1: Well plate modification indicated by red lines cut next to the wells [CellScale]

Table J-1: Percent Axial Strain of Well Pairs for Modified Well Plate												
Well	1a/b	2a/b	3a/b	4a/b	5a/b	6a/b	7a/b	8a/b	9a/b	10a/b	11a/b	12a/b
%Axial Strain	1.444	1.491	1.490	1.514	1.482	1.402	1.546	1.552	1.584	1.604	1.485	1.374

Table J-2: Percent Axial Strain of Well Pairs for Unmodified Well Plate												
Well	1a/b	2a/b	3a/b	4a/b	5a/b	6a/b	7a/b	8a/b	9a/b	10a/b	11a/b	12a/b
%Axial Strain	0.971	1.074	1.218	1.535	1.901	2.222	0.713	0.794	1.003	1.370	1.866	2.963

Begin Mechanical Stimulation of Cells:

1. Load the sterilized well plate into the well plate carrier.
2. Plate cells and add media, using a standard well plate lid to maintain sterility.
3. Program the Control Box using the MechanoCulture software.
4. Place the Well Plate Carrier Assembly with plated cells into the incubator.
5. Connect the Control Box to the Power Supply, and then to the Well Plate Carrier Assembly with the connection cable.
6. Press the button on the Control Box one time to begin stretching sequence .

References: “*MechanoCulture FX Mechanical Stimulation System.*” User Manual Version 1.2. CellScale Biomaterials Testing. 2016.

Appendix K

Legend of Photomask Stamp Designs

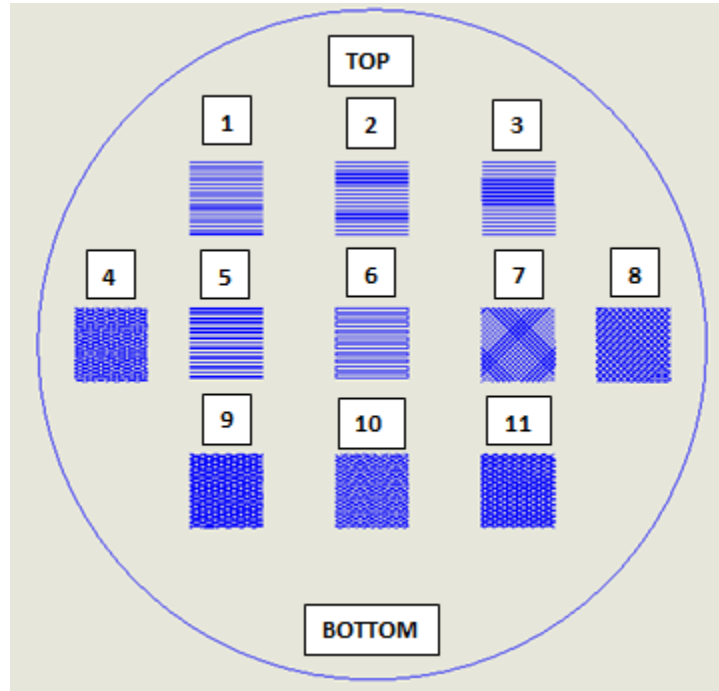



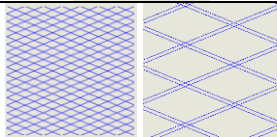

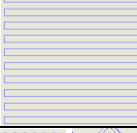
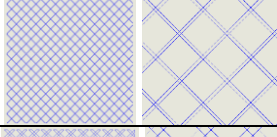
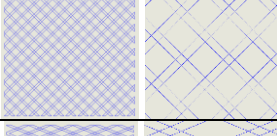
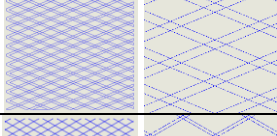
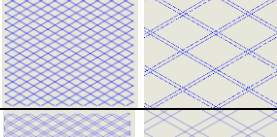
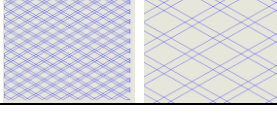


Figure K-1: Legend of Photomask Stamp Designs (corresponds with *Figure 3.6*)

Table K-1: Specifications of Stamp Designs corresponding to *Figure K-1*

STAMP #	PICTURE	DESCRIPTION
1		Parallel Lines 10 μm lanes 300 μm spacing
2		Parallel Lines 30 μm lanes 300 μm spacing
3		Parallel Lines 50 μm lanes 300 μm spacing
4		Diamonds, 45° 30 μm lanes 300 μm spacing
5		Parallel Lines 100 μm lanes 300 μm spacing
6		Parallel Lines 300 μm lanes 300 μm spacing
7		Diamonds, 90° 30 μm lanes 300 μm spacing
8		Diamonds, 90° 100 μm lanes 300 μm spacing
9		Diamonds, 45° 100 μm lanes 300 μm spacing
10		Diamonds, 60° 30 μm lanes 300 μm spacing
11		Diamonds, 60° 100 μm lanes 300 μm spacing

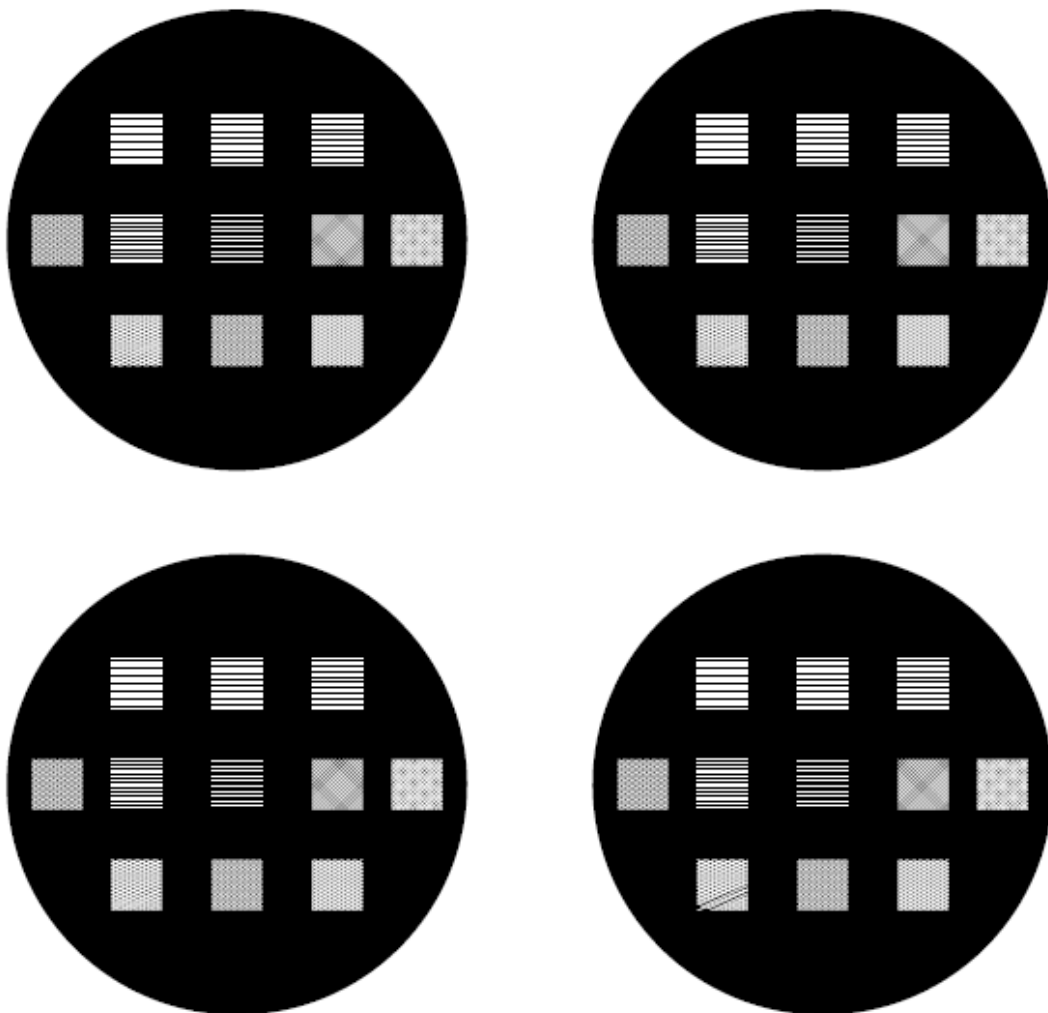


Figure K-2: Final proof of photomask from CAD/Art services

Appendix L

Results from Microstamping Trials

Microstamping procedures were optimized to develop the best patterns. A variety of substrates were used, including PDMS gels, polystyrene petri dishes, and glass petri dishes. Extracellular matrix proteins collagen and laminin were both patterned, with collagen demonstrating the best patterning ability. PDMS and silicone substrates were most effective at producing a complete, accurate protein pattern.

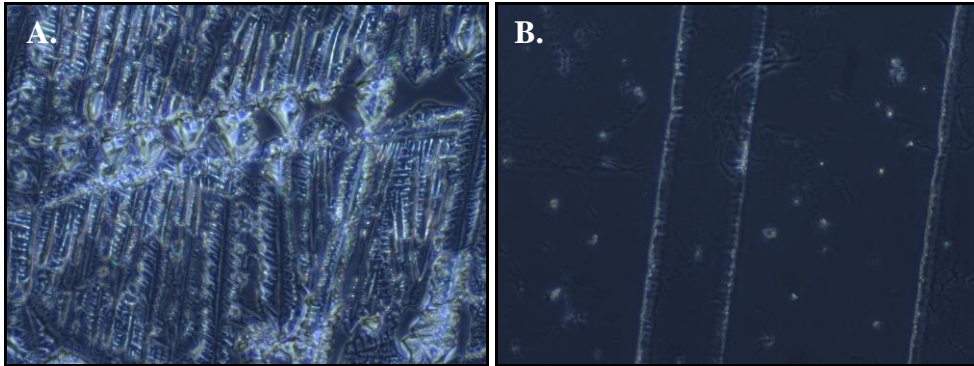


Figure L-1: A, B. Microstamping Collagen with a weight on PDMS gel (10X)

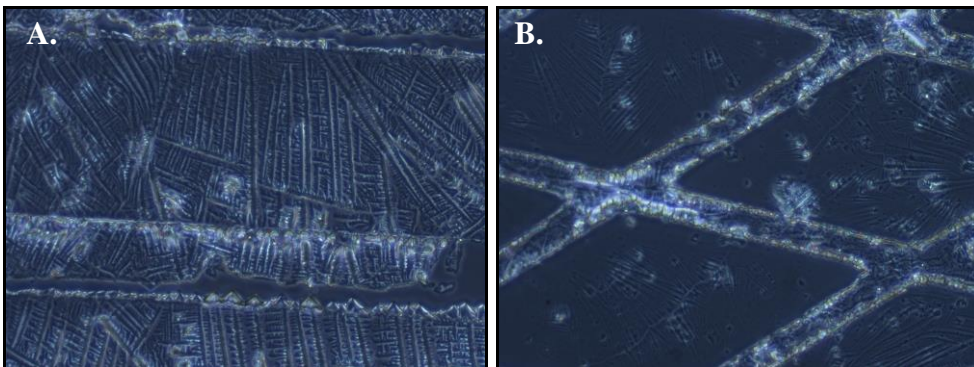


Figure L-2: A, B. Microstamping Laminin with a weight on PDMS gel (10X)

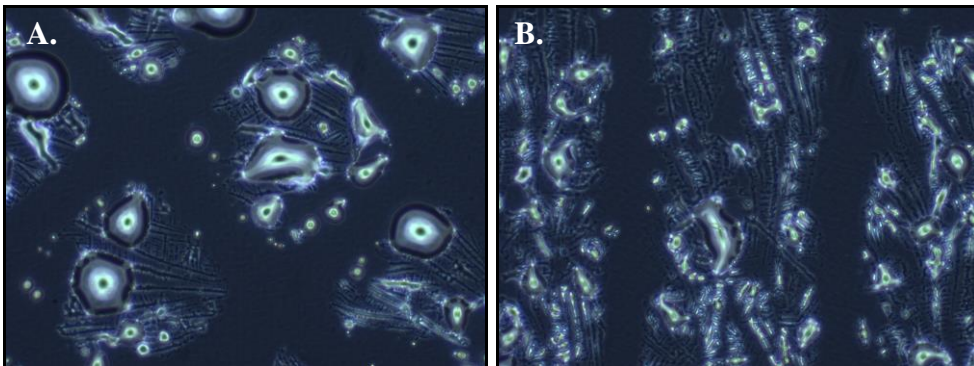


Figure L-3: A, B. Microstamping Collagen on polystyrene petri dish without rinsing or drying collagen (10X)

Appendix N

Proliferation Assay Data from Stretching Experiments

Tables N-1 to N-4 compare the viable cell numbers of control and stretched VSMCs plated with or without a stencil for the Trial One experiment of stretching VSMCs in stenciled line patterns. Tables N-5 to N-9 compare the viable cell numbers between wells in each sample group to determine the variance among each group. A two-tailed student's t-test with unequal variance was performed to determine if there is a statistically significant difference between the wells of each sample group.

Table N-1: Viable cell numbers of control and parallel or perpendicularly stretched VSMCs plated in a line pattern with a stencil (corresponds with *Figure 4.9*)

Viable Cell Numbers of Stenciled VSMCs		
Sample Group	Average Absorbance	Standard Deviation
Control (No Stretch)	0.266	0.023
Parallel Stretch	0.097	0.002
Perpendicular Stretch	0.095	0.001

Table N-2: Viable cell numbers of the control and stretched VSMCs without a stencil (corresponds with *Figure 4.8*)

Viable Cell Numbers of Non-Stenciled VSMCs			
Sample Group	Average Absorbance	Standard Deviation	T-Test
Control (No Stretch)	0.287	0.005	2.03 E-16
Stretch (Non-directional)	0.094	0.001	

Table N-3: Viable cell numbers of non-directional, parallel, and perpendicularly stretched VSMCs (corresponds with *Figure 4.11*)

Viable Cell Numbers of Stretched VSMCs		
Sample Group	Average Absorbance	Standard Deviation
No Stencil (Non-Directional)	0.094	0.001
Parallel Stretch	0.097	0.002
Perpendicular Stretch	0.095	0.001

Table N-4: Viable cell numbers of control VSMCs plated with or without a stencil (corresponds with *Figure 4.10*)

Viable Cell Numbers of Control (No-Stretch) VSMCs			
Sample Group	Average Absorbance	Standard Deviation	T-Test
No Stencil	0.287	0.005	0.044
Stencil	0.266	0.023	

Table N-5: Viable cell numbers of control samples plated without a stencil; p-value (0.297) indicates there is not a statistically significant difference between the wells

Viable Cell Numbers of Control VSMCs Plated without a Stencil						
Absorbance Values				Average Absorbance	Standard Deviation	T-Test
Well 1	0.286	0.282	0.287	0.285	0.003	0.297
Well 2	0.283	0.291	0.294	0.289	0.006	
Total Average Absorbance				0.287	0.004	

Table N-6: Viable cell numbers of stenciled control samples; p-values are listed for Well 1 vs. 2 (4.71 E-4), Well 1 vs. 3 (3.07 E -4), and Well 2 vs. 3 (5.11 E-3), respectively, and each indicates a statistically significant difference between the compared wells

Viable Cell Numbers of Control VSMCs Plated with a Stencil						
Absorbance Values				Average Absorbance	Standard Deviation	T-Tests
Well 1	0.293	0.290	0.291	0.291	0.002	4.71 E-4
Well 2	0.264	0.265	0.271	0.267	0.004	3.07 E-4
Well 3	0.232	0.240	0.247	0.240	0.008	5.11 E-3
Total Average Absorbance				0.266	0.004	

Table N-7: Viable cell numbers of stretched samples plated without a stencil; p-value (0.116) indicates there is not a statistically significant difference between the wells

Viable Cell Numbers of Stretched VSMCs Plated without a Stencil						
Absorbance Values				Average Absorbance	Standard Deviation	T-Test
Well 1	0.094	0.094	0.094	0.094	0.000	0.116
Well 2	0.093	0.094	0.093	0.093	0.001	
Total Average Absorbance				0.094	0.000	

Table N-8: Viable cell numbers of parallel stretch samples; p-values are listed for Well 1 vs. 2 (0.205), Well 1 vs. 3 (0.022), and Well 2 vs. 3 (0.016), respectively, and indicates a statistically significant difference between Wells 1 and 3, Wells 2 and 3

Viable Cell Numbers of Parallel Stretched VSMCs						
Absorbance Values				Average Absorbance	Standard Deviation	T-Tests
Well 1	0.097	0.094	0.096	0.096	0.002	0.205
Well 2	0.097	0.097	0.097	0.097	0.000	0.022
Well 3	0.099	0.099	0.101	0.100	0.001	0.016
Total Average Absorbance				0.097	0.001	

Table N-9: Viable cell numbers of perpendicular stretch samples; p-values are listed for Well 1 vs. 2 (0.205), Well 1 vs. 3 (0.158), and Well 2 vs. 3 (0.091), respectively, and each indicates there is not a statistically significant difference between the compared wells

Viable Cell Numbers of Perpendicular Stretched VSMCs						
Absorbance Values				Average Absorbance	Standard Deviation	T-Tests
Well 1	0.095	0.095	0.095	0.095	0.000	0.205
Well 2	0.096	0.095	0.098	0.096	0.002	0.158
Well 3	0.093	0.094	0.095	0.094	0.001	0.091
Total Average Absorbance				0.095	0.001	

Tables N-10 to N-11 compare the viable cell numbers of control and stretched VSMCs for the Trial Two experiment of stretching VSMCs in stenciled line patterns. Tables N-12 to N-16 compare the viable cell numbers between wells in each sample group to determine the variance among each group. A two-tailed student's t-test with unequal variance was performed to determine if there is a statistically significant difference between the wells of each sample group.

Table N-10: Viable cell numbers of control and stretched VSMCs (corresponds with Figure 4.18)

Viable Cell Numbers of Control and Stretched VSMCs		
Sample Group	Average Absorbance	Standard Deviation
Day 0 Control	0.131	0.007
Day 1 Control	0.114	0.002
Day 1 Stretch	0.095	0.002

Table N-11: Viable cell numbers of stretched VSMCs (corresponds with *Figure 4.19*)

Viable Cell Numbers of Parallel and Perpendicularly Stretched VSMCs			
Sample Group	Average Absorbance	Standard Deviation	T-Test
Parallel Stretch	0.095	0.001	0.493
Perpendicular Stretch	0.095	0.002	

Table N-12: Viable cell numbers of Day 0 Control samples, p-value (0.001) indicates there is a statistically significant difference between the wells

Viable Cell Numbers of Day 0 Control VSMCs						
Absorbance Values				Average Absorbance	Standard Deviation	T-Test
Well 1	0.124	0.126	0.126	0.125	0.001	0.001
Well 2	0.138	0.135	0.138	0.137	0.002	
Total Average Absorbance				0.131	0.007	

Table N-13: Viable cell numbers of Day 1 Control samples, p-value (0.742) indicates there is not a statistically significant difference between the wells

Viable Cell Numbers of Day 1 Control VSMCs						
Absorbance Values				Average Absorbance	Standard Deviation	T-Test
Well 1	0.116	0.116	0.111	0.114	0.003	0.742
Well 2	0.115	0.112	0.114	0.114	0.002	
Total Average Absorbance				0.114	0.002	

Table N-14: Viable cell numbers of Day 1 Parallel Stretch samples, p-value (0.742) indicates there is not a statistically significant difference between the wells

Viable Cell Numbers of Parallel Stretched VSMCs						
Absorbance Values				Average Absorbance	Standard Deviation	T-Test
Well 1	0.095	0.094	0.095	0.095	0.001	0.742
Well 2	0.094	0.093	0.096	0.094	0.002	
Total Average Absorbance				0.095	0.001	

Table N-15: Viable cell numbers of Day 1 Perpendicular Stretch samples, p-value (0.374) indicates there is not a statistically significant difference between the wells

Viable Cell Numbers of Perpendicular Stretched VSMCs						
Absorbance Values				Average Absorbance	Standard Deviation	T-Test
Well 1	0.099	0.094	0.095	0.096	0.003	0.374
Well 2	0.095	0.093	0.095	0.094	0.001	
Total Average Absorbance				0.095	0.002	

Table N-16: Viable cell numbers of Day 1 Stretch samples, p-value (0.493) indicates there is not a statistically significant difference between the parallel and perpendicular samples

Viable Cell Numbers of Parallel and Perpendicular Stretch VSMCs			
Absorbance Values	Average Absorbance	Standard Deviation	T-Test
Parallel Stretch	0.095	0.001	0.493
Perpendicular Stretch	0.095	0.002	
Total Average Absorbance	0.095	0.002	

Appendix O

VSMC Proliferation Assay Standard Curves

A standard curve for the proliferation assay was created to approximate viable cell number from absorbance readings. The protocol in *Appendix D* was used to obtain average absorbance and cell seeding density values to create a standard curve equation.

Table O-1: Seeding Density and Absorbance Values for Standard Curve #1

Average Absorbance	Cell Seeding Density
0.11642	1,000
0.12000	2,500
0.12758	5,000
0.15933	10,000
0.22992	25,000
0.33017	50,000
0.47400	100,000
0.80340	200,000

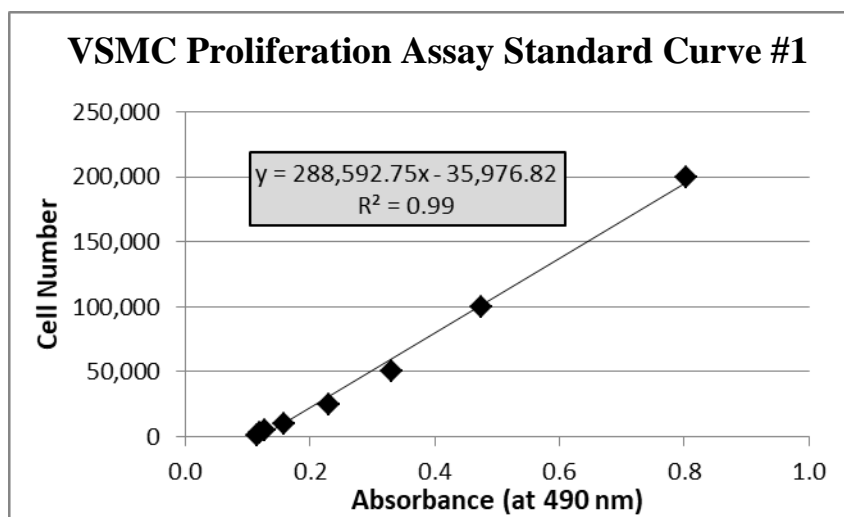


Figure O-1: VSMC Standard Curve #1

Standard Curve #1 Equation:

$$\text{CELL NUMBER} = 288,592.75(\text{ABSORBANCE}) - 35,976.82$$

Table O-2: Seeding Density and Absorbance Values for Standard Curve #2

Average Absorbance	Cell Seeding Density
0.11483	0
0.12217	1,000
0.13133	2,500
0.14675	5,000
0.17817	10,000
0.24792	25,000
0.38108	50,000
0.58708	100,000
0.84183	200,000

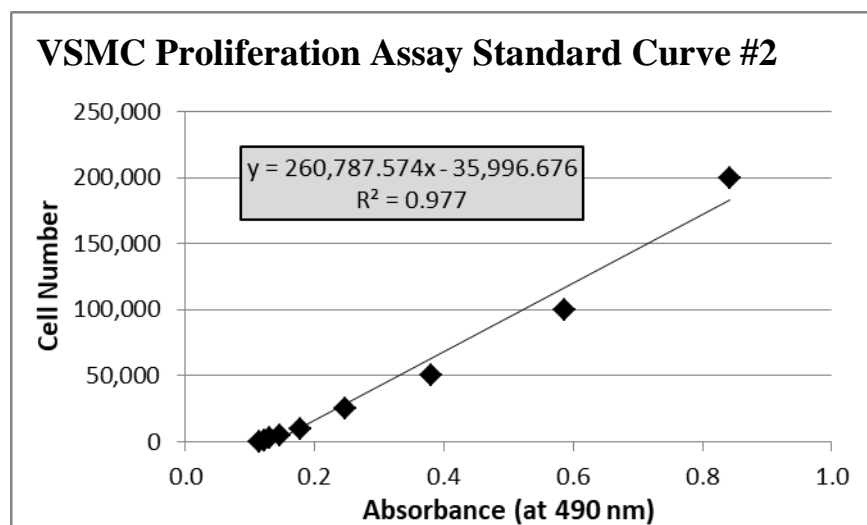


Figure O-2: VSMC Standard Curve #2

Standard Curve #2 Equation:

$$\text{CELL NUMBER} = 260,787.57(\text{ABSORBANCE}) - 35,996.68$$

Appendix P

Images of DAPI-Stained VSMCs for Number of Nuclei Analysis

Table P-1 shows the average number of nuclei for each sample group for the Trial One experiment of stretching VSMCs in stenciled line patterns. Figures P-1 to P-5 were used to compile the average number of VSMC nuclei for each sample group.

Table P-1: Average Number of Nuclei from DAPI-stained VSMCs at 10X
(corresponds with *Figure 4.12*)

Sample Group	Count 1	Count 2	Count 3	Count 4	Average Count	Standard Deviation
Control- No Stencil	320	542	232	198	323.000	154.786
Control- Stencil	187	399	333	100	254.750	135.976
Stretch- No Stencil	175	216	241	248	220.000	32.995
Stretch- Parallel	284	168	176	9	159.250	113.277
Stretch- Perpendicular	97	165	399	162	205.750	132.598

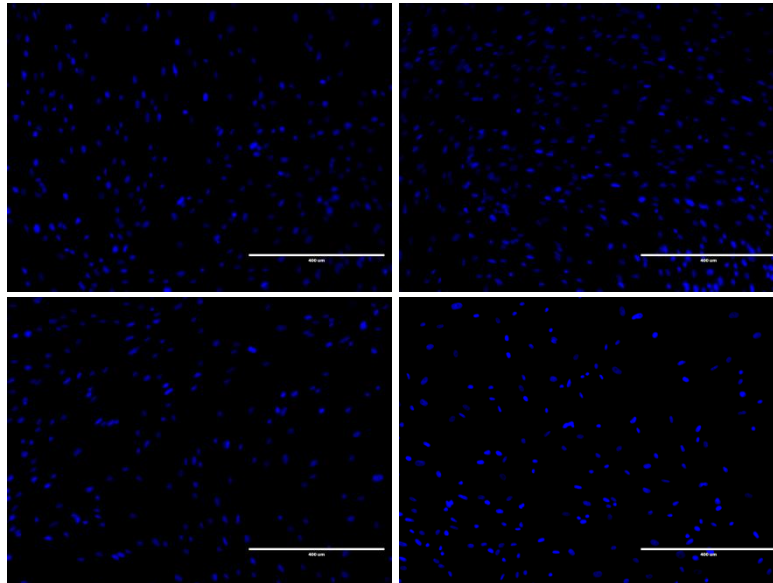


Figure P-1: A-D, Control VSMCs plated without a stencil, stained for DAPI (10X)

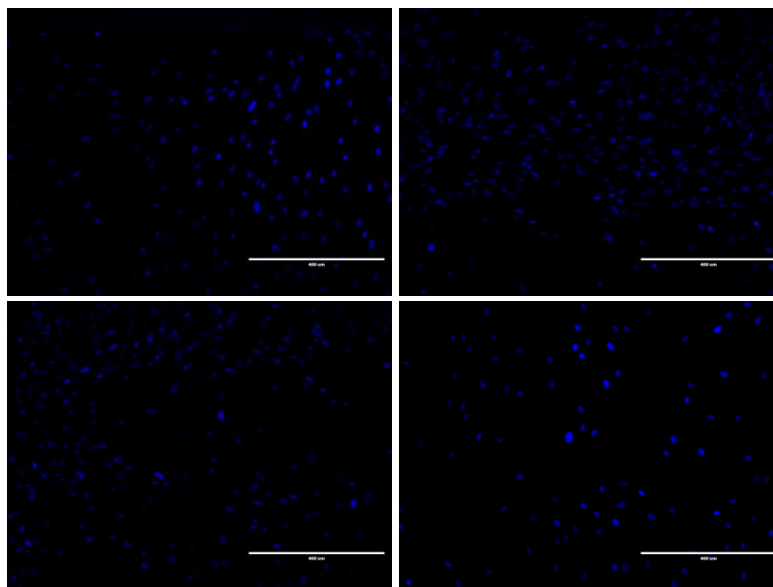


Figure P-2: A-D, Control VSMCs plated with a stencil, stained for DAPI (10X)

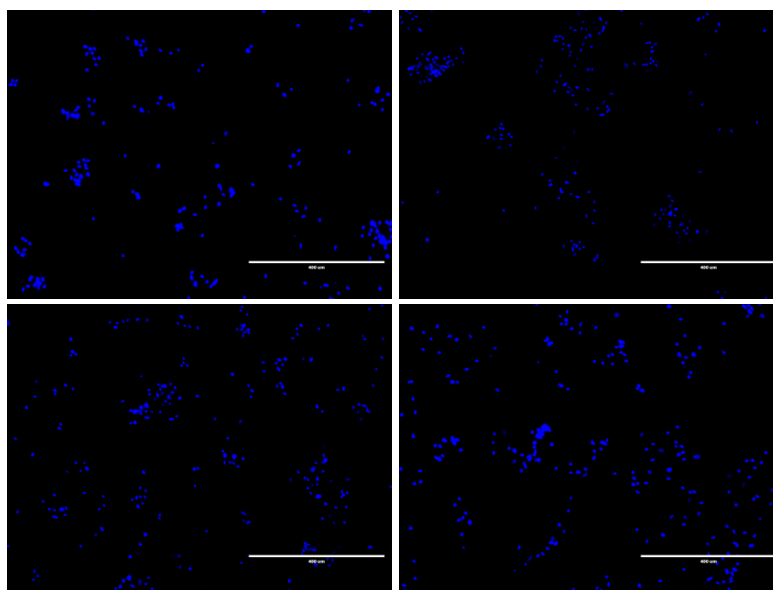


Figure P-3: A-D, Stretched VSMCs plated without a stencil, stained for DAPI (10X)

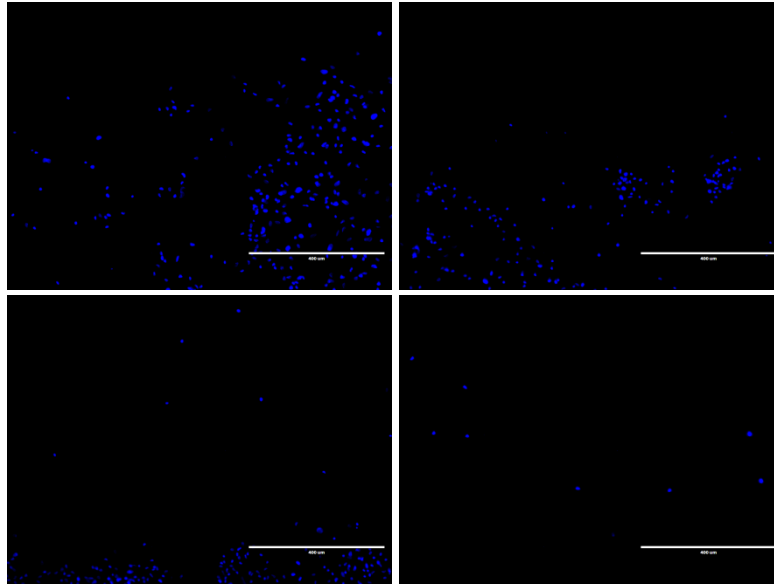


Figure P-4: A-D, Parallel-Stretched VSMCs plated with a stencil, stained for DAPI (10X)

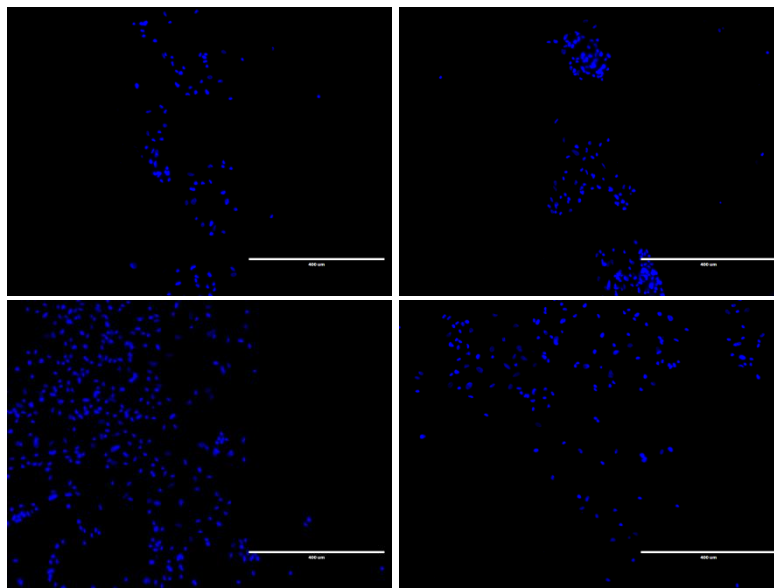


Figure P-5: A-D, Perpendicularly-Stretched VSMCs plated with a stencil, stained for DAPI (10X)

Table P-2 shows the average number of nuclei for each well of each sample group for the Trial One experiment of stretching VSMCs in stenciled line patterns. *Figures P-6 to P-12* were used to compile the average number of VSMC nuclei for each sample group.

Table P-2: Average Number of Nuclei from DAPI-stained VSMCs at 10X
(corresponds with *Figure 4.20*)

Sample Group	Well 1			Well 2			Average Count	Standard Deviation
	Count 1	Count 2	Count 3	Count 4	Count 5	Count 6		
Day 0 Control	75	84	84	61	67	128	83.167	23.794
Day 1 Control	14	53	55	57	42	58	46.500	16.932
Parallel	46	22	24	18	35	10	25.833	12.813
Perpendicular	38	13	19	0	0	0	11.667	15.214

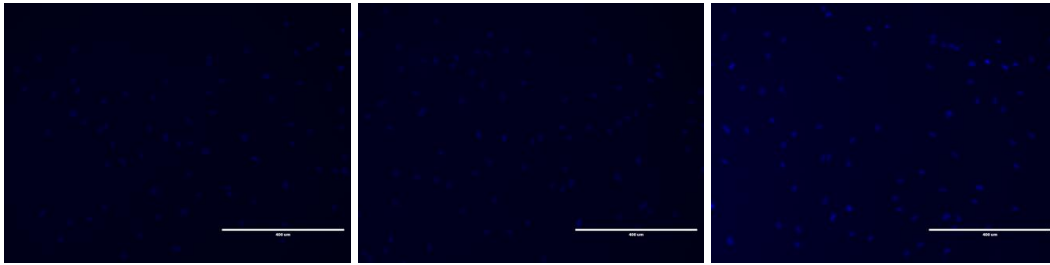


Figure P-6: A-C, Well 1 of Day 0 Control VSMCs, stained for DAPI (10X)

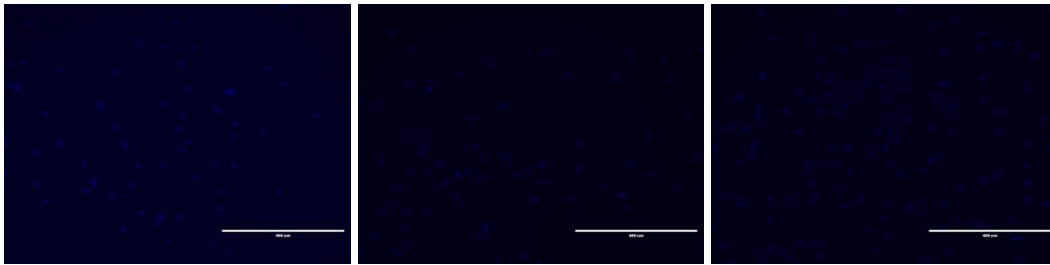


Figure P-7: A-C, Well 2 of Day 0 Control VSMCs, stained for DAPI (10X)

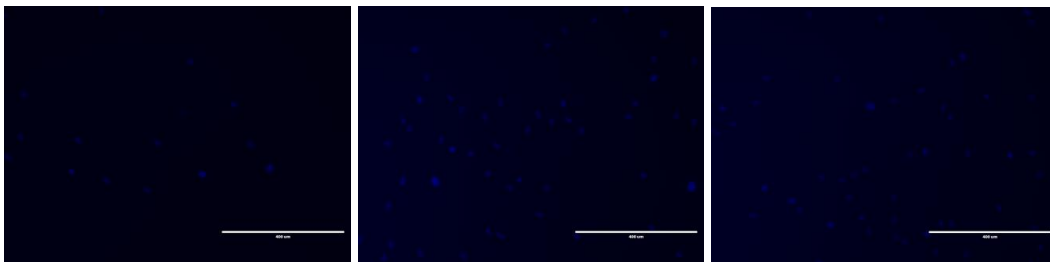


Figure P-8: A-C, Well 1 of Day 1 Control VSMCs, stained for DAPI (10X)

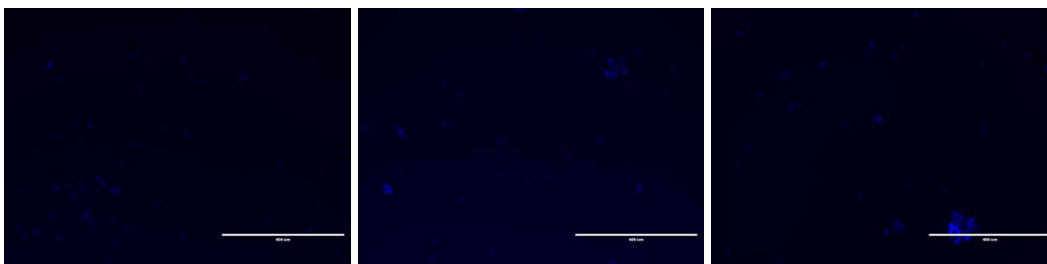


Figure P-9: A-C, Well 2 of Day 1 Control VSMCs, stained for DAPI (10X)

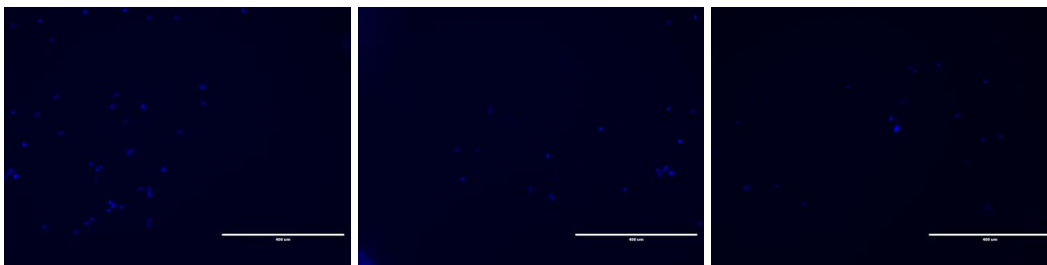


Figure P-10: A-C, Well 1 of Parallel-Stretched VSMCs, stained for DAPI (10X)

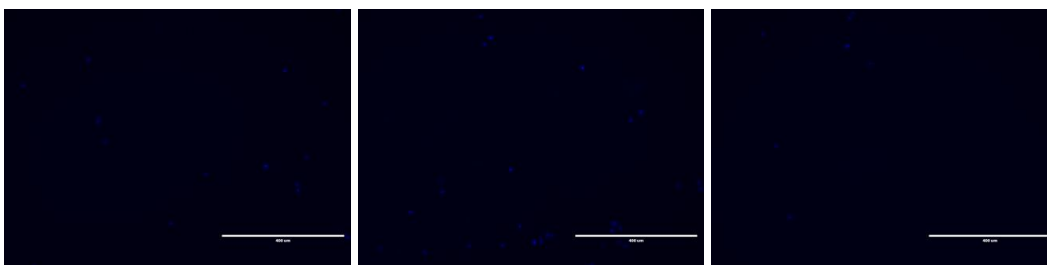


Figure P-11: A-C, Well 2 of Parallel-Stretched VSMCs, stained for DAPI (10X)

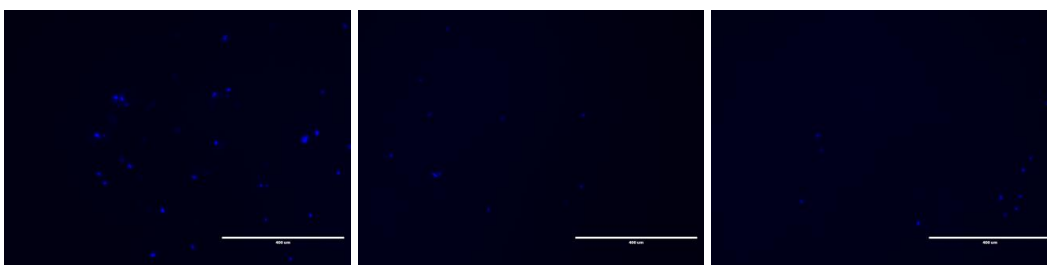


Figure P-12: A-C, Well 1 of Perpendicularly-Stretched VSMCs, stained for DAPI (10X)

***Note:** No pictures are available for Well 2 of Perpendicularly-Stretched VSMCs because no cells were visibly stained in the well.*